Title
Dimerization of Telomerase RNA During Telomerase Biogenesis Regulates Telomerase Activity

Author
Matsuguchi, Tetsuya

Publication Date
2011

Peer reviewed|Thesis/dissertation

Dimerization of Telomerase RNA During Telomerase Biogenesis Regulates Telomerase Activity

by

Tetsuya Matsuguchi

DISSERTATION

Submitted in partial satisfaction of the requirements for the degree of

DOCTOR OF PHILOSOPHY

in

Biochemistry and Molecular Biology

in the

GRADUATE DIVISION

of the

UNIVERSITY OF CALIFORNIA, SAN FRANCISCO

[redacted]

Acknowledgements

I would like to thank my thesis adviser, Elizabeth Blackburn, for her continued enthusiasm and endless patience, and for giving me the freedom to follow a number of questions. She always found interesting insights from what I thought were boring pieces of data, and I always left her office enthusiastic about the next set of experiments. I would also like to thank my thesis committee members: Hiten Madhani and Geeta Narlikar. Their insights, constructive criticisms and advice were always useful, and I would like to thank them especially for responding to my chronic last-minute requests.

I thank the past and present members of the Blackburn lab. Jue Lin and Laura Cassiday have patiently mentored me during my rotation in the lab when I had no idea what telomerase was or how to handle RNA. Jue has continued to provide advice and reagents for numerous experiments throughout my entire time in the lab, and I appreciate her keeping the promise that she would not leave the lab before I graduated. Svetlana Makovets and Shivani Nautiyal were very helpful in getting me up to speed in the lab; they have both taught me countless tricks for working with the yeast system. Sveta has also taught me an important lesson: Processing twice as many samples isn't twice as hard, so I should always process twice as many samples. I would like to thank Jeffrey Seidel and Shang Li not only for their expert scientific advice but also for their friendship. Jeff was especially helpful in teaching me yeast biochemistry techniques. Shang was always inspiring with his big ideas and dreams. Imke Listerman has given me much helpful advice on working with RNA. Brad Stohr, Tanya Williams, Lifeng Xu, and

Jason Lukas were always helpful in discussions of my projects. The discussions with Brad and Tanya were particularly fun and challenging. I am especially grateful for Carol Anderson as I write this thesis, for she had compiled many of the formatting tricks. I also thank the newer, younger additions to the lab: Beth Cimini, Francesca Gazzaniga, Kyle Jay, and Kyle Lapham. They have brought fresh ideas, energy, enthusiasm and more social environment to the lab. I would like to acknowledge special thanks to Kyle Lapham for bringing the high-throughput technologies into the lab, without which many of the experiments in this thesis would have been substantially more difficult. This work would not have been possible without Irma Easter, who prepared most of the reagents used and had always promptly responded my numerous requests. I would also like to thank Maura Clancy, Toni Hurley, and Dana Smith for keeping the lab running smoothly. I also thank Eric Jang, Rachel Ingraham, Ron Menorca, and Evelyn Chang, the students I had the privilege of mentoring, for their enduring my mentorship as I learned how to do it.

My classmates have been wonderful companions both academically and socially. Monica Carolina Rodrigo-Brenni and Brandon Toyama were helpful not only in the daily discharge of frustrations at the Adrenalin Hour, but also in the brainstorming sessions on overcoming experimental obstacles. Victoria Newman has also helped me cope with my gadgetophilia by teaching me how to use the capillary electrophoresis and automated nucleic acid purification machines. Stacy Chen, an honorary member of the Blackburn lab, was a wonderful partner-in-crime for daily lab mischiefs. Claire Rowe, Erin Quan

Toyama, and Katie Verges, the official models for the Mission Bay Housing, provided numerous brain foods (*e.g.* cupcakes) and a warm place to wind down from time to time.

I would also like to thank Quinn Mitrovich, David Breslow, Sean Collins, Clement Chu, Brian Lee, Antoine Roux, Ben Schiller, and Niall Cardin for helpful scientific discussions as well as sharing their expertise to help me with my project directions, presentations, and data analyses.

I thank the Howard Hughes Medical Institute for providing funding through the Predoctoral Fellowship for five years. I also thank the Larry L. Hillblom Foundation for the Hillblom Fellowship in aging research.

Finally, I would like to thank my family for allowing me to pursue my career without questioning and my friends who provided social environments outside the lab that kept me sane and happy all these years.

Dimerization of Telomerase RNA During Telomerase Biogenesis Regulates Telomerase Activity

by

Tetsuya Matsuguchi

Abstract

Telomerase is a ribonucleoprotein complex minimally composed of telomerase reverse transcriptase and telomerase RNA, which contains the template region encoding the telomeric repeat sequence. This minimal, monomeric complex is active for extending telomeric substrates *in vitro*, but several studies have indicated that telomerase reverse transcriptase as well as telomerase RNA can physically and functionally oligomerize or dimerize; however, the functional significance of dimerization is not known. Here we show that physical interaction between two (or more) molecules of the yeast telomerase RNA, TLC1, occurs *in vivo* by two independent modes: one involving the 3' region of TLC1 and the other by a Ku- and Sir4-mediated interaction. This telomerase RNA dimerization seems to be at least partially independent of the formation of the telomerase complex; in fact, no direct evidence for telomerase reverse transcriptase dimerization was found in our attempts. I propose a model in which TLC1 dimerization is an intermediate step during its biogenesis, and that the active telomerase complex either only has one catalytic site or that forms a dimer only transiently. Previous studies have shown that the template regions of two telomerase RNAs functionally interact, in yeast as well as in

human. I have shown that Est1 and Est3, essential factors for *in vivo* telomerase activity, are required for this functional interaction of the telomerase RNA templates in telomeric DNA synthesis. By integrating these results, I propose a model in which TLC1 physical dimerization can obscure the template region, and the activation of telomerase activity requires uncovering of this region. I suggest that Est1 and Est3 play a role in this step. Taken together, this provides a model in which yeast telomerase dimerization during its biogenesis requires subsequent reorganization and can act as a regulatory step in telomerase activity activation.

Table of Contents

List of Tables

List of Figures

Chapter 1: Introduction

Telomeres

Telomeres are specialized structures at the ends of linear chromosomes, in most eukaryotes, consisting of G-rich repetitive DNA sequence, multi-component complexes of proteins bound to the telomeric DNA, and associated RNAs including telomeric-repeat containing RNAs (de Lange *et al*. 2006; Feuerhahn *et al*. 2010). Telomeres play important roles in chromosome maintenance and dynamics throughout the life of a cell and an organism. A central role of telomeres is to act as caps protecting the ends of chromosomes from various insults including nucleases. The specialized telomeric structures are necessary for distinguishing the natural DNA ends from the ends resulting from DNA double-strand breaks (Jain and Cooper 2010). The earliest studies of telomeres have shown that natural DNA ends do not fuse to other ends as the double-strand break-induced ends do (McClintock 1931; Muller 1938). Interestingly, many of the double-strand break repair proteins reside on telomeres; the mechanism by which these repair proteins are prevented from recognizing telomeres as damaged DNA is not well understood (Jain and Cooper 2010).

Telomeric DNA is typically composed of repetitive sequences (tandem "TTAGGG" repeats in vertebrates; tandem $TG_{1\text{-}3}$ repeats in *S. cerevisiae*). The repetitive nature of the DNA sequence allows partial loss of telomeric DNA without any genetic information loss. Specific telomeric sequences also allow recruitment of specialized

telomeric proteins that help protect and maintain telomeres. These include double-stranded telomere binding proteins, such as Rap1 in yeast, and single-stranded telomere binding proteins, such as Cdc13, that bind the 3' overhanging, G-rich DNA strand at the end of the telomere (Jain and Cooper 2010). Such telomere sequence-specific, single-stranded DNA-binding proteins also have the potential to bind to any stretches of single-stranded telomeric DNA that may become exposed within the body of the telomeric repeat tract; such intermediates may exist during DNA replication or recombination processes.

In addition to all the forms of environmental damage that can cause telomeres to shorten, there is an obligatory shortening of telomeres every cell division that results from the incomplete DNA replication problem (Watson 1972). To date, all DNA polymerases catalyzing templated nucleic acid synthesis found in nature have 5' to 3' directionality in synthesis, and all replicative DNA polymerases require a nucleic acid primer. Hence, RNA primers are required for DNA replication, and Okazaki fragments initiated with short RNA stretches are created during the replication of lagging strand (Ogawa and Okazaki 1980). These facts lead to the inability of biomolecules to replicate DNA at the extreme termini. Minimally, the length of RNA primer used to replicate the extreme telomere terminus is lost during the semi-conservative replication of DNA.

In order to balance the loss of telomeric repeats from the ends of chromosomes, there is a specialized enzyme called telomerase that replenishes telomeric repeats to the telomeres. Almost all eukaryotic organisms have linear chromosomes with telomeres that depend on telomerase to maintain telomeres, with notable exceptions like *Drosophila*, in

which a retrotransposon is utilized. In addition, there are alternative recombination-based telomere-lengthening pathways that can operate under some conditions in many organisms. The majority of this thesis will focus on telomerase-dependent telomere maintenance.

Telomerase

Telomerase is a ribonucleoprotein (RNP) minimally composed of a protein catalytic subunit, telomerase reverse transcriptase (TERT; called hTERT in human and Est2 in budding yeast), and a telomerase RNA component, which contains the RNA template used by telomerase to extend telomeric DNA at the end of chromosomes (TER; called hTER or hTR in human and TLC1 in yeast). Telomerase is a unique class of polymerases that carries a self-contained template by which nucleotide additions are directed (C W Greider and E H Blackburn 1989). Natural telomerase substrates are single-stranded, telomere-repeat containing DNAs (together with their endogenously associated proteins). The single-stranded telomeric DNA can anneal to the 3' end of the template and act as the primer for elongation by telomerase. Once the end of the template is reached, the template and now the product must disengage in order to reposition and realign such that the 3' end of the DNA product is annealed to the 3' end of the template for the second round of extension (Autexier and Neal F. Lue 2006; Kelleher *et al*. 2002). This process is called the repeat addition processivity, and the mechanism by which the repositioning occurs is very poorly understood. This re-aligning step requires homology between the 5'

and 3' ends of the template, and it is important consideration when mutations are made in the template region, as it is done in Chapter 3.

Many aspects of telomerase are well conserved between yeast and human as well as *Tetrahymena* (Kelleher *et al*. 2002), in which the first telomerase activity was discovered (Carol W. Greider and Elizabeth H. Blackburn 1985). There are notable differences, such as robust repeat processivity seen in human telomerase *in vitro* while yeast telomerase shows no repeat processivity; however, yeast remains the most well-studied model organism in which telomerase is studied. The work described in this thesis focuses on the yeast telomerase.

Interestingly, both human and yeast telomerases remain bound to their extended DNA products, albeit in different contexts (Robart and Kathleen Collins 2011; John Prescott and Elizabeth H. Blackburn 1997). Purified human telomerase retains the repeat addition processivity, while yeast telomerases from *S. cerevisiae* and *K. lactis* can only extend the primer once (John Prescott and Elizabeth H. Blackburn 1997; Fulton and Elizabeth H. Blackburn 1998). The lack of repeat addition processivity by these two budding yeast telomerases *in vitro* is caused by the stable interaction of the DNA product stalled at the catalytic site, as evidenced by lack of extension of a DNA substrate (a "challenge" substrate) added at a later time (John Prescott and Elizabeth H. Blackburn 1997). The human telomerase, however, can extend the newly added "challenge" primer substrate while retaining an interaction with the previously extended primer product, suggesting that the stable interaction of the extended primer to telomerase is not at the catalytic site (Robart and Kathleen Collins 2011). The reason for why yeast telomerase

lacks the ability to remove its product *in vitro* is unknown. The ability of telomerase to retain telomeric oligonucleotides at and outside the catalytic site has important implications for interpretation of *in vitro* telomerase activity assays in Chapter 3.

A crystal structure of (a portion of) telomerase has only recently been available, but phylogenetic comparisons of telomerase reverse transcriptases and telomerase RNAs and molecular genetic approaches in model organism eukaryotes have been fruitful in identifying major structural elements of telomerase.

Telomerase reverse transcriptase

There are two major highly conserved domains in the telomerase reverse transcriptase (RT)-containing protein: the N-terminal region unique to telomerase that contains RNA and DNA binding domains, and the RT domain, located toward the C-terminal region of the protein (Autexier and Neal F. Lue 2006; Kelleher *et al*. 2002). The evolution of the telomerase RNP is ambiguous, but the telomerase protein TERT is thought to have evolved from viral reverse transcriptases, and the RT domain is well conserved, especially at the critical amino acid residues for catalysis, nucleotide addition processivity and nucleotide binding (Peng *et al*. 2001; Bosoy and Neal F. Lue 2001). Because the viral reverse transcriptases are well studied and many atomic-resolution structures exist, the comparable critical residues of telomerase have been identified well before the crystal structure of telomerase was available. One of the frequently used mutations in this thesis, *est2-D530A*, is the mutation in a residue critical for catalysis, in which one of the aspartate residues of the aspartate triad is mutated. This catalytically-

dead mutation is useful, because the protein remains stable, and, with the exception of the actual nucleotide addition step, *est2-D530A* can presumably carry out other steps involved in telomere addition *in vivo*, including assembling with other telomerase-associated factors, interacting with the telomeres, and binding to the DNA and dNTP substrates of telomerase.

The N-terminal regions of telomerase contain two major domains: the telomerase essential N-terminal (TEN) domain and the TERT RNA binding domain (TRBD). The TEN domain is thought to be important for DNA substrate binding and processivity (Jacobs *et al*. 2006). Recently, it has been shown that the TEN domain is not required for synthesis of a single repeat *in vitro*, however, the repeat processivity requires the presence of TEN domain, even as a *trans*-acting factor (Robart and Kathleen Collins 2011). The extreme N-terminus of yeast telomerase is part of this TEN domain, but the first 20 amino acids can be deleted without completely abolishing telomerase activity *in vivo* (Xia *et al*. 2000). This mutation, *est2-ΔN20*, results in an immediate growth defect, unlike senescence-causing mutations that take 40-60 generations before growth defect is apparent (Xia *et al*. 2000).

Telomerase RNA

Telomerase RNA, in addition to providing the template for reverse transcription, has extended base pairing to form secondary structures that create binding sites for telomerase RT as well as other telomerase factors (Theimer and Feigon 2006). Through

these interactions, the telomerase RNA, especially in yeast, acts as a scaffold for the telomerase enzyme (Zappulla and Thomas R. Cech 2004).

Telomerase RNA contains a core telomerase RT binding domain that includes a single-stranded template region followed by a boundary element that demarcates the end of the template, and a pseudoknot structure that also includes a required triple RNA helix formation (J. Lin *et al*. 2004). This pseudoknot structure is conserved from *Tetrahymena* to human and is critical for binding to telomerase RT.

Both human and yeast telomerase RNAs contain structures specific for binding RNA processing proteins that are used for other small nuclear RNAs (D. Fu and Kathleen Collins 2007; Seto *et al*. 1999). In the case of yeast, there is an Sm-protein binding site near the 3' end, which is important for the stability and processing of telomerase RNA as discussed later. Dyskerin binding to human telomerase RNA is also important for the stability of telomerase RNA, and several mutations in dyskerin binding have been found in humans that cause telomere shortening and premature aging (J. R. Mitchell *et al*. 1999; Errington *et al*. 2008).

Yeast telomerase RNA (TLC1) also has binding sites for Est1, an essential telomerase factor *in vivo*, and the Ku complex (Stellwagen *et al*. 2003; J. Zhou *et al*. 2000; Seto *et al*. 2002). Homologs of Est1 and Ku exist in humans, but they do not seem to bind directly to human telomerase RNA (hTER). Both Est1 and Ku play prominent roles in the recruitment of telomerase to telomeres in yeast, suggesting that a different recruitment pathway exists in humans, although no telomerase recruitment factors have been identified in humans. In addition, in both humans and in yeast, Est1 can bind

TERT/Est2 independently of telomerase RNA (Bianchi *et al*. 2004; Redon *et al*. 2007). TLC1 is also about 3-fold longer than the hTER, which may have provided additional sites for recruitment factors to bind that are not seen in hTER (Theimer and Feigon 2006).

Crystal structure of red flour beetle telomerase reverse transcriptase

While many attempts have been made by various groups to crystalize telomerase enzyme, only one group has managed to produce a crystal structure of telomerase reverse transcriptase (A. J. Gillis *et al*. 2008). This feat was accomplished by studying the red flour beetle telomerase. This telomerase, however, is missing the N-terminal TEN domain conserved in yeast and humans. There are still interesting features of telomerase enzyme discovered in the study of the crystal structure. The reverse transcriptase domain is very similar to that of HIV-1 reverse transcriptase, as expected. The RNA-binding N-terminal domain (TRBD) and the C-terminal end of the RT domain have an extensive surface interaction that results in a ring-like structure, resulting in an equivalent of the "closed" or active conformation in HIV reverse transcriptase. The cavity created by this interaction is just big enough (~26 Å wide and 21 Å deep) to fit seven base-pairs of a double-stranded nucleic acid (RNA-DNA hybrid), which is consistent with the number of bases in the template region hybridized to DNA in yeast telomerase (Forstemann and Lingner 2005). A co-crystal structure of the protein and a RNA-DNA hybrid hairpin mimicking the template bound to the substrate indeed shows that the base-paired substrate is in the cavity with the 3' end of the DNA situated in the active site (M.

Mitchell *et al*. 2010). The "open" or inactive conformation seen in HIV transcriptase would require disruption of the interaction between the N- and C-terminal domains. If such conformation exists in telomerase, it would most likely require an external factor. It is also possible that such conformation may require the presence of the full-length telomerase RNA, which this crystal lacked. It is unclear at this point whether the loading of telomerase RNA or DNA substrate require the catalytic site to "open," which may act as an "activation" step.

Other telomerase proteins

Several other factors are required for telomerase activity and regulation *in vivo*. Est1, Est3, and Cdc13 (formerly named as Est4) are essential *in vivo* for telomerase activity, although these are dispensable for activity *in vitro* (Lingner *et al*. 1997).

One of the key roles of Est1 is the recruitment of telomerase to telomeres, via binding to TLC1 and Cdc13, which in turn binds to single-stranded telomeric DNA (Qi and Zakian 2000; Pennock *et al*. 2001; J. Zhou *et al*. 2000; Seto *et al*. 2002). Est1 also has an "activation" function for telomerase activity: The essential recruitment function of Est1 can be bypassed by fusing Cdc13 with Est2, but the presence of Est1 in this setting leads to much longer telomeres, suggesting that even a such telomere-tethered telomerase is much more active in presence of Est1 (Evans and Victoria Lundblad 1999). The nature of this "activation" step is not well understood, but Est1 has been shown to be capable of promoting G-quartet formation of telomeric substrates *in vitro* (Zhang *et al*. 2010). Although Est1 is not required for telomerase activity *in vitro*, addition of purified Est1

has been shown to increase telomerase activity (DeZwaan and Freeman 2009). This is not due to the recruitment function of Est1, as this role requires Cdc13, but it is not clear whether this is due to the G-quartet formation of the substrates. The non-recruitment function of Est1 will be investigated in Chapter 3.

Est3, whose main function still remains unclear, is thought to play a role in the processivity of telomerase. Est3 from the budding yeast *S. castellii* increases telomerase activity *in vitro* (Lee *et al*. 2010). Telomerase from *S. castellii*, unlike the telomerases of *S. cerevisiae* and *K. lactis*, has a highly processive, multiple-repeat addition mode of telomerase activity *in vitro* (Cohn and E H Blackburn 1995). It also has been suggested that Est3 protein has RNA-DNA helicase and GTPase activities (Y. S. Sharanov *et al*. 2006; Shubernetskaya *et al*. 2011). Est3 can bind to Est1 and Est2 independently *in vivo*, but its recruitment to telomeres is dependent on all three factors Est1, Est2, and TLC1 (Tuzon *et al*. 2011).

Cdc13 is a sequence-specific, single-stranded telomeric DNA binding protein (Nugent *et al*. 1996). Cdc13 forms a complex with Stn1 and Ten1, and this complex is thought to play a role equivalent to the RPA complex during DNA replication (Gao *et al*. 2007). Cdc13 physically interacts with Est1, and this interaction is essential for telomerase recruitment to telomeres (Qi and Zakian 2000; Pennock *et al*. 2001). The telomerase recruitment function of Cdc13 is not passive, but rather cell-cycle dependent phosphorylation of Cdc13 modulates its ability to recruit telomerase (S. Li *et al*. 2009).

The recruitment functions of Est1 and Cdc13, and protein-protein interactions among these essential telomerase factors, have been studied in detail, mainly through *in*

vivo experiments; however, the mechanisms by which these proteins promote and activate telomerase activity at telomeres are less well studied. We will attempt to probe some of these questions in Chapter 3.

Telomerase Dimerization

As described above, telomerase is minimally composed of its protein catalytic component and the telomerase RNA. Indeed, *in vitro*, these are the only two components that seem to be required for telomeric substrate extension by telomerase in a template RNA-dependent manner. Human, yeast, and *Tetrahymena* telomerases have all been inferred to be active as a monomer *in vitro* (Alves *et al*. 2008; Shcherbakova *et al*. 2009; Bryan *et al*. 2003). However, there are many reports of telomerase complex existing in a dimeric or potentially even oligomeric form -- in yeast, *Euplotes*, and human (John Prescott and Elizabeth H. Blackburn 1997; L. Wang *et al*. 2002; Beattie *et al*. 2001; Wenz *et al*. 2001). A recent report (unpublished) of a single-molecule electron microscopic structural determination of human telomerase indicated that this RNP telomerase (a complex of hTER plus hTERT) was a dimer held together by interactions involving the RNA portions of the RNP complex (D. Rhodes, personal communication). The main goal of this thesis at the outset of this work was to ascertain whether telomerase does indeed exist in dimeric form and if so, whether the dimeric form plays an important role in telomere maintenance.

Many biomolecules form dimers or higher oligomers. Prominent examples include the replicative DNA polymerase complex of eukaryotes and prokaryotes, in

which synthesis at leading and lagging strands are coordinated; DNA binding proteins that dimerize to increase specificity and to cooperatively bind DNA; DNA damage signaling protein, ATM, in which dimerization auto-inhibits its phosphorylation activity (Bakkenist and Kastan 2003). In addition, HIV-1 reverse transcriptase heterodimerizes; the HIV-1 RT is a close relative of the reverse transcriptase domain of the TERT subunit core component of telomerase. These are only a few of many such examples. These examples led us to postulate the following non-mutually exclusive models for the role of telomerase dimerization: 1. Telomerase dimer extends two telomeres simultaneously. Chromosomes are replicated before telomerase acts, and both the leading and lagging strands can be extended by the dimeric telomerase. 2. Telomerase dimer is required for processive replication of telomeres. Telomerase must disengage the DNA substrate after each round of copying the template, and this repeat processivity may be facilitated by two catalytic sites and/or two templates within a single dimeric complex of telomerase. 3. Telomerase oligomeric state may act as a switch or modulate its own activity. 4. Telomerase has non-catalytic function in dimeric form, such as capping of telomere ends.

In addition to the core telomerase components, Est3 and Cdc13 have been shown to dimerize (C.-P. Yang *et al*. 2006; Sun *et al*. 2011). Although the Est3 dimerization *in vitro* has been originally reported to be likely too weak for *in vivo* dimerization (C.-P. Yang *et al*. 2006), a recent study has shown that the K_d can be increased two orders of magnitude in the presence of magnesium ions (Malyavko *et al*. 2010). Whether these factors contribute to the dimerization of telomerase complex has not been studied.

HIV-1 reverse transcriptase heterodimer

The HIV-1 reverse transcriptase is the structurally closest known relative to the RT domain of telomerase, and is found as a heterodimer of p66 and p51 subunits; the p51 subunit is the proteolytically truncated version of p66 (di Marzo Veronese *et al*. 1986). The full-length p66 contains the RNase H and reverse transcriptase domains, and the RNase H domain is cleaved off to make p51. Hence, the HIV RT complex has three catalytic sites: one RNase H and two reverse transcriptase sites. However, many studies show that only the reverse transcriptase catalytic site on p66 is active (Lowe *et al*. 1988; N. Cheng *et al*. 1991; J. C. Wu *et al*. 1991). The HIV RT has two conformations, open and closed. Both p66 and p51 monomers have the closed form, and the formation of the open form of p66 requires its heterodimerization with p51, while the p66-associated p51 RT remains in the closed conformation (J Wang *et al*. 1994). Although the RT domains of HIV-1 RT and telomerase are very similar, telomerase is distinct in that it has no RNase H domain, and instead has the RNA binding domain important for binding telomerase RNA. As described above, this RNA binding domain interacts with the C-terminal domain to form a closed conformation of the RT, and the crystal structure of the red flour beetle TERT (with or without a small RNA-DNA duplex bound in the putative active site) shows no dimerization (M. Mitchell *et al*. 2010).

Yeast telomerase dimerization

The initial discovery and inference of potential telomerase dimerization came from a special template mutation in yeast telomerase RNA, TLC1. A 3-base GUG substitution

mutation was introduced at various sites within the 14-base template such that each such triplet mutation within the template resulted in a GTGCAC palindromic telomeric sequence being synthesized by telomerase. One such mutant, *tlc1-476gug*, had no detectable telomerase activity *in vitro* or *in vivo* (J Prescott and E H Blackburn 1997). This was unusual for a template mutation, which generally is simply copied or leads to misusage of the template, not inactivity.

More importantly, the inactive template in *tlc1-476gug* regained its ability to be copied by the telomerase when a wild-type TLC1 was co-expressed, showing that there is some type of a functional interaction between the mutant and the wild-type TLC1 (J Prescott and E H Blackburn 1997). In addition, an extension product made by telomerase using a biotinylated telomeric DNA primer substrate that can only be extended by a wild-type template was able to pull down an untagged telomerase reaction product that was extended specifically by the tlc1-476gug telomerase, suggesting that the wild-type and mutant templates of TLC1 RNAs are physically associated (John Prescott and Elizabeth H. Blackburn 1997).

No evidence of telomerase RT dimerization itself has been reported, although as described above, the recent report of electron microscopic single-particle structural determination results indicated a human telomerase dimer consisting of two telomerase RNP subunits, held together by the RNA. In personal communications, however, yeast two-hybrid and co-immunoprecipitation assays have been reported to give no positive indications for dimerization.

Human telomerase dimerization

Many studies have taken advantage of the *in vitro* transcription and translation systems, which can produce active human telomerase, to test for human telomerase dimerization. Several of studies have shown that N-terminal and C-terminal regions of the hTERT can interact, including a study in *Euplotes* (Beattie *et al*. 2001; Moriarty *et al*. 2002; Moriarty *et al*. 2004; Arai *et al*. 2002; L. Wang *et al*. 2002). These results were taken as evidence of telomerase dimerization; however, the telomerase complex formed in these *in vitro* systems may not be properly folded in a physiologically-relevant form. The crystal structure of red flour beetle clearly shows that the N-terminal and C-terminal domains interact to form a ring-like structure with a significant surface region of contacts (M. Mitchell *et al*. 2010). In addition, the TEN domain of the human reverse transcriptase, which is missing in the crystal structure, has been shown to be able to promote repeat addition processivity in *trans*, but much less effectively than in *cis* (Robart and Kathleen Collins 2011). These intramolecular interactions can facilitate intermolecular interactions when the proteins are not folded correctly. The same argument can be applied to studies in which full-length hTERT was tested (Armbruster *et al*. 2001; Wenz *et al*. 2001).

There are some published studies that are notable exceptions, in which telomerase was prepared from HeLa cells, several immortalized cell lines, and primary dermal fibroblast cultures (Wenz *et al*. 2001; Cohen *et al*. 2007; Errington *et al*. 2008). When the size of the recombinant telomerase made in insect cells and native telomerase complex purified from HeLa cells were compared in a gel filtration assay, they showed the same profile (Wenz *et al*. 2001). However, this study was only able to conclude that there are

two hTER molecules per complex, not necessarily two active sites. Cohen *et al*. were able to isolate telomerase complex to purity from several immortal cell lines in its enzymatically active form by a clever biochemical method, in which the relatively stable binding of telomerase to its telomeric substrate was utilized to specifically affinity-purify active telomerase complexes. The purified telomerase complex was analyzed by mass spectroscopy and size fractionation to show that active telomerase complexes contain two copies each of telomerase RT, telomerase RNA and dyskerin (Cohen *et al*. 2007). However, size fractionation of RNPs is often misleading due to their non-globular shapes, and it is not ruled out as a possibility that an unknown RNA species is part of the active telomerase complex, obfuscating the actual molecular weight. Lastly, human telomerase purified from a primary dermal fibroblast cultures showed no dimerization (Errington *et al*. 2008). One caveat in this study is that it is possible that in the fibroblast cultures, in which telomerase is normally not highly expressed, telomerase dimerization naturally does not occur, even though other cancer or stem cell populations may have factors present that allow human telomerase to dimerize.

In addition, there are studies that show RNA-RNA interaction between two hTERs (Tesmer *et al*. 1999; Ly *et al*. 2003). In particular, a conserved pseudoknot structure found in telomerase RNA from *Tetrahymena*, yeast, and human were found to be important for human telomerase RNA dimerization (J. Lin *et al*. 2004; Ly *et al*. 2003). Again, these studies suffer in part from the criticism that *in vitro* transcribed RNA may be aberrant *in vitro*, or RNAs forced to express from artificial promoters at higher than the normal regulated levels may have aberrant biogenesis pathways *in vivo*. Generally, large

RNAs require chaperons to fold properly, and for telomerase RNA, as big as it is, folding in the *in vitro* setting and correctly assembling with telomerase RT may be difficult to accomplish in commonly used methods for *in vitro* reconstitution assays. Hence, it is possible that partial or abnormal folding of the telomerase RNAs allows two reverse transcriptases to bind.

Telomerase dimerization in other organisms

The only evidence available for telomerase oligomerization in *Tetrahymena* shows that telomerase is active as a monomer (Bryan *et al*. 2003). As mentioned above, the N-terminal and C-terminal regions of *Euplotes* telomerase have been shown to interact (L. Wang *et al*. 2002). Finally, the crystal structure of the red flour beetle telomerase TERT protein subunit shows no dimerization (A. J. Gillis *et al*. 2008; M. Mitchell *et al*. 2010). However, as mentioned above, this structure is missing the conserved N-terminal TEN domain, which may be important for dimerization of telomerase, and is missing the full length RNA, which was inferred to hold the human telomerase RNP dimer together in the electron microscopic single particle structural determination (D. Rhodes, personal communication). For these reasons, and related to the more fundamental concern that crystal formation occurs under non-physiological conditions, we cannot rule out the possibility that telomerase is a dimer from this crystal structure.

In summary, there are numerous experiments showing results consistent with telomerase dimerization model, but all these experiments have alternative explanations that do not involve dimerization of telomerase. It is not yet clear whether telomerase

complex *in vivo* is dimeric, and more importantly, the functional role of such dimeric telomerase remains unidentified. The literature in telomerase oligomerization has several conflicts and caveats; however, there is strong evidence for: 1. Monomeric telomerase is active (Bryan *et al*. 2003; Alves *et al*. 2008) and 2. Two telomerase RNAs can functionally interact (John Prescott and Elizabeth H. Blackburn 1997; Wenz *et al*. 2001). The main challenge here is to verify the oligomeric state of telomerase and to ascertain the functional significance of interacting telomerase RNAs in monomeric or dimeric telomerase complex. Chapter 2 will mainly focus on the physical dimerization of yeast telomerase RNA, TLC1. In this Chapter, this dimerization is inferred from TLC1-TLC1 intermolecular interaction (direct or indirect) quantified in extracts of cells expressing normal amounts of telomerase RNA, from the endogenous *TLC1* chromosomal locus. In Chapter 3, we will attempt to find the basis for the functional interaction of the template region of *TLC1* in enzymatically active telomerase. We have increasing evidence for the importance of interacting telomerase RNAs during the steps taken to form an active telomerase complex. The following sections will discuss these relevant processes in telomerase biogenesis and the regulation of telomerase activity.

Telomerase Biogenesis

Inability to detect dimerization of telomerase in most cases may be due to its transient state, perhaps during the biogenesis of telomerase. While the fully active telomerase may be in a monomeric form, it is possible that telomerase is dimeric at one or more assembly steps potentially as a regulatory mechanism (*e.g*. auto-inhibition in dimeric form).

There have been several studies probing steps required for building a functional telomerase. While there is much known about the steps required for maturation of telomerase components, the exact order and locality of each step have remained elusive. The major hurdle in understanding these mechanisms and localizations has been the low expression level of telomerase components. There are only about 40-80 copies of each protein and RNA subunit of telomerase in budding yeast (Mozdy and Thomas R. Cech 2006), thereby often requiring these studies to use overexpression of components under study.

There are no reports of any modification or processing of telomerase reverse transcriptase protein in yeast. Telomerase lacks any known RNase H domain. It is worth noting that in the HIV-1 viral reverse transcriptase dimer, the RNase H domain in one copy is cleaved off. Also, in human cells, there are several potential internally and N-terminally truncated telomerase RT species resulting from various alternative-splicing events and phosphorylation of hTERT protein has also been reported (Ulaner *et al*. 1998; Saeboe-Larssen *et al*. 2006; J. T. Chang *et al*. 2006).

Telomerase RNA biogenesis

In contrast to the protein subunit, however, several steps in budding yeast telomerase RNA biogenesis have been identified. Briefly, *TLC1* is transcribed by RNA polymerase II, polyadenylated, and hypermethylated at the 5' end to produce a tri-methyl G cap, and the 3' end region including the polyadenine tract is cleaved off to form the "mature" *TLC1* RNA. TLC1 is also shown to be shuttled between the cytoplasm and the nucleus.

The polyadenylation sites of RNA Polymerase II transcript *TLC1* are identified (Chapon *et al*. 1997). The "mature," shorter, polyA- form comprises the majority of the steady-state level of TLC1 in the cell (Chapon *et al*. 1997; Mozdy and Thomas R. Cech 2006). It likely derives from a longer polyA+ precursor. The enzyme responsible for the cleavage at the 3' end of TLC1 to produce the mature TLC1 has not been identified, though it has been shown that Rnt1, responsible for maturation of many non-coding RNAs, is not required for this step (Larose *et al*. 2007; MacRae and Doudna 2007). In asynchronous wild-type yeast cultures, only ~4-8% of TLC1 are in the polyA+ form (Mozdy and Thomas R. Cech 2006). The fraction that is polyA+ becomes much higher when TLC1 is overexpressed, indicating that TLC1 cleavage machinery may be limiting and that it is consistent with a precursor-product relationship between the longer, polyA+ form and the shorter, mature form of TLC1 (Mozdy and Thomas R. Cech 2006). This cleavage also seems to be only efficient during G1 phase of cell cycle, as cells arrested in S or G2/M phase show accumulation of the polyA+ form (Chapon *et al*. 1997).

There is an Sm-protein binding site near the cleavage site at the 3' end (Seto *et al*. 1999). Sm proteins form a seven-member protein complex that wraps around an RNA strand in a ring, and they are best known for their roles in processing spliceosomal RNAs. When the Sm site is mutated on *TLC1* (*tlc1-Sm*$^-$), the steady-state level of TLC1 is significantly reduced, and no polyA- form is detectable (Seto *et al*. 1999). However, the cells expressing tlc1-Sm$^-$ do not senesce, unlike deletion of *TLC1*, though telomeres are much shorter in these cells (Seto *et al*. 1999). This indicates that 3' processing of TLC1 is not essential for telomerase activity but is required for the full stable steady-state level.

In addition, TLC1 associated with telomerase is hypermethylated (trimethyl-G or TMG) at the 5' end (Franke *et al*. 2008); this TMG cap is shown to be put on by Tgs1 (Franke *et al*. 2008). In cells lacking Tgs1, TLC1 is not hypermethylated and accumulates in the nucleolus (Gallardo *et al*. 2008). Whether this is due to TMG requirement for export or assembly with telomerase is unclear. Hypermethylation of TLC1 is also not required for telomerase activity, as telomeres are slightly longer than the wild-type in length in *tgs1Δ* cells (Franke *et al*. 2008).

While several studies have shown via heterokaryon assays that TLC1 is exported out of and reimported into the nucleus, the importance of shuttling between the nucleus and cytoplasm is unclear (Ferrezuelo *et al*. 2002; Teixeira *et al*. 2002). Normally, TLC1 is mostly found in the nucleus. When other telomerase holoenzyme components are missing (in *est1Δ*, *est2Δ* or *est3Δ* strains), TLC1 is distributed both in the nucleus and cytoplasm (Gallardo *et al*. 2008). Overexpression of Est1 and Est2 can rescue the mis-localization of TLC1 in *est2Δ* and *est1Δ* cells, respectively. This suggests that either TLC1 forms a complex with Est1, Est2 and Est3 in the cytoplasm and that this step is important for reimport; or that TLC1 retention in the nucleus requires TLC1 association with Est1, Est2, and Est3. The same phenomenon is observed when the Ku complex is deleted (Gallardo *et al*. 2008). It is possible that the Ku complex is also required for the nuclear retention of TLC1 rather than for reimport.

In addition to the deletion of factors that are directly bound to TLC1, the loss of Tel1 and the MRX complex, which are required for the preferential recruitment of telomerase to the shortest telomeres, leads to TLC1 leaving the nucleus, albeit to a lesser

degree than the loss of Est1, Est2, or Est3 (Gallardo *et al*. 2008). Tel1 and the MRX complex are thought to direct the telomerase complex to telomeres indirectly (*i.e*. not via direct physical interaction), which suggests that the TLC1 retention in the nucleus is an active mechanism that Tel1 and the MRX complex control, rather than a passive sequestration mechanism.

Mtr10 is a karyopherin/importin, required for import various complexes, including snRNAs and tRNAs (Murthi *et al*. 2010). The deletion of *MTR10* results in very short telomeres (Ferrezuelo *et al*. 2002). While there is no evidence that TLC1 is directly bound to Mtr10, TLC1 localization distributes throughout the cell, and the steady-state level of TLC1 is substantially reduced in *mtr10*$^{-}$ strains (Ferrezuelo *et al*. 2002). In addition, 3' processing of TLC1 is abrogated, leaving all of TLC1 in the polyA+ form. The phenotype of *mtr10Δ* is very similar to that of *tlc1-Sm*$^{-}$ (Sm-protein binding site mutation). However, all other Sm protein dependent snRNAs are at normal levels, suggesting the defect may be specific to TLC1 (Ferrezuelo *et al*. 2002).

In Chapter 2, we show that TLC1 dimerization is one of the steps during the TLC1 biogenesis.

Telomerase holoenzyme assembly

It is unclear, both in humans and in yeast, when and where the meeting of telomerase RT and telomerase RNA occurs. Over-expression of telomerase RT (Est2) and Est1 both result in their accumulation in the nucleolus when they are tagged with GFP; overexpression of TLC1, however, forces nucleolar foci of Est1- and Est2-GFP to diffuse

throughout the nucleus (Teixeira *et al*. 2002). This suggests perhaps the protein components remain in the nucleolus until telomerase holoenzyme is assembled there. However, because of the overexpression condition, this may be due to nonspecific consequence of overloading telomerase assembly pathway.

Similarly in human cells, telomerase RT and telomerase RNA are observed to colocalized in the Cajal body, a region concentrated with ribosomal RNAs (Zhu *et al*. 2004; Tomlinson *et al*. 2008). The colocalization of hTR and the Cajal body requires hTERT and is not observed in telomerase-negative cells; ectopic expression of hTERT can induce hTR localization at Cajal body (Zhu *et al*. 2004). The hTERT and hTR localizations are both cell cycle regulated (Tomlinson *et al*. 2006). During the G1/G2 phase, hTERT is found in the nucleolus, as it is in yeast. In the early S-phase, both hTERT and hTR colocalize in the Cajal body, though whether they are fully assembled at this point is unclear. During the mid- to late-S phase, hTERT, hTR, as well as Cajal body colocalize with telomeres (Tomlinson *et al*. 2006). The telomerase holoenzyme is presumably assembled, as this is when telomerase is active.

In both human and yeast cells, PinX1, a nucleolar protein, has been shown to bind telomerase RT (X. Z. Zhou and K. P. Lu 2001; J. Lin and Elizabeth H. Blackburn 2004). Deletion of segments of the *EST2* gene indicated that PinX1 binds to the telomerase RT in the same region that is required for telomerase RNA binding to the telomerase RT. Indeed, pull-down assays showed that TLC1 and PinX1 were in separate complexes and that a given telomerase RT molecule is not associated with PinX1 and telomerase RNA simultaneously (J. Lin and Elizabeth H. Blackburn 2004). The accumulation of

overexpressed Est2 in the nucleolus may therefore be explained by this PinX1 interaction.

In Chapter 2, we show that the telomerase holoenzyme assembly is not an absolutely necessary step for TLC1 dimerization.

Regulation of Telomerase Activity

Dimerization of telomerase might hypothetically act as a switch in regulation of telomerase activity. Any number of factors controlling telomerase activity may be facilitating dimerization or disruption of dimerization. Therefore, telomerase activity regulators make good candidates for factors important in controlling the oligomeric state of telomerase.

Telomerase acts at telomeres, or at the ends of chromosomes. Sometimes, however, a double strand break can mimic ends of chromosomes. Addition of telomeres at these breaks is deleterious as it results in a chromosomal fragment without a centromere. Through various regulatory mechanisms distinguishing double-strand break from natural telomeres, including Pif1 helicase (Schulz and Zakian 1994; Makovets and Elizabeth H. Blackburn 2009), telomerase recruitment and activity are inhibited at double strand breaks.

Cell cycle-dependent regulation of telomerase

While levels of Est2 and TLC1 remain similar throughout the cell cycle, Est1, an essential cofactor, is tightly cell cycle regulated at both the mRNA and protein levels.

Rnt1, an RNA nuclease, controls the amount of *EST1* mRNA (Larose *et al*. 2007). The Est1 protein level is also regulated proteolytically (Osterhage *et al*. 2006). These processes lead to the presence of Est1 at telomeres specifically at the late S and G2/M phase (Taggart *et al*. 2002). This coincides with, and may create, the window of opportunity in which telomerase can act at telomeres.

Additionally, Est2 association with telomeres is cell cycle-regulated (Chan *et al*. 2008). During the G1 phase of the cell cycle, Est2 is physically recruited to telomeres in a manner that requires TLC1-Ku interaction, while Est1-TLC1 interaction is required for Est2 to be physically recruited to telomeres during the late S and G2/M phases (Taggart *et al*. 2002; Fisher *et al*. 2004). While these experiments show the TLC1 requirement for Est2 localization to telomeres, it remains to be tested whether TLC1 can localize to telomeres in the absence of Est2.

Est1's role in telomerase activation does not seem to be limited to recruitment. When Est2 is fused to Cdc13, Est1 becomes dispensable for recruitment of telomerase to telomeres (Evans and Victoria Lundblad 1999). However, when Est1 is expressed in cells expressing Cdc13-Est2 fusion, the telomere lengths are significantly longer than when Est1 is not expressed (Evans and Victoria Lundblad 1999). Additionally, *in vitro*, Est1 promotes the G-quartet formation of telomeric substrates, which in turn allow more efficient extension by telomerase (Zhang *et al*. 2010). These attributes are defined as Est1's activation function, and mutations in *EST1* specifically affecting either recruitment or activation as defined by these assays have been reported (Evans and Victoria Lundblad 2002). One of these activation mutants was also shown to be lacking in the ability to

promote processivity that was seen with wild-type Est1 in *in vitro* telomerase activity assays (DeZwaan and Freeman 2009).

Telomerase activity and telomere length regulation

In yeast, it is estimated that telomerase only acts on ~10% of telomeres in any one cell cycle (~3-4 telomeres per haploid cell; Teixeira *et al*. 2004). At telomeres shorter than 100 bp, the length and the frequency of telomerase-dependent telomere extension are significantly more than at longer telomeres (Teixeira *et al*. 2004). This increased telomerase activity at short telomeres is largely attributed to the increase in the processivity of telomerase; telomerase has been shown to be not processive *in vivo* at telomeres greater than 100 bp *in vitro* (M. Chang *et al*. 2007; John Prescott and Elizabeth H. Blackburn 1997). This is intriguing as it suggests that there may be two distinct forms of telomerase *in vivo*: processive and non-processive. This raises the possibility that the distinction could be the oligomeric/dimeric state of telomerase. In addition, telomerase is recruited to shorter telomeres preferentially (Sabourin *et al*. 2007). This is dependent on Tel1, a signaling protein kinase that promotes telomerase-dependent telomere length maintenance, and Rif1 and Rif2, negative regulators of telomere length that interact with the telomeric DNA binding protein Rap1 (Sabourin *et al*. 2007). The mechanisms by which these proteins direct telomerase preferentially to short telomeres are still unknown.

Whether or not the increased extension of telomeres at shorter telomeres is due mechanistically to an increase in processivity in the classic sense or simply to more frequent events of telomerase visiting shorter telomeres, Est1 and Est3 have each been

suggested as the relevant processivity factor. It is possible that Est1, Est3, or both are involved in the regulation of telomerase dimerization, which in turn can regulate the processivity of telomerase.

Overview of the Work Described in This Thesis

The main goal of the work described here is to explore the telomerase dimerization model and to identify the functional significance of telomerase dimerization. The initial attempts at examining the Est2-Est2 interactions are omitted, as we found no positive evidence for this interaction; in hindsight, the lack of positive interaction is consistent with the model we propose in Chapter 2.

In Chapter 2, we show evidence for physical dimerization of TLC1. We found two classes of TLC1 dimers and two modes by which TLC1 can dimerize. One class of TLC1 dimer was sensitive to protease treatment, and another (possibly overlapping) class was sensitive to high concentration of anti-sense oligonucleotides. The Ku complex association with TLC1, as well as the silent information regulator protein Sir4, but not the classic silencing via heterochromatin formation, is critical in one of the modes of TLC1 dimerization. The other mode requires the 3' region of TLC1 that is cleaved off in the mature version of TLC1. Surprisingly, TLC1 dimerization was not substantially affected by the essential telomerase components, although some partial dependence was quantifiable. We also show that Est2-Est2 interaction is not stable enough *in vitro* to be observed by the methods applied in this work.

In Chapter 3, we explore the functional interaction of *TLC1* templates. While this study uses a particularly specialized mutation, *tlc1-476gug*, it allowed us to uncover important functions of Est1 and Est3 in "activation" of telomerase activity. This activation model proposes that the physical dimerization of TLC1, shown in Chapter 2, creates a physical obstacle for telomerase activity and may act as a regulatory step. We will also attempt to resolve the disparity in the assessment of the oligomerization state of telomerase from these experimental setups.

Finally in Chapter 4, we will summarize the findings in Chapter 2 and Chapter 3 to form a cohesive picture of the nature of telomerase oligomerization. Furthermore, we will attempt to reconcile the differences and controversies, as well as consistencies, of our findings with the previously proposed models. Implications for the model we propose and the future directions will be discussed.

References

Alves, D., Li, H., Codrington, R., Orte, A., Ren, X., Klenerman, D. and Balasubramanian, S., 2008. Single-molecule analysis of human telomerase monomer. *Nat Chem Biol*, 4(5), pp.287-289.

Arai, K., Masutomi, K., Khurts, S., Kaneko, S., Kobayashi, K. and Murakami, S., 2002. Two Independent Regions of Human Telomerase Reverse Transcriptase Are Important for Its Oligomerization and Telomerase Activity. *Journal of Biological Chemistry*, 277(10), pp.8538 -8544.

Armbruster, B.N., Banik, S.S.R., Guo, C., Smith, A.C. and Counter, C.M., 2001. N-Terminal Domains of the Human Telomerase Catalytic Subunit Required for Enzyme Activity *in vivo*. *Mol. Cell. Biol.*, 21(22), pp.7775-7786.

Autexier, C. and Lue, Neal F., 2006. The Structure and Function of Telomerase Reverse Transcriptase. *Annual Review of Biochemistry*, 75(1), pp.493-517.

Bakkenist, C.J. and Kastan, M.B., 2003. DNA damage activates ATM through intermolecular autophosphorylation and dimer dissociation. *Nature*, 421(6922), pp.499-506.

Beattie, T.L., Zhou, W., Robinson, M.O. and Harrington, L., 2001. Functional Multimerization of the Human Telomerase Reverse Transcriptase. *Mol. Cell. Biol.*, 21(18), pp.6151-6160.

Bianchi, A., Negrini, S. and Shore, D., 2004. Delivery of Yeast Telomerase to a DNA Break Depends on the Recruitment Functions of Cdc13 and Est1. *Molecular Cell*, 16(1), pp.139-146.

Bosoy, D. and Lue, Neal F., 2001. Functional Analysis of Conserved Residues in the Putative "Finger" Domain of Telomerase Reverse Transcriptase. *Journal of Biological Chemistry*, 276(49), pp.46305 -46312.

Bryan, T.M., Goodrich, K.J. and Cech, Thomas R., 2003. Tetrahymena Telomerase Is Active as a Monomer. *Molecular Biology of the Cell*, 14(12), pp.4794-4804.

Chan, A., Boulé, J.-B. and Zakian, V.A., 2008. Two Pathways Recruit Telomerase to Saccharomyces cerevisiae Telomeres. *PLoS Genet*, 4(10), p.e1000236.

Chang, J.T., Lu, Y.-C., Chen, Y.-J., Tseng, C.-P., Chen, Y.-L., Fang, C.-W. and Cheng, A.-J., 2006. hTERT phosphorylation by PKC is essential for telomerase holoprotein integrity and enzyme activity in head neck cancer cells. *Br J Cancer*, 94(6), pp.870-878.

Chang, M., Arneric, M. and Lingner, J., 2007. Telomerase repeat addition processivity is increased at critically short telomeres in a Tel1-dependent manner in Saccharomyces cerevisiae. *Genes & Development*, 21(19), pp.2485 -2494.

Chapon, C., Cech, T R and Zaug, A J, 1997. Polyadenylation of telomerase RNA in budding yeast. *RNA (New York, N.Y.)*, 3(11), pp.1337-1351.

Cheng, N., Painter, G.R. and Furman, P.A., 1991. Crosslinking of substrates occurs exclusively to the p66 subunit of heterodimeric HIV-1 reverse transcriptase. *Biochemical and Biophysical Research Communications*, 174(2), pp.785-789.

Cohen, S.B., Graham, M.E., Lovrecz, G.O., Bache, N., Robinson, P.J. and Reddel, R.R., 2007. Protein Composition of Catalytically Active Human Telomerase from Immortal Cells. *Science*, 315(5820), pp.1850-1853.

Cohn, M. and Blackburn, E H, 1995. Telomerase in yeast. *Science (New York, N.Y.)*, 269(5222), pp.396-400.

DeZwaan, D.C. and Freeman, B.C., 2009. The conserved Est1 protein stimulates telomerase DNA extension activity. *Proceedings of the National Academy of Sciences*, 106(41), pp.17337 -17342.

Errington, T.M., Fu, D., Wong, J.M.Y. and Collins, Kathleen, 2008. Disease-Associated Human Telomerase RNA Variants Show Loss of Function for Telomere Synthesis without Dominant-Negative Interference. *Mol. Cell. Biol.*, 28(20), pp.6510-6520.

Evans, S.K. and Lundblad, Victoria, 1999. Est1 and Cdc13 as Comediators of Telomerase Access. *Science*, 286(5437), pp.117 -120.

Evans, S.K. and Lundblad, Victoria, 2002. The Est1 Subunit of Saccharomyces cerevisiae Telomerase Makes Multiple Contributions to Telomere Length Maintenance. *Genetics*, 162(3), pp.1101 -1115.

Ferrezuelo, F., Steiner, B., Aldea, M. and Futcher, B., 2002. Biogenesis of yeast telomerase depends on the importin mtr10. *Molecular and Cellular Biology*, 22(17), pp.6046-6055.

Feuerhahn, S., Iglesias, N., Panza, A., Porro, A. and Lingner, J., 2010. TERRA biogenesis, turnover and implications for function. *FEBS Letters*, 584(17), pp.3812-3818.

Fisher, T.S., Taggart, A.K.P. and Zakian, V.A., 2004. Cell cycle-dependent regulation of yeast telomerase by Ku. *Nat Struct Mol Biol*, 11(12), pp.1198-1205.

Forstemann, K. and Lingner, J., 2005. Telomerase limits the extent of base pairing between template RNA and telomeric DNA. *EMBO Rep*, 6(4), pp.361-366.

Franke, J., Gehlen, J. and Ehrenhofer-Murray, A.E., 2008. Hypermethylation of yeast telomerase RNA by the snRNA and snoRNA methyltransferase Tgs1. *Journal of Cell Science*, 121(21), pp.3553 -3560.

Fu, D. and Collins, Kathleen, 2007. Purification of human telomerase complexes identifies factors involved in telomerase biogenesis and telomere length regulation. *Molecular Cell*, 28(5), pp.773-785.

Fulton, T.B. and Blackburn, Elizabeth H., 1998. Identification of Kluyveromyces lactis Telomerase: Discontinuous Synthesis along the 30-Nucleotide-Long Templating Domain. *Mol. Cell. Biol.*, 18(9), pp.4961-4970.

Gallardo, F., Olivier, C., Dandjinou, A.T., Wellinger, R.J. and Chartrand, P., 2008. TLC1 RNA nucleo-cytoplasmic trafficking links telomerase biogenesis to its recruitment to telomeres. *EMBO J*, 27(5), pp.748-757.

Gao, H., Cervantes, R.B., Mandell, E.K., Otero, J.H. and Lundblad, Victoria, 2007. RPA-like proteins mediate yeast telomere function. *Nat Struct Mol Biol*, 14(3), pp.208-214.

Gillis, A.J., Schuller, A.P. and Skordalakes, E., 2008. Structure of the Tribolium castaneum telomerase catalytic subunit TERT. *Nature*, 455(7213), pp.633-637.

Greider, C W and Blackburn, E H, 1989. A telomeric sequence in the RNA of Tetrahymena telomerase required for telomere repeat synthesis. *Nature*, 337(6205), pp.331-337.

Greider, Carol W. and Blackburn, Elizabeth H., 1985. Identification of a specific telomere terminal transferase activity in tetrahymena extracts. *Cell*, 43(2, Part 1), pp.405-413.

Jacobs, S.A., Podell, E.R. and Cech, Thomas R, 2006. Crystal structure of the essential N-terminal domain of telomerase reverse transcriptase. *Nature Structural & Molecular Biology*, 13(3), pp.218-225.

Jain, D. and Cooper, J.P., 2010. Telomeric strategies: means to an end. *Annual Review of Genetics*, 44, pp.243-269.

Kelleher, C., Teixeira, M.T., Förstemann, K. and Lingner, J., 2002. Telomerase: biochemical considerations for enzyme and substrate. *Trends in Biochemical Sciences*, 27(11), pp.572-579.

de Lange, T., Lundblad, Vicki and Blackburn, E., 2006. *Telomeres, Second Edition* 2nd ed., Cold Spring Harbor Laboratory Press.

Larose, S., Laterreur, N., Ghazal, G., Gagnon, J., Wellinger, R.J. and Elela, S.A., 2007. RNase III-dependent Regulation of Yeast Telomerase. *Journal of Biological Chemistry*, 282(7), pp.4373 -4381.

Lee, J., Mandell, E.K., Rao, T., Wuttke, D.S. and Lundblad, Victoria, 2010. Investigating the role of the Est3 protein in yeast telomere replication. *Nucleic Acids Research*, 38(7), pp.2279 -2290.

Li, S., Makovets, S., Matsuguchi, T., Blethrow, J.D., Shokat, K.M. and Blackburn, Elizabeth H., 2009. Cdk1-Dependent Phosphorylation of Cdc13 Coordinates Telomere Elongation during Cell-Cycle Progression. *Cell*, 136(1), pp.50-61.

Lin, J. and Blackburn, Elizabeth H., 2004. Nucleolar protein PinX1p regulates telomerase by sequestering its protein catalytic subunit in an inactive complex lacking telomerase RNA. *Genes & Development*, 18(4), pp.387 -396.

Lin, J., Ly, H., Hussain, A., Abraham, M., Pearl, S., Tzfati, Y., Parslow, T.G. and Blackburn, Elizabeth H, 2004. A universal telomerase RNA core structure includes structured motifs required for binding the telomerase reverse transcriptase protein. *Proceedings of the National Academy of Sciences of the United States of America*, 101(41), pp.14713-14718.

Lingner, J., Cech, Thomas R., Hughes, Timothy R. and Lundblad, Victoria, 1997. Three Ever Shorter Telomere (EST) genes are dispensable for *in vitro* yeast telomerase activity. *Proceedings of the National Academy of Sciences*, 94(21), pp.11190 -11195.

Lowe, D.M., Aitken, A., Bradley, C., Darby, G.K., Larder, B.A., Powell, K.L., Purifoy, D.J., Tisdale, M. and Stammers, D.K., 1988. HIV-1 reverse transcriptase:

crystallization and analysis of domain structure by limited proteolysis. *Biochemistry*, 27(25), pp.8884-8889.

Ly, H., Xu, L., Rivera, M.A., Parslow, T.G. and Blackburn, Elizabeth H., 2003. A role for a novel "trans-pseudoknot" RNA–RNA interaction in the functional dimerization of human telomerase. *Genes & Development*, 17(9), pp.1078 -1083.

MacRae, I.J. and Doudna, J.A., 2007. Ribonuclease revisited: structural insights into ribonuclease III family enzymes. *Current Opinion in Structural Biology*, 17(1), pp.138-145.

Makovets, S. and Blackburn, Elizabeth H., 2009. DNA damage signalling prevents deleterious telomere addition at DNA breaks. *Nat Cell Biol*, 11(11), pp.1383-1386.

Malyavko, A.G., Logvina, N.A., Zvereva, M.E. and Dontsova, O.A., 2010. *In vitro* dimerization of telomerase protein Est3p is stimulated by magnesium cations. *Doklady Biochemistry and Biophysics*, 433(1), pp.152-154.

di Marzo Veronese, F., Copeland, T.D., DeVico, A.L., Rahman, R., Oroszlan, S., Gallo, R.C. and Sarngadharan, M.G., 1986. Characterization of highly immunogenic p66/p51 as the reverse transcriptase of HTLV-III/LAV. *Science (New York, N.Y.)*, 231(4743), pp.1289-1291.

McClintock, B., 1931. *Cytological observations of deficiencies involving known genes, translocations and an inversion in Zea mays*, Columbia Mo.: University of Missouri College of Agriculture Agricultural Experiment Station.

Mitchell, J.R., Wood, E. and Collins, K, 1999. A telomerase component is defective in the human disease dyskeratosis congenita. *Nature*, 402(6761), pp.551-555.

Mitchell, M., Gillis, A., Futahashi, M., Fujiwara, H. and Skordalakes, E., 2010. Structural basis for telomerase catalytic subunit TERT binding to RNA template and telomeric DNA. *Nat Struct Mol Biol*, 17(4), pp.513-518.

Moriarty, T.J., Huard, S., Dupuis, S. and Autexier, C., 2002. Functional Multimerization of Human Telomerase Requires an RNA Interaction Domain in the N Terminus of the Catalytic Subunit. *Mol. Cell. Biol.*, 22(4), pp.1253-1265.

Moriarty, T.J., Marie-Egyptienne, D.T. and Autexier, C., 2004. Functional Organization of Repeat Addition Processivity and DNA Synthesis Determinants in the Human Telomerase Multimer. *Mol. Cell. Biol.*, 24(9), pp.3720-3733.

Mozdy, A.D. and Cech, Thomas R., 2006. Low abundance of telomerase in yeast: Implications for telomerase haploinsufficiency. *RNA*, 12(9), pp.1721 -1737.

Muller, H., 1938. The remaking of chromosomes. *The Collecting Net*, (8), pp.182-195.

Murthi, A., Shaheen, H.H., Huang, H.-Y., Preston, M.A., Lai, T.-P., Phizicky, E.M. and Hopper, A.K., 2010. Regulation of tRNA Bidirectional Nuclear-Cytoplasmic Trafficking in Saccharomyces cerevisiae. *Mol. Biol. Cell*, 21(4), pp.639-649.

Nugent, C.I., Hughes, T R, Lue, N F and Lundblad, V, 1996. Cdc13p: a single-strand telomeric DNA-binding protein with a dual role in yeast telomere maintenance. *Science (New York, N.Y.)*, 274(5285), pp.249-252.

Ogawa, T. and Okazaki, T., 1980. Discontinuous DNA Replication. *Annual Review of Biochemistry*, 49(1), pp.421-457.

Osterhage, J.L., Talley, J.M. and Friedman, K.L., 2006. Proteasome-dependent degradation of Est1p regulates the cell cycle-restricted assembly of telomerase in Saccharomyces cerevisiae. *Nat Struct Mol Biol*, 13(8), pp.720-728.

Peng, Y., Mian, I.S. and Lue, Neal F, 2001. Analysis of Telomerase Processivity: Mechanistic Similarity to HIV-1 Reverse Transcriptase and Role in Telomere Maintenance. *Molecular Cell*, 7(6), pp.1201-1211.

Pennock, E., Buckley, K. and Lundblad, Victoria, 2001. Cdc13 Delivers Separate Complexes to the Telomere for End Protection and Replication. *Cell*, 104(3), pp.387-396.

Prescott, J and Blackburn, E H, 1997. Telomerase RNA mutations in Saccharomyces cerevisiae alter telomerase action and reveal nonprocessivity *in vivo* and *in vitro*. *Genes & Development*, 11(4), pp.528 -540.

Prescott, John and Blackburn, Elizabeth H., 1997. Functionally interacting telomerase RNAs in the yeast telomerase complex. *Genes & Development*, 11(21), pp.2790 - 2800.

Qi, H. and Zakian, V.A., 2000. The Saccharomyces telomere-binding protein Cdc13p interacts with both the catalytic subunit of DNA polymerase α and the telomerase-associated Est1 protein. *Genes & Development*, 14(14), pp.1777 - 1788.

Redon, S., Reichenbach, P. and Lingner, J., 2007. Protein–RNA and protein–protein interactions mediate association of human EST1A/SMG6 with telomerase. *Nucleic Acids Research*, 35(20), pp.7011 -7022.

Robart, A.R. and Collins, Kathleen, 2011. Human Telomerase Domain Interactions Capture DNA for TEN Domain-Dependent Processive Elongation. *Molecular Cell*, 42(3), pp.308-318.

Sabourin, M., Tuzon, C.T. and Zakian, V.A., 2007. Telomerase and Tel1p preferentially associate with short telomeres in S. cerevisiae. *Molecular Cell*, 27(4), pp.550-561.

Saeboe-Larssen, S., Fossberg, E. and Gaudernack, G., 2006. Characterization of novel alternative splicing sites in human telomerase reverse transcriptase (hTERT): analysis of expression and mutual correlation in mRNA isoforms from normal and tumour tissues. *BMC Molecular Biology*, 7(1), p.26.

Schulz, V.P. and Zakian, V.A., 1994. The saccharomyces PIF1 DNA helicase inhibits telomere elongation and de novo telomere formation. *Cell*, 76(1), pp.145-155.

Seto, A.G., Livengood, A.J., Tzfati, Y., Blackburn, Elizabeth H. and Cech, Thomas R., 2002. A bulged stem tethers Est1p to telomerase RNA in budding yeast. *Genes & Development*, 16(21), pp.2800 -2812.

Seto, A.G., Zaug, Arthur J., Sobel, S.G., Wolin, S.L. and Cech, Thomas R., 1999. Saccharomyces cerevisiae telomerase is an Sm small nuclear ribonucleoprotein particle. *Nature*, 401(6749), pp.177-180.

Sharanov, Y.S., Zvereva, M.I. and Dontsova, O.A., 2006. Saccharomyces cerevisiae telomerase subunit Est3p binds DNA and RNA and stimulates unwinding of RNA/DNA heteroduplexes. *FEBS Letters*, 580(19), pp.4683-4690.

Shcherbakova, D.M., Sokolov, K.A., Zvereva, M.I. and Dontsova, O.A., 2009. Telomerase from yeast Saccharomyces cerevisiae is active *in vitro* as a monomer. *Biochemistry (Moscow)*, 74(7), pp.749-755.

Shubernetskaya, O., Logvina, N., Sharanov, Y. and Zvereva, M., 2011. Yeast telomerase protein Est3 is a novel type of GTPase. *Biochimie*, 93(2), pp.202-206.

Stellwagen, A.E., Haimberger, Z.W., Veatch, J.R. and Gottschling, D.E., 2003. Ku interacts with telomerase RNA to promote telomere addition at native and broken chromosome ends. *Genes & Development*, 17(19), pp.2384 -2395.

Sun, J., Yang, Y., Wan, K., Mao, N., Yu, T.-Y., Lin, Y.-C., DeZwaan, D.C., Freeman, B.C., Lin, J.-J., Lue, Neal F and Lei, M., 2011. Structural bases of dimerization of yeast telomere protein Cdc13 and its interaction with the catalytic subunit of DNA polymerase [alpha]. *Cell Res*, 21(2), pp.258-274.

Taggart, A.K.P., Teng, S.-C. and Zakian, V.A., 2002. Est1p As a Cell Cycle-Regulated Activator of Telomere-Bound Telomerase. *Science*, 297(5583), pp.1023 -1026.

Teixeira, M.T., Forstemann, K., Gasser, S.M. and Lingner, J., 2002. Intracellular trafficking of yeast telomerase components. *EMBO Reports*, 3(7), pp.652-659.

Teixeira, M.T., Arneric, M., Sperisen, P. and Lingner, J., 2004. Telomere Length Homeostasis Is Achieved via a Switch between Telomerase- Extendible and -Nonextendible States. *Cell*, 117(3), pp.323-335.

Tesmer, V.M., Ford, L.P., Holt, S.E., Frank, B.C., Yi, X., Aisner, D.L., Ouellette, M., Shay, J.W. and Wright, W.E., 1999. Two Inactive Fragments of the Integral RNA

Cooperate To Assemble Active Telomerase with the Human Protein Catalytic Subunit (hTERT) *In vitro*. *Mol*. *Cell*. *Biol*., 19(9), pp.6207-6216.

Theimer, C.A. and Feigon, J., 2006. Structure and function of telomerase RNA. *Current Opinion in Structural Biology*, 16(3), pp.307-318.

Tomlinson, R.L., Abreu, E.B., Ziegler, T., Ly, H., Counter, C.M., Terns, R.M. and Terns, M.P., 2008. Telomerase Reverse Transcriptase Is Required for the Localization of Telomerase RNA to Cajal Bodies and Telomeres in Human Cancer Cells. *Mol*. *Biol*. *Cell*, 19(9), pp.3793-3800.

Tomlinson, R.L., Ziegler, T.D., Supakorndej, T., Terns, R.M. and Terns, M.P., 2006. Cell Cycle-regulated Trafficking of Human Telomerase to Telomeres. *Mol*. *Biol*. *Cell*, 17(2), pp.955-965.

Tuzon, C.T., Wu, Y., Chan, A. and Zakian, V.A., 2011. The Saccharomyces cerevisiae Telomerase Subunit Est3 Binds Telomeres in a Cell Cycle– and Est1–Dependent Manner and Interacts Directly with Est1 *In vitro*. *PLoS Genet*, 7(5), p.e1002060.

Ulaner, G.A., Hu, J.F., Vu, T.H., Giudice, L.C. and Hoffman, A.R., 1998. Telomerase activity in human development is regulated by human telomerase reverse transcriptase (hTERT) transcription and by alternate splicing of hTERT transcripts. *Cancer Research*, 58(18), pp.4168-4172.

Wang, J, Smerdon, S.J., Jäger, J., Kohlstaedt, L.A., Rice, P.A., Friedman, J.M. and Steitz, T.A., 1994. Structural basis of asymmetry in the human immunodeficiency virus type 1 reverse transcriptase heterodimer. *Proceedings of the National Academy of Sciences*, 91(15), pp.7242 -7246.

Wang, L., Dean, S.R. and Shippen, D.E., 2002. Oligomerization of the telomerase reverse transcriptase from Euplotes crassus. *Nucleic Acids Research*, 30(18), pp.4032 - 4039.

Watson, J.D., 1972. Origin of concatemeric T7 DNA. *Nature: New Biology*, 239(94), pp.197-201.

Wenz, C., Enenkel, B., Amacker, M., Kelleher, C., Damm, K. and Lingner, J., 2001. Human telomerase contains two cooperating telomerase RNA molecules. *EMBO J*, 20(13), pp.3526-3534.

Wu, J.C., Warren, T.C., Adams, J., Proudfoot, J., Skiles, J., Raghavan, P., Perry, C., Potocki, I., Farina, P.R. and Grob, P.M., 1991. A novel dipyridodiazepinone inhibitor of HIV-1 reverse transcriptase acts through a nonsubstrate binding site. *Biochemistry*, 30(8), pp.2022-2026.

Xia, J., Peng, Y., Mian, I.S. and Lue, Neal F., 2000. Identification of Functionally Important Domains in the N-Terminal Region of Telomerase Reverse Transcriptase. *Mol. Cell. Biol.*, 20(14), pp.5196-5207.

Yang, C.-P., Chen, Y.-B., Meng, F.-L. and Zhou, J.-Q., 2006. Saccharomyces cerevisiae Est3p dimerizes *in vitro* and dimerization contributes to efficient telomere replication *in vivo*. *Nucleic Acids Research*, 34(2), pp.407 -416.

Zappulla, D.C. and Cech, Thomas R., 2004. Yeast telomerase RNA: A flexible scaffold for protein subunits. *Proceedings of the National Academy of Sciences of the United States of America*, 101(27), pp.10024 -10029.

Zhang, M.-L., Tong, X.-J., Fu, X.-H., Zhou, B.O., Wang, Jianyong, Liao, X.-H., Li, Q.-J., Shen, N., Ding, J. and Zhou, J.-Q., 2010. Yeast telomerase subunit Est1p has guanine quadruplex-promoting activity that is required for telomere elongation. *Nat Struct Mol Biol*, 17(2), pp.202-209.

Zhou, J., Hidaka, K. and Futcher, B., 2000. The Est1 Subunit of Yeast Telomerase Binds the Tlc1 Telomerase RNA. *Mol. Cell. Biol.*, 20(6), pp.1947-1955.

Zhou, X.Z. and Lu, K.P., 2001. The Pin2/TRF1-Interacting Protein PinX1 Is a Potent Telomerase Inhibitor. *Cell*, 107(3), pp.347-359.

Zhu, Y., Tomlinson, R.L., Lukowiak, A.A., Terns, R.M. and Terns, M.P., 2004. Telomerase RNA Accumulates in Cajal Bodies in Human Cancer Cells. *Mol. Biol. Cell*, 15(1), pp.81-90.

Chapter 2: TLC1 Dimerization Is a Telomerase Biogenesis Step

Tetsuya Matsuguchi and Elizabeth H. Blackburn

Department of Biochemistry and Biophysics

University of California, San Francisco

San Francisco, CA 94158

Results

The 3' region of TLC1 is important for TLC1-TLC1 interaction

A previous study by Gipson *et al*. has identified a palindromic sequence at 3' end of TLC1 only present in the immature form of TLC1 that is required for TLC1-TLC1 dimerization *in vitro*. This region has been shown to be critical for maintaining wild-type telomere length *in vivo* (Gipson *et al*. 2007). To directly test whether this region leads to TLC1 dimerization *in vivo*, we developed a co-immunoprecipitation (coIP) assay using lysed yeast cell extracts to detect TLC1-TLC1 interaction. A tandem pair of RNA hairpins that specifically bind to MS2 Coat Protein was inserted at the BclI restriction site of TLC1, a region that has previously been shown to accommodate insertions of modular protein binding domains (Bernardi and Spahr 1972; Zappulla and Cech 2004) (Figure 2-1A). This insertion of the RNA hairpins (*TLC1-MS2*) resulted in a stable and slightly shorter telomere length compared to wild-type.

TLC1-MS2 was co-expressed along with untagged, wild-type TLC1 from the endogenous locus. MS2 Coat Protein was fused to 3xMyc tag and was expressed from

the *CYC1* promoter in experimental strains. Generally, we found that 50-80% of the tagged TLC1-MS2 is immunoprecipitated by this method, and about 10% of TLC1 is present in a TLC1-TLC1 dimeric form *in vivo* (Figure 2-1B, see Materials and Methods for calculation). To ensure that there are no transcripts containing both TLC1 and TLC1-MS2 in the same molecule expressed from the genomic locus (two copies are in tandem flanking a URA3 marker), TLC1-MS2 was also expressed from a CEN-ARS plasmid. Regardless of the loci, both TLC1 and TLC1-MS2 were expressed at similar levels to wild-type strains (Figure 2-1C), and the coIP of untagged TLC1 did not change (Figure 2-1D).

Mutations that disrupt the evolutionarily conserved palindromic sequence that allows predicted intermolecular base pairing were reported to abrogate *in vitro* dimerization (Gipson *et al*. 2007). These same mutations were incorporated into the strains also expressing TLC1-MS2. The separate mutations reduced TLC1-TLC1 coIP by half, although the compensatory mutations predicted to restore the TLC1-TLC1 base-pairing did not restore TLC1-TLC1 coIP, unlike the finding previously reported *in vitro* (Figure 2-2A).

The *TLC1* gene region containing the palindromic sequence mutation encompasses a 3' extension of *TLC1* RNA that is normally cleaved off to form the mature, major form of TLC1, with only 2-4% of TLC1 in the cells being in the longer, presumably immature form (Chapon *et al*. 1997; Mozdy and Cech 2006). Because 8-12% of TLC1 is in the dimer form, most of the TLC1 in dimeric form must be the cleaved form of TLC1. However, because this 3' extension region is important for TLC1-TLC1

coIP, we tested whether the immature form is enriched in the co-immunoprecipitated TLC1. Neither the TLC1-MS2 nor the untagged TLC1 was enriched with the immature form in the immunoprecipitate and co-immunoprecipitate (Figure 2-2B). These findings, together with reduction in coIP caused by mutating the 3' region downstream of the cleavage site producing the mature form of TLC1, suggest that the dimerization of TLC1 initializes in the immature form, possibly in the 3' extension region, and persists after the cleavage of the 3' end.

Identification of regions important for TLC1-TLC1 dimerization

Gipson *et al*. previously suggested that the palindromic sequence at the 3' region may act as "kissing loop" to initiate base-pairing of two TLC1 molecules. In other RNA-RNA interactions, such trans-base-pairing can extend beyond the site of the original kissing loop contacts, as found for example in the ColE1 plasmid replication-regulating RNAI and RNAII. However, we note that unlike TLC1 molecules, the RNAI and II ColE1 RNAs are anti-sense, and thus can undergo much more extensive base-pairing than TLC1, by "zipping up" between the two molecules after the kissing-loop interaction has initiated (Tomizawa 1984). Nonetheless, in order to test whether the TLC1-TLC1 interaction measured by coIP is held together by intermolecular base-pairings that is similarly initiated within the 3' extension region but then spreads to regions within the cleaved mature TLC1, DNA oligonucleotides were used to attempt to disrupt the base-pairing. We designed 72 DNA oligonucleotides, 30 bases in length, complementary to the full-length of *TLC1* and also including the 3' region of the immature TLC1 that is cleaved off

in the mature form. These oligonucleotides were added to the wash buffer during the washing step of immunoprecipitation (see Materials and Methods). As a control, 72 DNA oligonucleotides designed against other regions of the genome were used. We observed that when all 72 oligonucleotides against *TLC1* were incubated with the immunoprecipitates, about 30% of untagged TLC1 remained on the beads (Figure 2-3A). The amount of MS2-coat protein binding site-tagged TLC1 remaining on the MS2 coat-protein beads did not appreciably change, suggesting that the disruption by oligonucleotides was specific to TLC1-TLC1 interaction. This disruption can be through a direct competition of base-paired regions between two *TLC1* RNAs or also through an unwinding of some structural elements of TLC1.

To further probe the regions and structures important for holding TLC1 molecules in a dimer, different subset of oligonucleotides were used in the same experimental setup. The 72 oligonucleotides were subdivided into thirds and ninths, and each region was probed separately, and the level of TLC1 that remained in the dimer form was measured (Figure 2-3B). In all experiments, the concentration of each oligonucleotide was kept constant. The oligonucleotides directed to the first third of TLC1 did not significantly reduce the coIP of the untagged TLC1 (Figure 2-3B, Row 2). While the second and third interval oligonucleotides had the greater effect on disrupting TLC1 dimerization, each of the thirds individually disrupted the dimerization at a significantly lower level than when all oligonucleotides were included. Even adding up the effect from each of the three regions was not enough to explain the whole effect, suggesting that there is a synergistic effect in adding all oligonucleotides. Similarly, probing the TLC1 dimer with each of the

one-ninth regions had small effect, especially in the 5' regions of TLC1 (Figure 2-3B, Row 3). The most effect was seen at the 3' end, where only two oligonucleotides were complementary to the mature form of TLC1, and the rest of the six oligonucleotides were complementary to the un-cleaved, immature form of TLC1. This suggested that the 3' end is either most critical or most vulnerable to the disruption of TLC1 dimerization.

Dimerization is cell cycle-regulated

The dependence of the TLC1 dimerization on the 3' region not present in the mature TLC1 suggested that dimerization initiates before the 3' regions is cleaved. A previous study has shown that cells arrested in S and G2/M phase accumulate immature TLC1, while alpha-factor arrested cells show no accumulation of immature TLC1 (Chapon *et al*. 1997). This suggests that mechanisms required for TLC1 processing is not active during S and G2/M phase (Chapon *et al*. 1997). To test whether TLC1-TLC1 association was cell cycle-controlled, yeast lysates were prepared at 15-minute intervals from cells following a release from the alpha-factor arrest. Cell cycle progression and synchrony was confirmed by analysis of the cyclin mRNA levels throughout the time course (Figure 2-4C).

During the first cell cycle after the release from the alpha-factor arrest, the fraction of TLC1 in dimer form remained relatively constant (Figure 2-4A). The coIP assay on these samples showed an increase in TLC1 dimerization after mitosis, as the cell population re-entered the next G1 phase after the first cell cycle following release. This is consistent with the model suggested above, that TLC1 dimerization occurs during the

biogenesis of telomerase complex, a process that is active only during G1 phase. As previously reported, TLC1 levels did not change significantly in a cell-cycle dependent manner (Figure 2-4B).

TLC1 dimerization depends on nuclear export factors

TLC1 RNA is an RNA Polymerase II transcript that is polyadenylated and trimethyl-G capped at its 5' end by Tgs1 (Chapon *et al*. 1997; Franke *et al*. 2008). Co-immunoprecipitation assays on *tgs1Δ* showed that this cap is only slightly important for dimerization of TLC1 (Figure 2-5A), which is consistent with the slightly longer than wild-type telomere length of *tgs1Δ*, suggesting that the cap does not play a major role in TLC1 biogenesis or telomerase activity (Franke *et al*. 2008). At some stage during its biogenesis, TLC1 is exported into the cytoplasm and re-imported back into the nucleus. Nup133 is a subunit of the nuclear pore complex, and it is required for the export of polyadenylated RNAs. When the *NUP133* gene was deleted, the TLC1 dimerization was reduced by more than half (Figure 2-5A).

Once TLC1 is exported, it is thought to interact with other telomerase components, Est1, Est2, and Est3, before it is re-imported back in the nucleus (Gallardo *et al*. 2008). In the absence of Est1, Est2, and Est3, TLC1 is diffused throughout the cell instead of localizing in the nucleus. The Ku complex is also required for the nuclear localization of TLC1 (Gallardo *et al*. 2008). To test, initially, whether nuclear localization or reimport is required for TLC1 dimerization, coIP assays were carried out in *est1Δ*, *est2Δ*, *est3Δ*, *yku70Δ*, and *yku80Δ* strains. There was a modest reduction of TLC1 dimerization in

est1Δ, *est2Δ*, and *est3Δ*, and strikingly, more than half of TLC1 dimerization was lost in *yku70Δ* and *yku80Δ* (Figure 2-5B). It is not clear from this set of data whether nuclear reimport is necessary for TLC1 dimerization, as defects in these mutants may be related to nuclear retention or reimport of TLC1.

TLC1 dimerization is held together by proteins

The Ku complex binds to TLC1 directly (Stellwagen *et al*. 2003). To test whether TLC1 dimerization is held together by the Ku complex or any other protein, sensitivity of TLC1 dimerization to protease treatment was tested. The whole lysate was treated with magnetic bead-bound trypsin, which allows the removal of trypsin before immunoprecipitation. The condition used for trypsin treatment resulted in precipitations in the lysate, but enough TLC1 remained in the solution for immunoprecipitation. Trypsin- and mock-treated lysates were incubated with MS2 coat protein bound to magnetic beads for the immunoprecipitation. Pre-treating the whole lysate with trypsin resulted in ~40% reduction in the coIP of untagged TLC1 (Figure 2-6), suggesting that there are some protein factors that are holding *TLC1* RNAs together.

Ku and Sir4 are required for TLC1 dimerization

Ku has many functions in the regulation of telomeres in yeast, including recruitment of telomerase to telomeres, recruitment of telomeres to nuclear periphery, and silencing at telomeres. Although there is no evidence that Ku plays a role in biogenesis of TLC1, Ku binds directly to the stem-loop structure in TLC1 (Stellwagen *et al*. 2003). To test

whether the Ku complex binding to TLC1 is required for TLC1 dimerization, *yku80-135i* allele was tested for its ability to support TLC1 dimerization. The small insertion in *yku80-135i* results in abrogation of TLC1-Ku interaction, but this mutant Ku complex retains all the other known *in vivo* functions of the Ku complex. This mutation disrupted the TLC1 dimerization to the same extent as the deletions of *YKU70* and *YKU80* (Figure 2-7B), showing that Ku-TLC1 interaction is necessary for the TLC1 dimerization function of Ku.

The deletion of the Ku complex as well as *yku80-135i* mutation result in a marked reduction in steady-state level of TLC1 (~50%; Figure 2-7A). To test whether the reduction in TLC1 dimerization is due solely to the reduced level of the steady-state TLC1 level, *CTR9* and *CDC73* genes, that are part of the Paf1 complex important for TLC1 expression, were deleted (Mozdy *et al*. 2008). These deletions each resulted in a reduction of the total TLC1 level down to ~20-25% of the wild-type TLC1 level, but the fraction of TLC1 in dimeric form did not appreciably change from that of the wild-type strain (Figure 2-7). Additionally, the deletion of *EST2* did not have as much effect as the deletions of Ku in TLC1 dimerization, but the amount of TLC1 is reduced to a similar extent in *est2Δ* cells as the Ku mutants (Figure 2-5B and see Appendix 2).

To determine whether any of the processes in which the Ku complex participates are important for TLC1 dimerization, coIP assays were carried out in strains deleted for *ESC1* and *CTF18* (telomere tethering to nuclear periphery; Taddei *et al*. 2004; Hiraga *et al*. 2006); and *SIR2*, *SIR3*, and *SIR4* (telomere silencing; Boulton and Jackson 1998) genes. Both *esc1Δ* and *ctf18Δ* cells showed modestly lower fraction of TLC1 dimers,

while *sir2Δ* and *sir3Δ* had no effect on TLC1 dimerization. Surprisingly, *sir4Δ* showed a TLC1 dimer fraction as low as that of *yku80-135i*. Thus, telomere silencing is clearly not required for TLC1 dimerization, because *sir2Δ* and *sir3Δ* had the wild-type levels of TLC1 dimers. The only known Sir4 function that is unique from the other members of the Sir complex is its role in telomere binding near the distal tip. The Ku complex is also thought to bring the telomerase to the telomere near the distal tip, and the Ku complex is known to physically interact with Sir4 (Tsukamoto *et al*. 1997). This led to the question of whether the Ku complex and Sir4 are acting together in the same pathway for TLC1 dimerization. Indeed, when *yku80Δ* or *yku80-135i* was combined with *sir4Δ*, there was no further reduction in the TLC1 dimer fraction (Figure 2-8A).

Ku/Sir4 and the 3' region promote TLC1 dimerization in different modes

To test whether Ku and Sir4 promote TLC1 dimerization through interacting with the 3' region of TLC1, *sir4Δ* and *yku80Δ* were combined with the 3' mutation *tlc1-42G*. When the mutations were combined, the fraction of TLC1 in the dimer form was further reduced, nearly down to the level of the negative control (Figure 2-8). This suggests that TLC1 dimerizes through the 3' region of TLC1 at least partially independently of Ku and Sir4. While it is unknown when Ku and Sir4 are associated with TLC1, they are thought to function at telomeres, where TLC1 is presumably already processed to the mature form (*i.e*. missing the 3' region). A process involving two separate modes of TLC1 dimerization is consistent with this model.

The majority of telomerase RNP complexes contain only one Est2 subunit

There have been a number of studies suggesting that telomerase RNP is a dimer, with two copies each of telomerase RNAs and telomerase reverse transcriptases. Such studies include a recent electron microscope-single-particle structural determination of human telomerase, which indicates a dimer containing two TERT subunits held together at the central region of the complex by RNA regions (D. Rhodes, personal communication, 2011). It was surprising; therefore, that deletion of protein components of telomerase had little effect on TLC1 dimerization. Est2 binding to TLC1 requires the pseudoknot structure at the core of TLC1 near the template region; the conserved sequence regions CS3 and CS4 form base-pairs necessary for the pseudoknot (Lin *et al*. 2004). When the base pairing in these regions were mutated (*tlc1-cs3* and *tlc1-cs4* mutations), TLC1 dimerization was abrogated (Figure 2-10A). When *tlc1-cs3* and *tlc1-cs4* mutations are combined in *cis*, the base-pairings and the pseudoknot structure are restored. TLC1 dimerization was also restored when the compensatory mutations are introduced (Figure 2-10A; *cs3-cs4*). The requirement for the pseudoknot structure is puzzling as the loss of Est2-binding caused by these particular mutations and the deletion of *EST2* do not have the same extent of TLC1 dimerization disruption. This suggests that the pseudoknot structure is an important feature during the biogenesis of telomerase complex. Pseudoknot formation could be required for a proper RNA folding pathway that allows the stable TLC1-TLC1 interaction that is detected in our TLC1-TLC1 dimerization assay experiments.

TLC1 dimerization was slightly reduced in *est1Δ*, *est2Δ*, and *est3Δ* strains (Figure 2-5). To test whether this is due to the absence of dimeric telomerase RNP, an attempt was made to immunoprecipitate an Est2-Est2 complex. To this end, Est2 was tagged at the C-terminus with 3xFLAG or 13xMyc, and these constructs were co-expressed in a diploid strain. As a positive control, both 3xFLAG and 13xMyc were fused in a single *EST2* ORF. Lysates from these strains were subjected to sequential immunoprecipitation (IP), anti-FLAG IP followed by anti-Myc IP. As expected, we observed a robust enrichment of TLC1 in positive control strain containing Est2 tagged with both epitopes (Figure 2-10B). In contrast, strains carrying Est2-3xFLAG and Est2-13xMyc showed the same amount of TLC1 in the precipitates as the negative control that only contained Est2-3xFLAG. While we cannot exclude the possibility that Est2-Est2 interaction exists *in vivo*, the results is consistent with the model in which TLC1-TLC1 interaction is independent of Est2 or Est-Est2 interaction. Previous study has shown that TLC1-containing telomerase RNP has a single, stable, dominant form *in vitro* (Prescott and Blackburn 1997), suggesting that telomerase complex *in vitro* is monomeric.

Discussion

The series of co-immunoprecipitation assay show that TLC1-TLC1 interaction occurs *in vivo*, complementing the *in vitro* study (Gipson *et al*. 2007). We also show that the 3' region identified as necessary for *in vitro* dimerization is also important for dimerization *in vivo*. However, the compensatory mutation, which restores base pairing in the 3' region and rescues the *in vitro* TLC1 dimerization, does not rescue dimerization *in vivo*

(Gipson *et al*. 2007). The concentration at which the *in vitro* study was done is much higher than it is *in vivo*; only about 40 copies of TLC1 RNA are present in the haploid cell (Mozdy and Cech 2006). It is possible that restoration of base pairing in this region requires a higher concentration than it is available *in vivo*. Alternatively, the 3' region may be important for binding some factors necessary for dimerization, and the rescue *in vitro* was an artifact of high concentration.

The properties of TLC1 dimer

Probing the dimeric TLC1 immunoprecipitated with anti-sense oligonucleotides allowed us to identify regions that are important for dimerization. When the entire length of *TLC1* was targeted by the oligonucleotides, most of the dimerization was lost. The experiments probing smaller regions of *TLC1* for oligonucleotide targeting resulted in disruption that did not simply add up to the disruption when the entire length of *TLC1* was targeted. This suggests a model reminiscent of unzipping caused by the oligonucleotides. The region that was most affected by the oligonucleotides was the 3' region. We propose a model in which the 3' region has a weaker base-pairing or tertiary structure that can be more easily disrupted by oligonucleotide probing; once this region is "unzipped," oligonucleotides have better and easier access to the rest of the TLC1 dimer structure, allowing it to disassociate further. Perhaps time course experiments with oligonucleotides targeted to different regions added in different order can further probe potential tertiary structures that are formed in the TLC1 dimer.

The oligonucleotide-driven disruption left about 30% of TLC1 dimers intact; treating the lysate with trypsin resulted in about 30-40% reduction in TLC1 dimers. While this is only circumstantial evidence, it is possible that there are two fractions of TLC1 dimers: a fraction that is mostly stabilized by RNA-RNA interaction and a fraction that is held together by proteins. This is consistent with the results that show two predominant modes by which TLC1 dimerizes: through the 3' region and through Ku/Sir4 interaction. This should be tested by treating the lysate prepared from mutations in the 3' region and *yku70Δ* / *yku80Δ* / *sir4Δ* with the anti-sense oligonucleotides assay and trypsin treatment.

Formation of TLC1 dimer

As discussed earlier, the 3' region that is required for TLC1 dimerization is cleaved off during one of the steps of TLC1 maturation, which means this process must initiate before or during one of the TLC1's biogenesis steps (Figure 2-11, A and B). The cleavage of the polyadenylated downstream 3' region of TLC1 occurs only during the G1 phase, as evidenced by the lack of polyA+ TLC1 in alpha-factor arrested cells and the persistence of increased levels of polyA+ TLC1 in nocodazole- and HU-arrested cells (Chapon *et al*. 1997). The cell cycle-dependent increase of TLC1 dimers in G1 phase of the cell-cycle is thus consistent with TLC1 dimerization occurring at least in part during or before the biogenesis step in which the 3' region is cleaved. The polyadenylated tail is important for the stability of mRNAs. It is unknown what role polyadenylation plays in the stability of TLC1; however, upon the cleavage of polyadenylation, TLC1

dimerization may help with its stabilization. The lack of a higher fraction of TLC1 in the dimer form during the G1 phase immediately following the release from the alpha-factor arrest is also consistent with dimerization formation during the biogenesis step, as in this situation, cells have been sitting in G1 phase with active biogenesis machinery for 120 minutes at the point of release from alpha-factor. Taken together, we favor the model in which about half of the TLC1 dimers observed in asynchronous cultures come from TLC1 biogenesis intermediates.

Sir4 and the Ku complex are nuclear proteins, with Sir4 concentrated around the nuclear periphery (Huh *et al*. 2003). Sir4 binds the more distal end of telomeres through its interaction with Rap1, while Sir2, Sir3, and Sir4 binding to, and heterochromatin formation at, subtelomeres are interdependent on each other (Luo *et al*. 2002). This is the only known function of Sir4 that is unique to Sir4 in the sense that it does not require Sir2 and Sir3 (Rap1-Sir4 interaction can also inhibit nonhomologous end-joining at telomeres independently of Sir2 and Sir3; Marcand *et al*. 2008). The Ku complex is a DNA-end biding complex and is also thought to bind telomeres at the distal end. Taken together, we propose a model in which Sir4- and the Ku complex-dependent dimerization of TLC1 occur at telomeres (Figure 2-11B). While we cannot exclude the possibility that Sir4 and the Ku complex have functions off DNA, such functions for neither protein have been observed.

This parsimonious model for the independent roles played by the 3' region and Ku/Sir4 in the formation of TLC1 dimerization is also consistent with the model mentioned above: that there are two forms of TLC1 dimers: the anti-sense

oligonucleotide-sensitive form, especially the 3' region, and the trypsin-sensitive form. The apparent lack of epistatic relationship between the 3' region and Ku/Sir4 in TLC1 dimerization is not a conundrum, as the biogenesis step can occur in the absence of Ku/Sir4, and the cleavage of the 3' region seems largely unimportant for telomerase RNP formation (data not shown).

TLC1 dimerization and telomerase RNP

The oligomeric state of telomerase has been controversial for some time, with studies supporting both monomeric and dimeric forms of telomerase in multiple organisms. Such studies include a recent electron microscope-single-particle structural determination of human telomerase, which indicates a dimer containing two TERT subunits held together at the central region of the complex by RNA regions (D. Rhodes, personal communication, 2011). Here we have shown that Est2-Est2 interaction that contains TLC1 does not survive immunoprecipitation assays. Previous study showed that on a glycerol gradient, there is a single oligomeric form of TLC1-containing complex resolvable by this method (Prescott and Blackburn 1997). Because the immunoprecipitation condition used here is no less mild, we propose that the predominant form of telomerase RNP contains a single Est2 (Figure 2-11C). We cannot rule out the possibility that telomerase RNP is dimeric *in vivo*; however, we can say that any Est2-Est2 interaction detectable by experiments using normal coIP conditions is not as stable as TLC1-TLC1 interaction *in vitro*. It remains to be seen whether telomerase RNP *in vitro* contains one or two TLC1's (Figure 2-11C). An attempt was made at

looking at the dimerization state of TLC1 in Est2 immunoprecipitates, but the amount collected was too small to be certain that there was no dimeric TLC1 (data not shown). A larger scale version of this experiment and another glycerol gradient experiment (or perhaps native gel RNP fractionation, with or without prior cross-linking) with two TLC1's of different sizes will need to be done to answer this question.

As shown by several studies in various organisms, a seemingly monomeric telomerase RNP has the full complement of factors necessary for its activity (Bryan *et al*. 2003; Alves *et al*. 2008; Shcherbakova *et al*. 2009); the functional significance of telomerase dimerization has remained a mystery. Some of the models suggested that such dimeric telomerase RNP may act as a switch for telomerase activity or be able to increase processivity. Consistent with the model that there is no such dimeric telomerase RNP and that TLC1 dimerization is mostly independent of the formation of telomerase RNP, the TLC1 dimerization level did not change during S and G2/M phases of the cell cycle, the window in which telomerase is active in polymerization at telomeres. Furthermore, mutating genes that modulate telomerase polymerization action on telomeres, *TEL1*, *RIF1*, and *RIF2,* had no effect on TLC1 dimerization (data not shown).

Functional significance of TLC1 dimerization

The mutations in Ku, Sir4, and the 3' region of TLC1 result not only in a lower fraction of TLC1 in the dimer form but also in shorter telomeres. This suggests that TLC1 dimerization is functionally important for telomerase activity. However, as discussed above, TLC1 dimerization does not seem to directly affect the DNA polymerizing action

of the telomerase complex on telomeres. How, then, does dimerization affect the activity of telomerase? We postulated that perhaps TLC1 dimerization before forming a complex with telomerase protein subunits could either increase the stability of naked RNA or allow TLC1 to more efficiently assemble into active telomerase. Some mutations that reduced TLC1-TLC1 dimerization did in fact reduce the steady-state level of TLC1 (*tlc1-42G*), but others did not affect the steady state level (*nup133Δ*). However, the Paf1 complex mutations that significantly reduced TLC1 levels had no effect on the fraction of TLC1-TLC1 dimers in cells, showing that reduction of the steady state of telomerase RNA is not sufficient to reduce its dimerization. To test the possibility that TLC1 requires dimerizing in order to efficiently assemble into an active telomerase complex, we will carry out coIP assays to determine the level of TLC1-Est2 association in telomerase dimerization-defective mutants. The functional significance of TLC1 dimerization and the mechanism by which it affects telomere length remain largely unresolved.

Future Directions

In addition to experiments mentioned above, the following experiments will be important in deciphering the role of TLC1 dimerization. To study the dimerization of TLC1 through its biogenesis pathway, an inducible TLC1 construct will be useful. Time course experiments with the induced TLC1 can follow various aspects of TLC1 processing, such as capping, polyadenylation, dimerization, cleavage of the 3' region, and interactions with other protein components (Sm, Ku, Est1, Est2, and Est3). Mutations in Sm-binding

site and *MTR10*, which are both required for TLC1 maturation and *MTR10* for nuclear retention of TLC1 (Seto *et al*. 1999; Ferrezuelo *et al*. 2002), will also be informative determining the step at which TLC1 dimerizes during its biogenesis.

Materials and Methods

Plasmids

The integrating vector, pRS306-TLC1, was provided by Jue Lin. The MS2 CP-binding RNA hairpins were constructed by annealing overlapping oligonucleotide in a standard PCR protocol. The hairpin construct was cloned into the BclI site of pRS306-TLC1. The fusion PCR method was used to construct *tlc1-42G* and *tlc1-42C* alleles, which were cloned between the BclI and XhoI sites of pRS306-TLC1. CEN-ARS versions of the plasmids were made by subcloning BamHI-XhoI fragments of the integrating vectors into the vector pRS316.

Yeast strains and growth media

Yeast strains were in the S288c background and are isogenic with BY4746, except as noted in Table 2-1 (Baker Brachmann *et al*. 1998). Yeast cultures were grown in standard rich medium or minimal media (YEPD or CSM). Deletion strains were made using a PCR-based transformation method (Longtine *et al*. 1998).

Immunoprecipitation of MS2 hairpin-tagged TLC1

TLC1 was tagged with two MS2 coat-protein-binding RNA hairpins at the BclI restriction site in the *TLC1* coding region sequence. This gene construct with its native promoter was integrated at the endogenous chromosomal *TLC1* locus, in tandem with untagged, wild-type *TLC1*, flanking the *URA3* marker. MS2 coat protein fused to 3 Myc epitope tags was expressed either in *tlc1Δ* or in experimental strains containing both tagged and untagged *TLC1*. Whole cell lysates were prepared from cultures in log-phase of growth in YEPD (OD_{600}=0.6-1.0) using glass beads and bead beaters. The lysis buffer contained 50mM HEPES-KCl pH8.0, 2 mM EDTA, 2 mM EGTA, 0.1% Nonidet P40, 10% glycerol, cOmplete EDTA-free protease inhibitors (Roche) and RNasin (Promega; 1 uL / mL). The lysate concentrations were adjusted to A_{260nm} = 40 before immunoprecipitation. For lysates containing co-expressed MS2 coat protein, 400 uL of lysate was mixed with 1.5 mg Dynal ProA magnetic beads (Invitrogen) and 1 ug of monoclonal anti-Myc antibody (9E11, Santa Cruz Biotechnology). For experiments in which MS2 coat protein was purified separately, ProA magnetic beads, anti-Myc antibody, and whole cell lysate containing MS2 coat protein (at A_{260nm}=60-80) were incubated for 1-2 hours. The beads were washed and used for tagged TLC1 precipitation. The immunoprecipitation was allowed to take place at 4 °C for 4-hours to overnight. For oligonucleotide-directed displacement experiments, the immunoprecipitates were washed in presence of oligonucleotides each at 0.5 uM in the lysis buffer.

Immunoprecipitation of tagged proteins

For immunoprecipitation of tagged proteins (Est2-13xMyc, Est2-3xFLAG), lysates were prepared as described above. For Myc-tagged proteins, the lysate was mixed with 1.5 mg Dynal ProA magnetic beads, and 1 ug 9E11 antibody. For FLAG-tagged proteins, lysate was incubated with 50uL of M2-conjugated agarose beads. For sequential immunoprecipitation of FLAG-tagged proteins followed by Myc-tagged proteins, 15 ug of 3xFLAG peptide was added to the M2-conjugated agarose beads. The eluate was then used for Myc-tag immunoprecipitation as described.

Quantitative reverse transcription and PCR

RNA from input and immunoprecipitates were isolated using RNeasy Mini Kit (Qiagen), including the DNase step as described by the manufacturer. The primer set for PGK1 was designed using IDT's PrimerQuest program. The reverse primers used to distinguish tagged and untagged TLC1 were designed within and at the insertion junction, respectively, of the MS2 hairpin tag. One-step reverse transcription and PCR kits were used for all RNA quantifications, except for the quantification of immature TLC1 (Stratagene, Invitrogen). For quantification of immature TLC1, or 3' regions of TLC1, SuperScript III and random hexamer were used for reverse transcription. Subsequently, SYBR Green I Master mix kit (Roche) was used for quantitative PCR. All quantitative PCR runs included serially diluted RNA samples to make standard curve, from which relative quantitative values were derived using the LightCycler software. The oligonucleotide sequences used in qRT-PCR reactions are listed in Table 2-2.

Telomere length analysis

Genomic DNA was digested with XhoI and separated on a 0.85% agarose gel. DNA was denatured and transferred to a Nylon membrane, and UV-crosslinked with a Stratalinker. The membrane was blotted with telomeric oligonucleotide (5'-CACACCCACACCACACCCACAC-3') labeled with WellRED D3 fluorescent dye at the 5' end. The blotted membrane was scanned and analyzed using the Odyssey Infrared Imaging System (LI-COR). A linear plasmid containing an S. cerevisiae telomeric DNA sequence was included as a marker.

References

Alves, D., Li, H., Codrington, R., Orte, A., Ren, X., Klenerman, D. and Balasubramanian, S., 2008. Single-molecule analysis of human telomerase monomer. *Nat Chem Biol*, 4(5), pp.287-289.

Baker Brachmann, C., Davies, A., Cost, G.J., Caputo, E., Li, J., Hieter, P. and Boeke, J.D., 1998. Designer deletion strains derived from Saccharomyces cerevisiae S288C: A useful set of strains and plasmids for PCR-mediated gene disruption and other applications. *Yeast*, 14(2), pp.115-132.

Bernardi, A. and Spahr, P.-F., 1972. Nucleotide Sequence at the Binding Site for Coat Protein on RNA of Bacteriophage R17. *Proceedings of the National Academy of Sciences of the United States of America*, 69(10), pp.3033-3037.

Boulton, S.J. and Jackson, S.P., 1998. Components of the Ku-dependent non-homologous end-joining pathway are involved in telomeric length maintenance and telomeric silencing. *The EMBO Journal*, 17(6), pp.1819-1828.

Bryan, T.M., Goodrich, K.J. and Cech, T.R., 2003. Tetrahymena Telomerase Is Active as a Monomer. *Molecular Biology of the Cell*, 14(12), pp.4794-4804.

Chapon, C., Cech, T.R. and Zaug, A.J., 1997. Polyadenylation of telomerase RNA in budding yeast. *RNA (New York, N.Y.)*, 3(11), pp.1337-1351.

Ferrezuelo, F., Steiner, B., Aldea, M. and Futcher, B., 2002. Biogenesis of yeast telomerase depends on the importin mtr10. *Molecular and Cellular Biology*, 22(17), pp.6046-6055.

Franke, J., Gehlen, J. and Ehrenhofer-Murray, A.E., 2008. Hypermethylation of yeast telomerase RNA by the snRNA and snoRNA methyltransferase Tgs1. *Journal of Cell Science*, 121(21), pp.3553 -3560.

Gallardo, F., Olivier, C., Dandjinou, A.T., Wellinger, R.J. and Chartrand, P., 2008. TLC1 RNA nucleo-cytoplasmic trafficking links telomerase biogenesis to its recruitment to telomeres. *EMBO J*, 27(5), pp.748-757.

Gipson, C.L., Xin, Z.-T., Danzy, S.C., Parslow, T.G. and Ly, H., 2007. Functional Characterization of Yeast Telomerase RNA Dimerization. *Journal of Biological Chemistry*, 282(26), pp.18857 -18863.

Hiraga, S.-ichiro, Robertson, E.D. and Donaldson, A.D., 2006. The Ctf18 RFC-like complex positions yeast telomeres but does not specify their replication time. *EMBO J*, 25(7), pp.1505-1514.

Huh, W.-K., Falvo, J.V., Gerke, L.C., Carroll, A.S., Howson, R.W., Weissman, J.S. and O'Shea, E.K., 2003. Global analysis of protein localization in budding yeast. *Nature*, 425(6959), pp.686-691.

Lin, J., Ly, H., Hussain, A., Abraham, M., Pearl, S., Tzfati, Y., Parslow, T.G. and Blackburn, E.H., 2004. A universal telomerase RNA core structure includes structured motifs required for binding the telomerase reverse transcriptase protein. *Proceedings of the National Academy of Sciences of the United States of America*, 101(41), pp.14713-14718.

Longtine, M.S., Mckenzie III, A., Demarini, D.J., Shah, N.G., Wach, A., Brachat, A., Philippsen, P. and Pringle, J.R., 1998. Additional modules for versatile and economical PCR-based gene deletion and modification in Saccharomyces cerevisiae. *Yeast*, 14(10), pp.953-961.

Luo, K., Vega-Palas, M.A. and Grunstein, M., 2002. Rap1–Sir4 binding independent of other Sir, yKu, or histone interactions initiates the assembly of telomeric heterochromatin in yeast. *Genes & Development*, 16(12), pp.1528 -1539.

Marcand, S., Pardo, B., Gratias, A., Cahun, S. and Callebaut, I., 2008. Multiple pathways inhibit NHEJ at telomeres. *Genes & Development*, 22(9), pp.1153 -1158.

Mozdy, A.D. and Cech, T.R., 2006. Low abundance of telomerase in yeast: Implications for telomerase haploinsufficiency. *RNA*, 12(9), pp.1721 -1737.

Mozdy, A.D., Podell, E.R. and Cech, T.R., 2008. Multiple Yeast Genes, Including Paf1 Complex Genes, Affect Telomere Length via Telomerase RNA Abundance. *Mol. Cell. Biol.*, 28(12), pp.4152-4161.

Prescott, J. and Blackburn, E.H., 1997. Functionally interacting telomerase RNAs in the yeast telomerase complex. *Genes & Development*, 11(21), pp.2790 -2800.

Seto, A.G., Zaug, A.J., Sobel, S.G., Wolin, S.L. and Cech, T.R., 1999. Saccharomyces cerevisiae telomerase is an Sm small nuclear ribonucleoprotein particle. *Nature*, 401(6749), pp.177-180.

Shcherbakova, D.M., Sokolov, K.A., Zvereva, M.I. and Dontsova, O.A., 2009. Telomerase from yeast Saccharomyces cerevisiae is active *in vitro* as a monomer. *Biochemistry (Moscow)*, 74(7), pp.749-755.

Stellwagen, A.E., Haimberger, Z.W., Veatch, J.R. and Gottschling, D.E., 2003. Ku interacts with telomerase RNA to promote telomere addition at native and broken chromosome ends. *Genes & Development*, 17(19), pp.2384 -2395.

Taddei, A., Hediger, F., Neumann, F.R., Bauer, C. and Gasser, S.M., 2004. Separation of silencing from perinuclear anchoring functions in yeast Ku80, Sir4 and Esc1 proteins. *EMBO J*, 23(6), pp.1301-1312.

Tomizawa, J.-ichi, 1984. Control of cole 1 plasmid replication: The process of binding of RNA I to the primer transcript. *Cell*, 38(3), pp.861-870.

Tsukamoto, Y., Kato, J.-ichi and Ikeda, H., 1997. Silencing factors participate in DNA repair and recombination in Saccharomyces cerevisiae. *Nature*, 388(6645), pp.900-903.

Zappulla, D.C. and Cech, T.R., 2004. Yeast telomerase RNA: A flexible scaffold for protein subunits. *Proceedings of the National Academy of Sciences of the United States of America*, 101(27), pp.10024 -10029.

Figure Legends

Figure 2-1. Co-immunoprecipitation strategy to detect TLC1 dimerization.
(A) *TLC1* RNA before it is polyadenylated is represented (+1-1301). A tandem MS2 hairpins was inserted at BclI site (+1033). The binding sites for Ku (+288-335), Est1 (+660-664), and Sm (+1153-1160) proteins are indicated. The telomeric repeat template (+468-484), CGCGCG sequence (+1204), and the 3' end of the mature TLC1 (+1167) are also shown. (B) The amount of untagged TLC1 co-immunoprecipitated with MS2-tagged TLC1 was used to estimate the fraction of total TLC1 that is dimeric. (C) The amount of untagged and MS2-tagged TLC1 in total RNA normalized to PGK1 mRNA level is shown. TLC1 was expressed from the genomic locus or on a CEN-ARS plasmid. (D) The fraction of TLC1 in dimer form is calculated based on the amount of untagged TLC1 co-immunoprecipitated. The values are normalized to the average of the wild-type samples

for each experiment. The error bars indicate the standard errors among the samples. "Mix" samples represent mixed lysates from strains carrying untagged and tagged TLC1 independently.

Figure 2-2. The 3' region that is cleaved off plays a role in TLC1 dimerization.
(A) The fraction of TLC1 in dimer form is calculated in strains that carry mutations that disrupt palindromic sequence in the 3' region of TLC1. WT=CGCGCG, 42G=CGGGGG, 42C=CCCCCG, 42GC=CGGGGG+CCCCCG. (B) The ratios of the amount of 3' region to the total TLC1 were measured in the total RNA and immunoprecipitated RNA. The values were normalized to the average of all values. The error bars indicate the standard errors among the samples. The one-sample t-test values for the comparison with the wild-type indicate $p < 0.002$ for samples marked with ***. The pair-wise t-test values among the bracketed samples are indicated.

Figure 2-3. Anti-sense oligonucleotides can disrupt TLC1 dimers.
Anti-sense oligonucleotides were designed against *TLC1* and added during the washing step of immunoprecipitation. (A) The amount of TLC1 that remained in dimer is shown. All 72 anti-*TLC1* primers or random primers were added. The error bars indicate the standard errors among the experiments. (B) Different subsets of oligonucleotides were added during the wash step of immunoprecipitation. Each box represents the regions against which oligonucleotides added targeted. Each ninth and third region contained 8

and 24 oligonucleotides targeting that region. In each box is the fraction of TLC1 that remained on the beads after the wash with the standard deviation in the parentheses.

Figure 2-4. Cell cycle-dependent dimerization of TLC1.

The cells arrested in alpha-factor were released and were collected every 15 minutes. The first sample (t=0 min) is from alpha-factor arrested cells. (A) The fraction of TLC1 in dimer form is calculated from coIP experiments. (B) TLC1 levels, tagged and untagged, were measured. In both (A) and (B), the values are normalized to the asynchronous sample and the error bars represent the standard deviation between two experiments. (C) The level of cyclin mRNAs was measured to track the cell-cycle progress. The values are normalized so that the lowest value is 0 and the highest value is 1. The horizontal bars show cell cycle phase ascertained from the cyclin mRNA expression levels.

Figure 2-5. TLC1 dimer levels in deletion mutants.

The fraction of TLC1 in the dimer form is calculated from the coIP assays and normalized to the average of the wild-type samples in each experiment. (A) Indicated genes involved in TLC1 biogenesis pathway is deleted. (B) Deletion mutations that result in diffused TLC1 throughout the cell were tested. The error bars represent standard errors among the samples. The one-sample t-test values for the comparison with the wild-type are denoted: * $p > 0.01$, ** $p > 0.001$, *** $p < 0.0001$. The pair-wise t-test values among the bracketed samples are indicated.

Figure 2-6. TLC1 dimer is sensitive to trypsin treatment.

The fraction of TLC1 that remained in the dimer form was measured. The values were normalized to the average of trypsin-treated samples. The error bars represent the standard deviation between samples. The one-sample t-test value for the comparison with the wild-type is indicated.

Figure 2-7. Total TLC1 levels do not affect the fraction of TLC1 in the dimer form.

(A) TLC1 levels, both tagged and untagged, in the total RNA were measured in strains deleted for the indicated genes. The levels were normalized to PGK1 mRNA levels first and then to the wild-type levels. (B) Fraction of TLC1 in the dimer form was calculated from the coIP assay in strains deleted from indicated genes. The values are normalized to the average of the wild-type samples in each experiment. The error bars indicate the standard error among the samples, except for *ctr9Δ* sample, which was done only once. The one-sample t-test values for the comparison with the wild-type are denoted: * $p > 0.8$, ** $p > 0.3$, *** $p < 0.00005$. The pair-wise t-test values among the bracketed samples are indicated.

Figure 2-8. The Ku complex and Sir4 are required for TLC1 dimerization.

Fraction of TLC1 in the dimer form was calculated from the coIP assay in mutant strains as indicated. (A) Mutations defective in either telomere tethering to nuclear periphery or telomere silencing. (B) The Ku mutations were combined with *SIR4* deletion. The values are normalized to the average of the wild-type samples in each experiment. The error bars

indicate the standard deviation among the samples. The one-sample t-test values for the comparison with the wild-type are denoted: * $p > 0.1$, ** $p < 0.05$, *** $p < 0.0002$. The pair-wise t-test values among the bracketed samples are indicated.

Figure 2-9. The Ku and Sir4 combined with the mutation in the 3' region.
Fraction of TLC1 in the dimer form was calculated from the coIP assay in mutant strains as indicated. The values are normalized to the average of the wild-type samples in each experiment. The error bars indicate the standard error among the samples. The one-sample t-test values for the comparison with the wild-type indicate $p < 0.005$ for samples marked with **. The pair-wise t-test values among the bracketed samples are indicated.

Figure 2-10. Est2 interactions with TLC1.
(A) Pseudoknot structure critical for Est2 binding to TLC1 was mutated (cs3 and cs4) and compensatory mutation (cs3-cs4) was introduced. The fraction of TLC1 in the dimer form was calculated from the coIP assay. The values are normalized to the average of the wild-type samples in each experiment. The error bars indicate the standard error between two experiments. The one-sample t-test values for the comparison with the wild-type indicate $p < 0.05$ for samples marked with **. (B) The amount of TLC1 immunoprecipitated after sequential immunoprecipitation, anti-FLAG then anti-MYC, was measured. Amount of TLC1 remained in the MYC IP is represented as the fraction of TLC1 immunoprecipitated in the FLAG IP. The table below indicates EST2 fusions with specified tags present in each IP.

Figure 2-11. TLC1 dimerization model.

(A) A schematic of TLC1 polyadenylation and the cleavage of 3' region is shown. Tick marks represent the template region of TLC1. CGCGCG denotes the sequence at the 3' region that is important in TLC1 dimerization. AAA represents the polyadenylation. The stem-loop structure that the Ku complex binds is indicated. (B) We propose that there are two modes by which *TLC1* RNAs dimerize. The dimerization dependent on the 3' region is initiated before the 3' region is cleaved. TLC1 dimerization dependent on Sir4 and the Ku complex is at telomeres. The rectangles represent the telomeric repeats. (C) TLC1 in the telomerase RNP is either monomeric or dimeric, but each RNP contains only one Est2.

Table 2-1. Strains used in Chapter 2

All strains are in the S288c strain background and are isogenic, except as noted below.

Strain number	Relevant genotype
yEHB22,321	*ADE2 his3Δ1 leu2Δ0 lys2Δ0 met15Δ0 trp1Δ63 ura3Δ0 bar1Δ0 MATa*
yEHB22,465	*ADE2 his3Δ1 leu2Δ0 lys2Δ0 met15Δ0 trp1Δ63 ura3Δ0 bar1Δ0 MATa*
yEHB22,495	yEHB22,321 but *TLC1-MS2*
yEHB22,496	yEHB22,465 but *TLC1-MS2*
yEHB22,720	yEHB22,321 but *HIS3-P_{CYC1}-CP-3xMyc*
yEHB22,721	yEHB22,465 but *HIS3-P_{CYC1}-CP-3xMyc*
yEHB22,722	yEHB22,720 but *TLC1-MS2*
yEHB22,723	yEHB22,721 but *TLC1-MS2*
yEHB22,662	yEHB22,720 but *TLC1-URA3-TLC1-MS2*
yEHB22,663	yEHB22,721 but *TLC1-URA3-TLC1-MS2*
yEHB22,750	yEHB22,720 but *TLC1-LEU2-TLC1-MS2*
yEHB22,751	yEHB22,721 but *TLC1-LEU2-TLC1-MS2*
yEHB22,799	yEHB22,720 but *TLC1-URA3-TLC1*
yEHB22,800	yEHB22,721 but *TLC1-URA3-TLC1*
yEHB22,801	yEHB22,720 but *TLC1-MS2-URA3-TLC1-MS2*
yEHB22,802	yEHB22,721 but *TLC1-MS2-URA3-TLC1-MS2*
yEHB22,742	yEHB22,720 but *tlc1-42G-URA3-TLC1-MS2*
yEHB22.743	yEHB22,721 but *tlc1-42G-URA3-TLC1-MS2*
yEHB22.744	yEHB22,720 but *tlc1-42C-URA3-TLC1-MS2*
yEHB22.745	yEHB22,721 but *tlc1-42C-URA3-TLC1-MS2*
yEHB22.776	yEHB22,720 but *tlc1-42C-URA3-tlc1-42G-MS2*
yEHB22.777	yEHB22,721 but *tlc1-42C-URA3-tlc1-42G-MS2*
yEHB22,704	yEHB22,662 but *tgs1Δ::KanMX6*
yEHB22,705	yEHB22,663 but *tgs1Δ::KanMX6*
yEHB22,768	yEHB22,750 but *nup133Δ::KanMX6*
yEHB22,769	yEHB22,751 but *nup133Δ::KanMX6*
yEHB22,698	yEHB22,662 but *est1Δ::KanMX6*
yEHB22,699	yEHB22,663 but *est1Δ::KanMX6*
yEHB22,724	yEHB22,662 but *est2Δ::KanMX6*
yEHB22,725	yEHB22,663 but *est2Δ::KanMX6*
yEHB22,700	yEHB22,662 but *est3Δ::KanMX6*
yEHB22,701	yEHB22,663 but *est3Δ::KanMX6*
yEHB22,682	yEHB22,662 but *yku70Δ::KanMX6*
yEHB22,683	yEHB22,663 but *yku70Δ::KanMX6*
yEHB22,686	yEHB22,662 but *yku80Δ::KanMX6*

yEHB22,687	yEHB22,663 but *yku80Δ::KanMX6*
yEHB22,758	yEHB22,750 but *yku80-135i*
yEHB22,759	yEHB22,751 but *yku80-135i*
yEHB22,702	yEHB22,662 but *arf1Δ::KanMX6*
yEHB22,703	yEHB22,663 but *arf1Δ::KanMX6*
yEHB22,706	yEHB22,662 but *cdc73Δ::KanMX6*
yEHB22,707	yEHB22,663 but *cdc73Δ::KanMX6*
yEHB22,726	yEHB22,662 but *ctr9Δ::KanMX6*
yEHB22,727	yEHB22,663 but *ctr9Δ::KanMX6*
yEHB22,764	yEHB22,750 but *ctf18Δ::KanMX6*
yEHB22,765	yEHB22,751 but *ctf18Δ::KanMX6*
yEHB22,766	yEHB22,750 but *esc1Δ::KanMX6*
yEHB22,767	yEHB22,751 but *esc1Δ::KanMX6*
yEHB22,728	yEHB22,662 but *sir2Δ::KanMX6*
yEHB22,729	yEHB22,663 but *sir2Δ::KanMX6*
yEHB22,762	yEHB22,750 but *sir3Δ::KanMX6*
yEHB22,763	yEHB22,751 but *sir3Δ::KanMX6*
yEHB22,730	yEHB22,662 but *sir4Δ::KanMX6*
yEHB22,731	yEHB22,663 but *sir4Δ::KanMX6*
yEHB22,787	yEHB22,662 but *sir4-42::KanMX6*
yEHB22,788	yEHB22,663 but *sir4-42::KanMX6*
yEHB22,789	yEHB22,662 but *rif1Δ::KanMX6*
yEHB22,790	yEHB22,663 but *rif1Δ::KanMX6*
yEHB22,791	yEHB22,662 but *rif2Δ::KanMX6*
yEHB22,792	yEHB22,663 but *rif2Δ::KanMX6*
yEHB22,770	yEHB22,750 but *tel1Δ::KanMX6*
yEHB22,771	yEHB22,751 but *tel1Δ::KanMX6*
yEHB22,774	yEHB22,662 but *sir4Δ::KanMX6 yku80Δ::TRP1*
yEHB22,775	yEHB22,663 but *sir4Δ::KanMX6 yku80Δ::TRP1*
yEHB22,776	yEHB22,720 but *tlc1-42G-URA3-TLC1-MS2 yku80Δ::TRP1*
yEHB22,777	yEHB22,721 but *tlc1-42G-URA3-TLC1-MS2 yku80Δ::TRP1*
yEHB22,803	*LYS2 can1Δ::STE2$_P$-HIS5 lyp1Δ::STE3$_P$-LEU2*
yEHB22,804	*LYS2 can1Δ::STE2$_P$-HIS5 lyp1Δ::STE3$_P$-LEU2*
yEHB22,805	yEHB22,803 but *TLC1-MS2*
yEHB22,806	yEHB22,804 but *TLC1-MS2*
yEHB22,807	yEHB22,803 but *TLC1-URA3-TLC1-MS2*
yEHB22,808	yEHB22,804 but *TLC1-URA3-TLC1-MS2*
yEHB22,809	yEHB22,803 but *tlc1-42G-URA3-TLC1-MS2*
yEHB22,810	yEHB22,804 but *tlc1-42G-URA3-TLC1-MS2*
yEHB22,811	yEHB22,803 but *tlc1-42C-URA3-TLC1-MS2*

yEHB22,812	yEHB22,804 but *tlc1-42C-URA3-TLC1-MS2*
yEHB22,813	yEHB22,803 but *tlc2-42C-URA3-tlc1-42G-MS2*
yEHB22,814	yEHB22,804 but *tlc2-42C-URA3-tlc1-42G-MS2*
yEHB22,815	yEHB22,807 but *yku80-135i*
yEHB22,816	yEHB22,808 but *yku80-135i*
yEHB22,817	yEHB22,807 but *sir4Δ::KanMX6*
yEHB22,818	yEHB22,808 but *sir4Δ::KanMX6*
yEHB22,819	yEHB22,807 but *sir2Δ::KanMX6*
yEHB22,820	yEHB22,808 but *sir2Δ::KanMX6*
yEHB22,821	yEHB22,807 but *sir4Δ::KanMX6 yku80-135i*
yEHB22,822	yEHB22,808 but *sir4Δ::KanMX6 yku80-135i*
yEHB22,823	yEHB22,803 but *tlc1-42G-URA3-TLC1-MS2 yku80-135i*
yEHB22,824	yEHB22,804 but *tlc1-42G-URA3-TLC1-MS2 yku80-135i*
yEHB22,825	*EST2-3xFLAG/EST2-13xMyc MATa/α*
yEHB22,826	*EST2-3xFLAG/EST2 MATa/α*
yEHB22,827	*EST2-3xFLAG-13xMyc/EST2 MATa/α*

Table 2-2. Primer sequences for qRT-PCR

Amplicon	Primer number	Sequence (5' to 3')
PGK1	oEHB22,0716	GGCTGGTGCTGAAATCGTTCCAAA
	oEHB22,0717*	AGCCAGCTGGAATACCTTCCTTGT
Untagged *TLC1*	oEHB22,0561	CATCGAACGATGTGACAGAGAA
	oEHB22,0801*	GACAAAAATACCGTATTGATCATTAA
MS2-tagged *TLC1*	oEHB22,0563	ATGCCTGCAGGTCGACTCTAGAAA
	oEHB22,0338*	TGCGACAAAAATACCGTATTGATCA
Uncleaved, untagged *TLC1*	oEHB22,1015	TATCTATTAAAACTACTTTGATGATCAGTA
	oEHB22,1038*	AGCGATATACAAGTACAGTACGCGCG
Uncleaved, MS2-tagged *TLC1*	oEHB22,0339	AGCTTGCATGCCTGCAGGTCGACTC
	oEHB22,1038*	AGCGATATACAAGTACAGTACGCGCG
CLN2	oEHB22,712	TTGTTCGAGCTGTCTGTGGTCACT
	oEHB22,713*	AATTTGGCTTGGTCCCGTAACACG
CLN3	oEHB22,837	AAGGCCGCTGTACAACCTGACTAA
	oEHB22,838*	TGAACCGCGAGGAATACTTGTCCA

*Primer used in the reverse transcription step

Figure 2-1

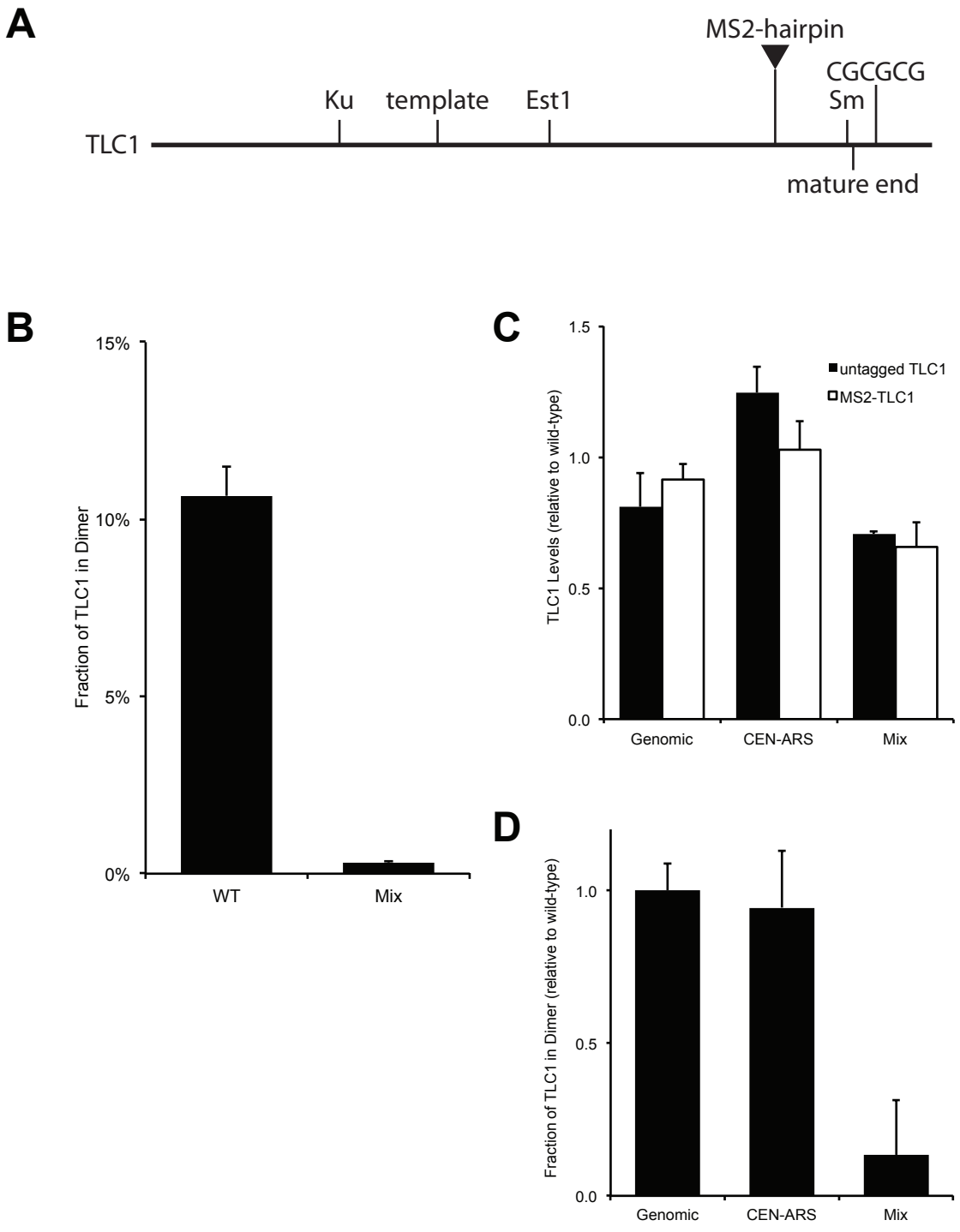
A
MS2-hairpin
CGCGCG
Sm
Ku
template
Est1
TLC1
mature end
B
15%
10%
5%
0%
Fraction of TLC1 in Dimer
WT
Mix
C
1.5
1.0
0.5
0.0
TLC1 Levels (relative to wild-type)
untagged TLC1
MS2-TLC1
Genomic
CEN-ARS
Mix
D
1.0
0.5
0.0
Fraction of TLC1 in Dimer (relative to wild-type)
Genomic
CEN-ARS
Mix

Figure 2-2

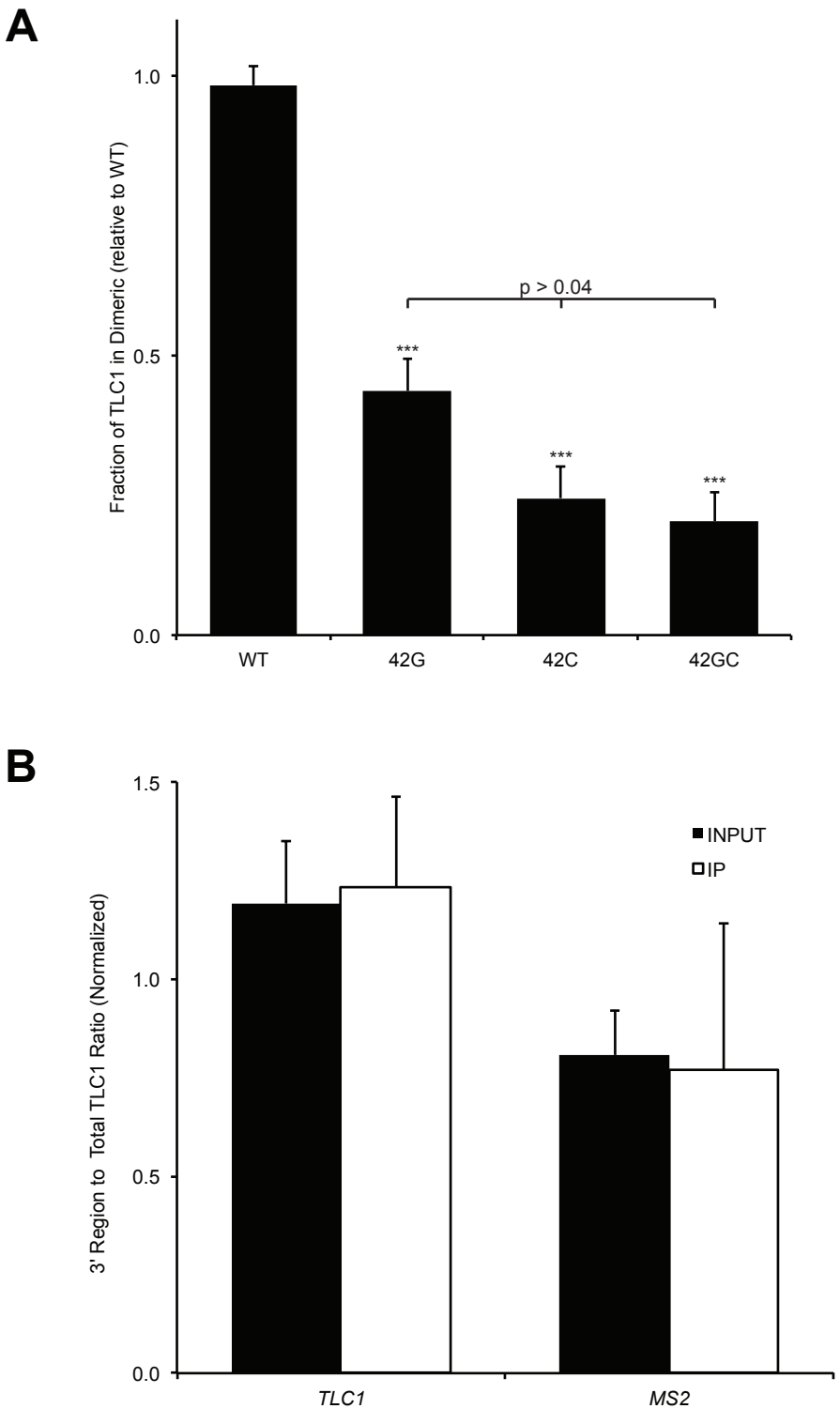
A
1.0
0.5
0.0
Fraction of TLC1 in Dimeric (relative to WT)
p > 0.04
***
***
***
WT
42G
42C
42GC
B
1.5
1.0
0.5
0.0
3' Region to Total TLC1 Ratio (Normalized)
INPUT
IP
TLC1
MS2

Figure 2-3

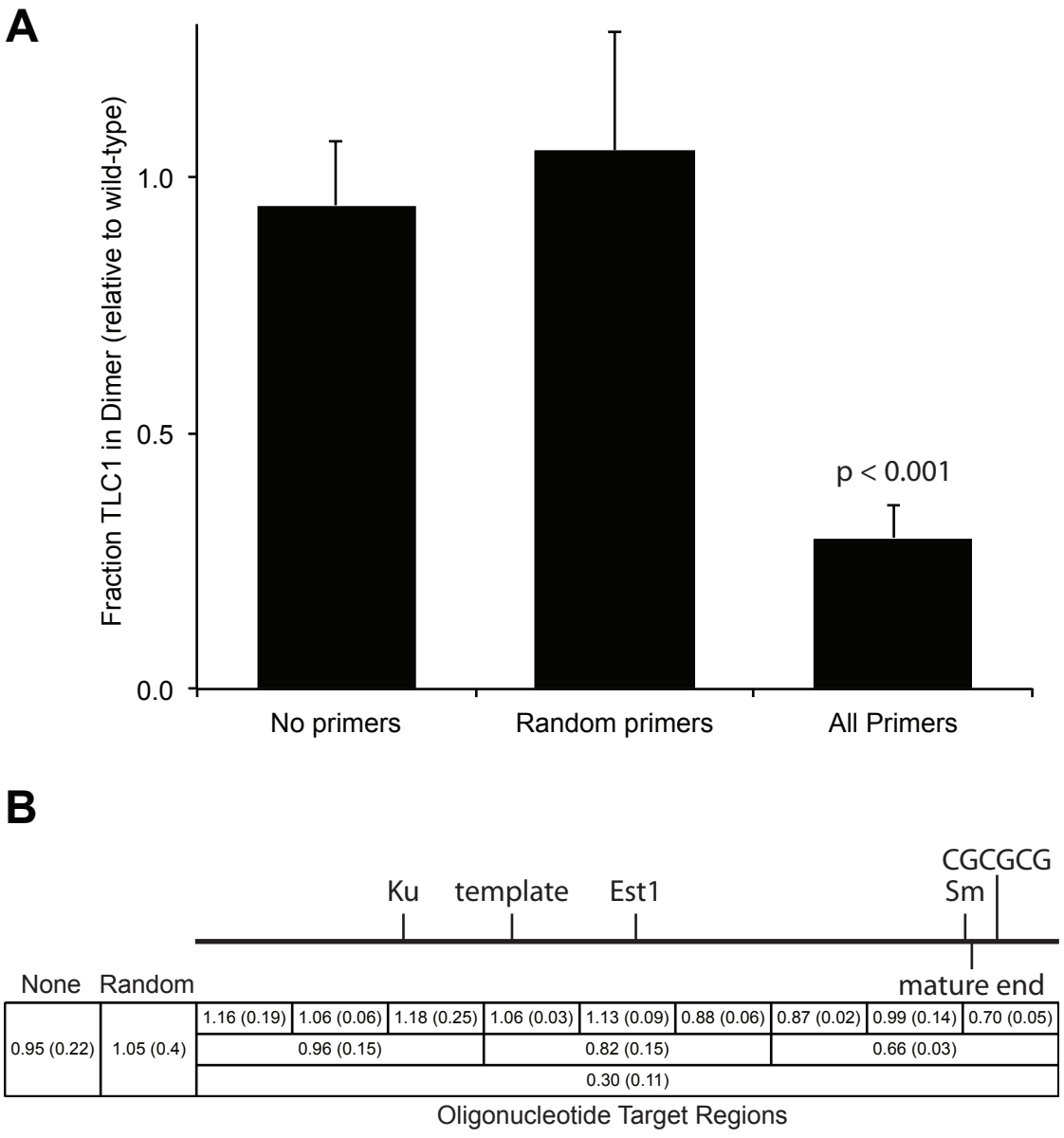
A
Fraction TLC1 in Dimer (relative to wild-type)
1.0
0.5
0.0
p < 0.001
No primers
Random primers
All Primers
B
Ku
template
Est1
CGCGCG
Sm
mature end
None
Random
0.95 (0.22)
1.05 (0.4)
1.16 (0.19)
1.06 (0.06)
1.18 (0.25)
1.06 (0.03)
1.13 (0.09)
0.88 (0.06)
0.87 (0.02)
0.99 (0.14)
0.70 (0.05)
0.96 (0.15)
0.82 (0.15)
0.66 (0.03)
0.30 (0.11)
Oligonucleotide Target Regions

Figure 2-4

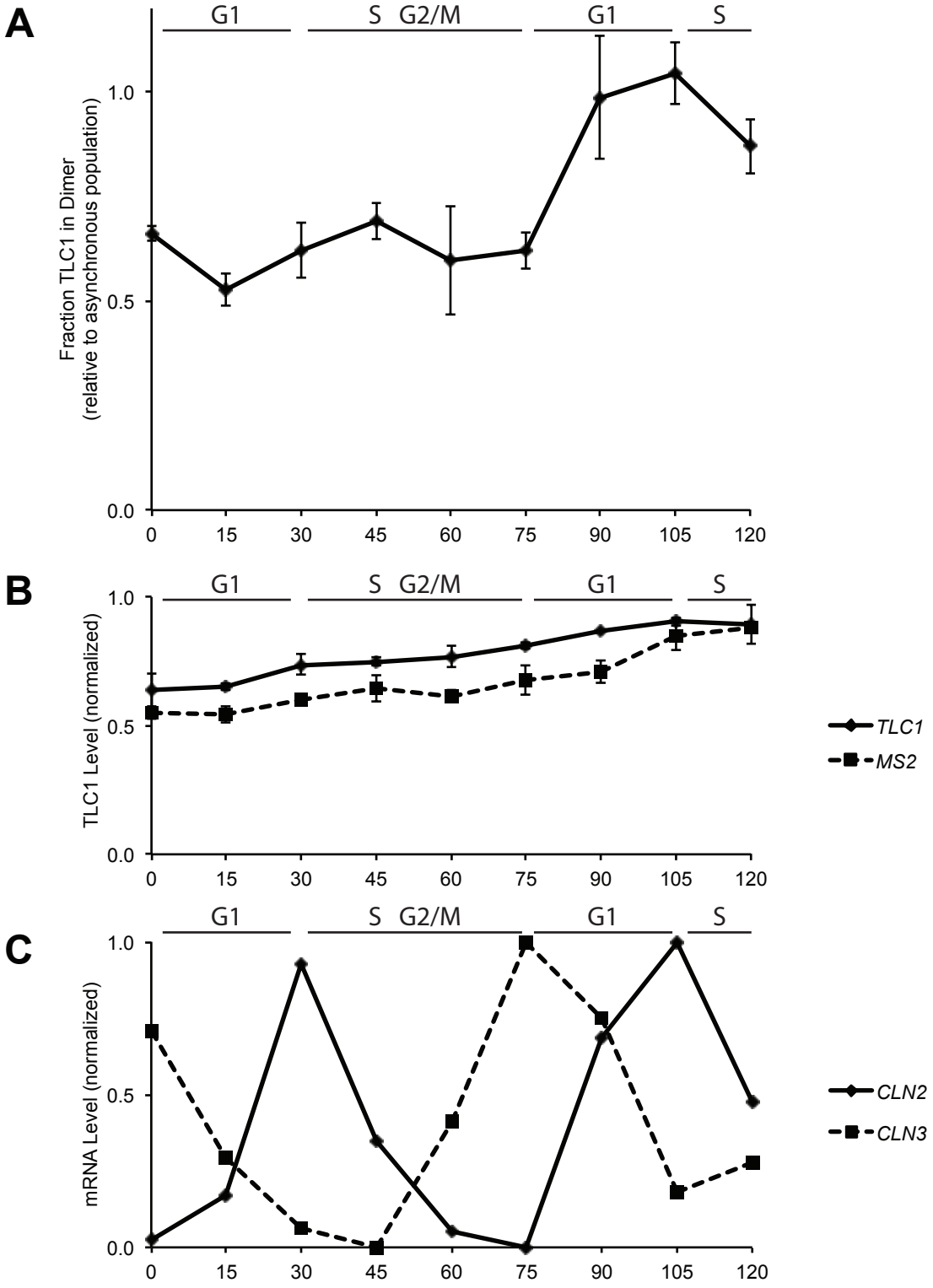
A
G1
S
G2/M
G1
S
Fraction TLC1 in Dimer
(relative to asynchronous population)
1.0
0.5
0.0
0
15
30
45
60
75
90
105
120
B
G1
S
G2/M
G1
S
TLC1 Level (normalized)
1.0
0.5
0.0
0
15
30
45
60
75
90
105
120
TLC1
MS2
C
G1
S
G2/M
G1
S
mRNA Level (normalized)
1.0
0.5
0.0
0
15
30
45
60
75
90
105
120
CLN2
CLN3

Figure 2-5

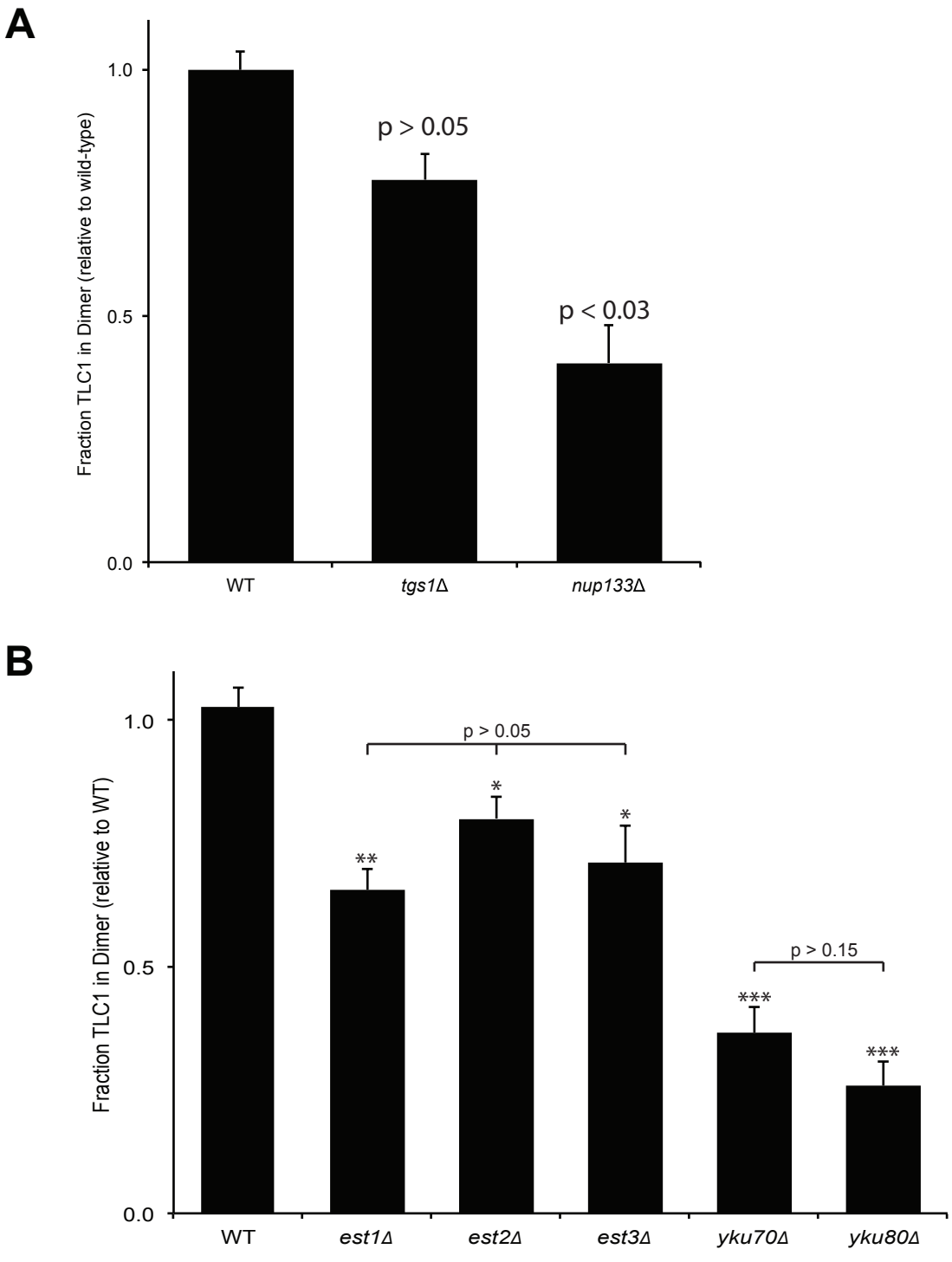
A
Fraction TLC1 in Dimer (relative to wild-type)
1.0
0.5
0.0
p > 0.05
p < 0.03
WT
tgs1Δ
nup133Δ
B
Fraction TLC1 in Dimer (relative to WT)
1.0
0.5
0.0
p > 0.05
p > 0.15
**
*
*
***
***
WT
est1Δ
est2Δ
est3Δ
yku70Δ
yku80Δ

Figure 2-6

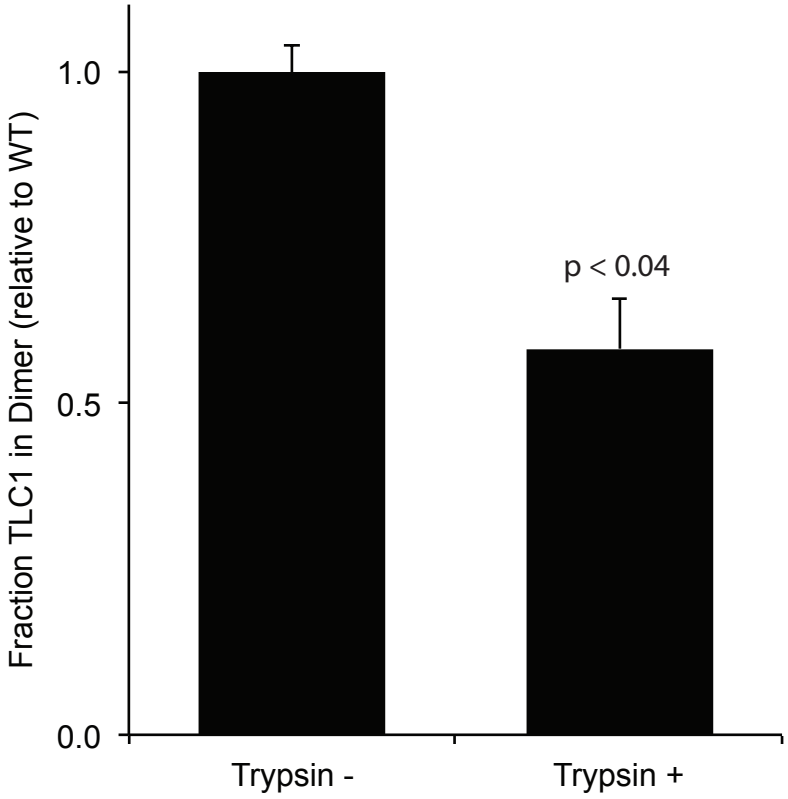
Fraction TLC1 in Dimer (relative to WT)
1.0
0.5
0.0
p < 0.04
Trypsin -
Trypsin +

Figure 2-7

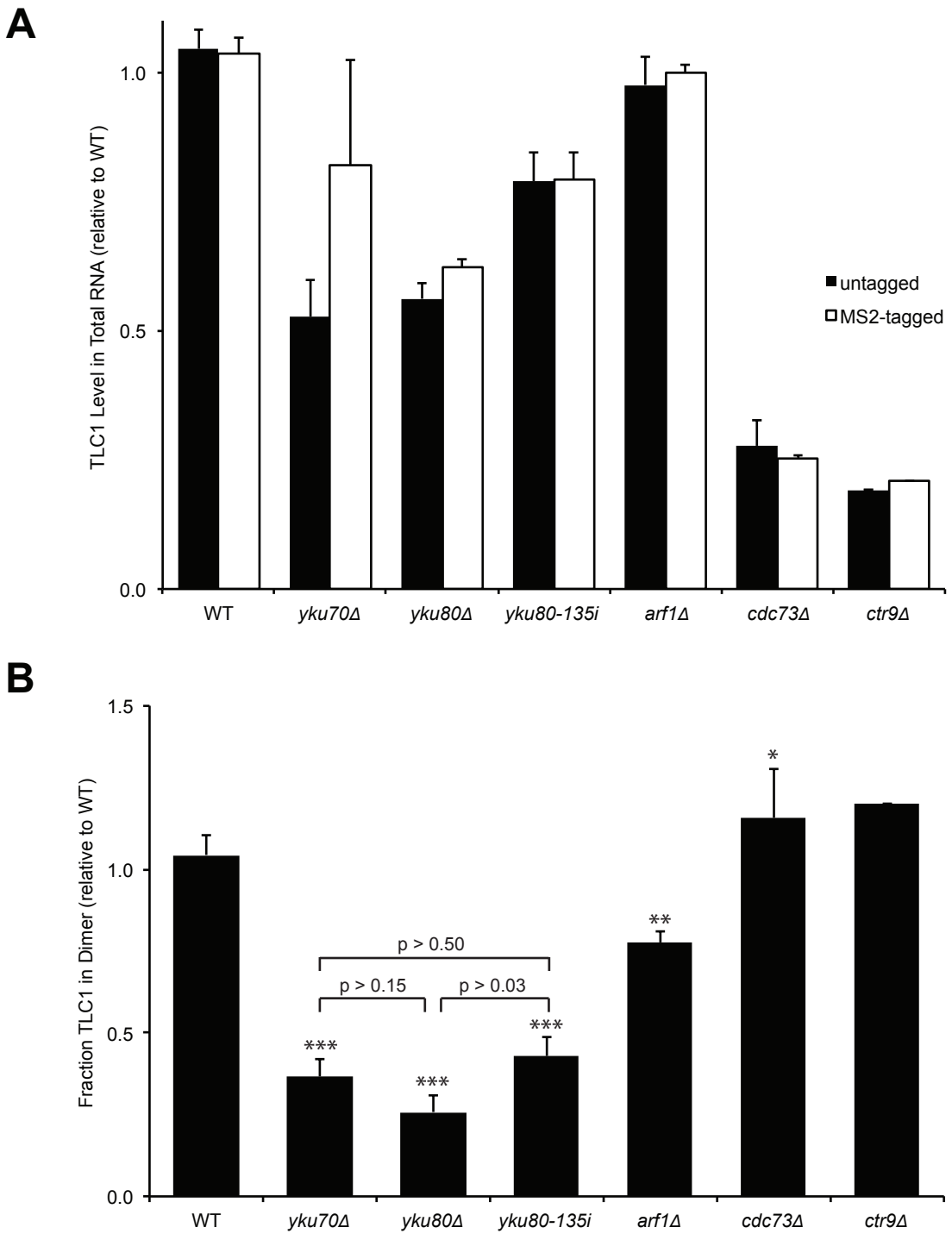
A
TLC1 Level in Total RNA (relative to WT)
1.0
0.5
0.0
untagged
MS2-tagged
WT
yku70Δ
yku80Δ
yku80-135i
arf1Δ
cdc73Δ
ctr9Δ
B
Fraction TLC1 in Dimer (relative to WT)
1.5
1.0
0.5
0.0
p > 0.50
p > 0.15
p > 0.03
***
***
***
**
*
WT
yku70Δ
yku80Δ
yku80-135i
arf1Δ
cdc73Δ
ctr9Δ

Figure 2-8

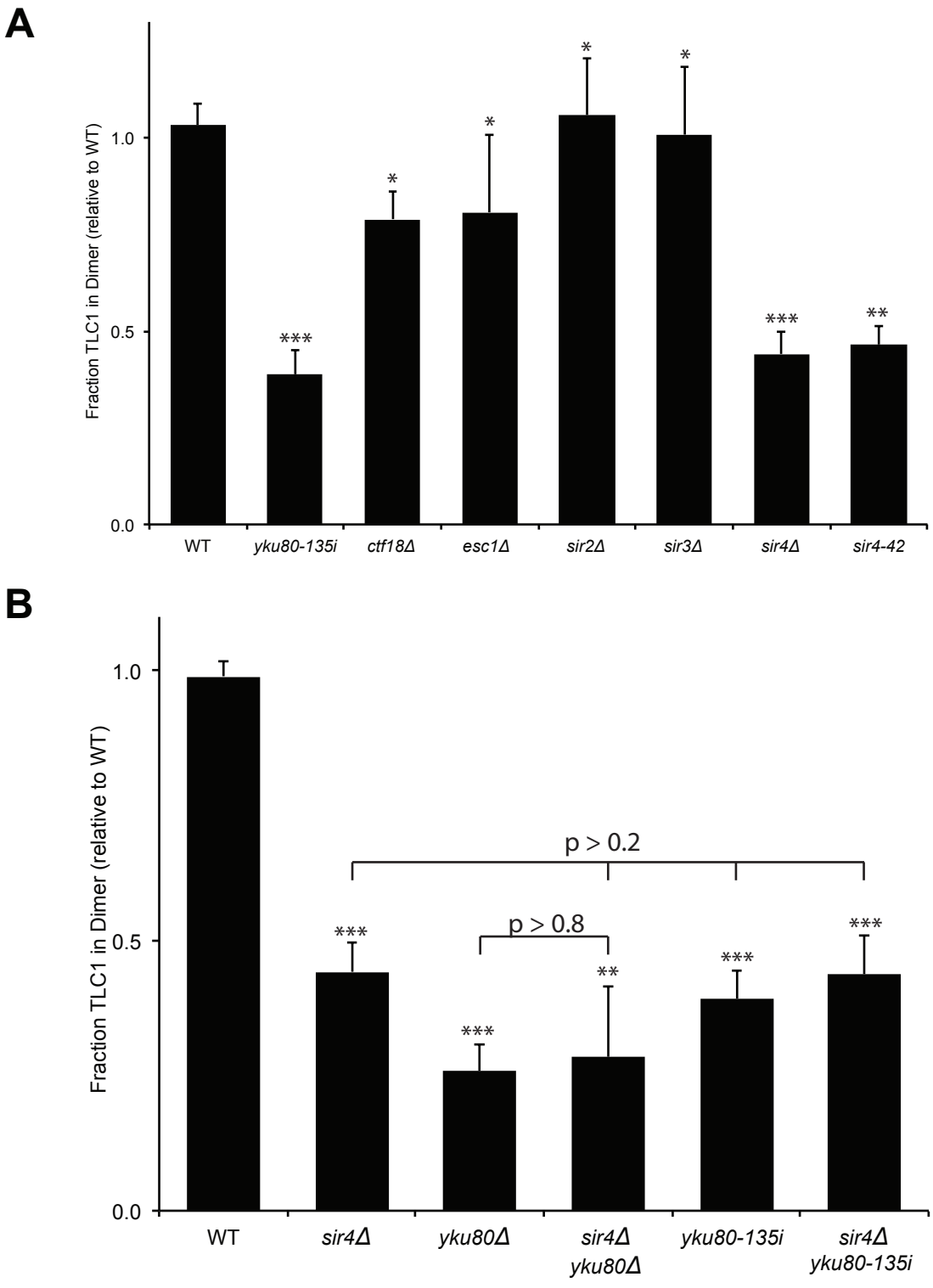
A
Fraction TLC1 in Dimer (relative to WT)
1.0
0.5
0.0
***
*
*
*
*
***
**
WT
yku80-135i
ctf18Δ
esc1Δ
sir2Δ
sir3Δ
sir4Δ
sir4-42
B
Fraction TLC1 in Dimer (relative to WT)
1.0
0.5
0.0
p > 0.2
p > 0.8
***
***
**
***
***
WT
sir4Δ
yku80Δ
sir4Δ yku80Δ
yku80-135i
sir4Δ yku80-135i

Figure 2-9

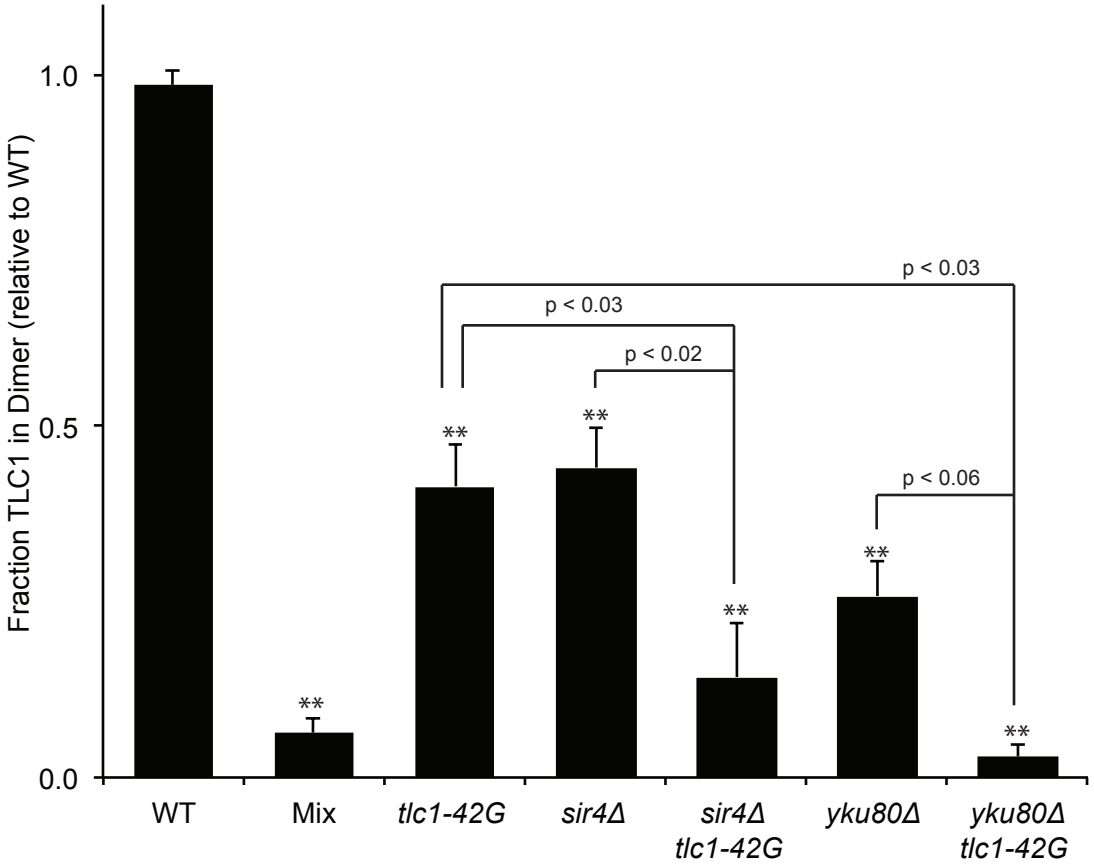
Fraction TLC1 in Dimer (relative to WT)
1.0
0.5
0.0
p < 0.03
p < 0.03
p < 0.02
p < 0.06
**
WT
Mix
tlc1-42G
sir4Δ
sir4Δ tlc1-42G
yku80Δ
yku80Δ tlc1-42G

Figure 2-10

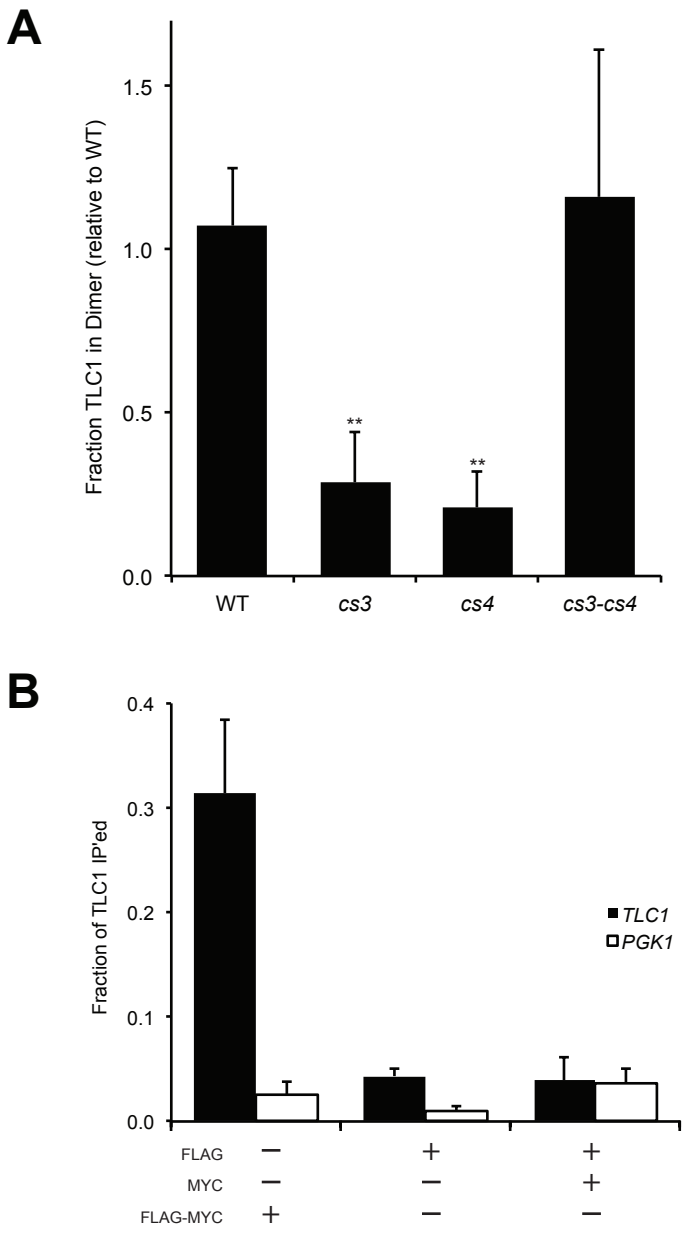
A
Fraction TLC1 in Dimer (relative to WT)
1.5
1.0
0.5
0.0
**
**
WT
cs3
cs4
cs3-cs4
B
Fraction of TLC1 IP'ed
0.4
0.3
0.2
0.1
0.0
TLC1
PGK1
FLAG
MYC
FLAG-MYC
− + +
− − +
+ − −

Figure 2-11

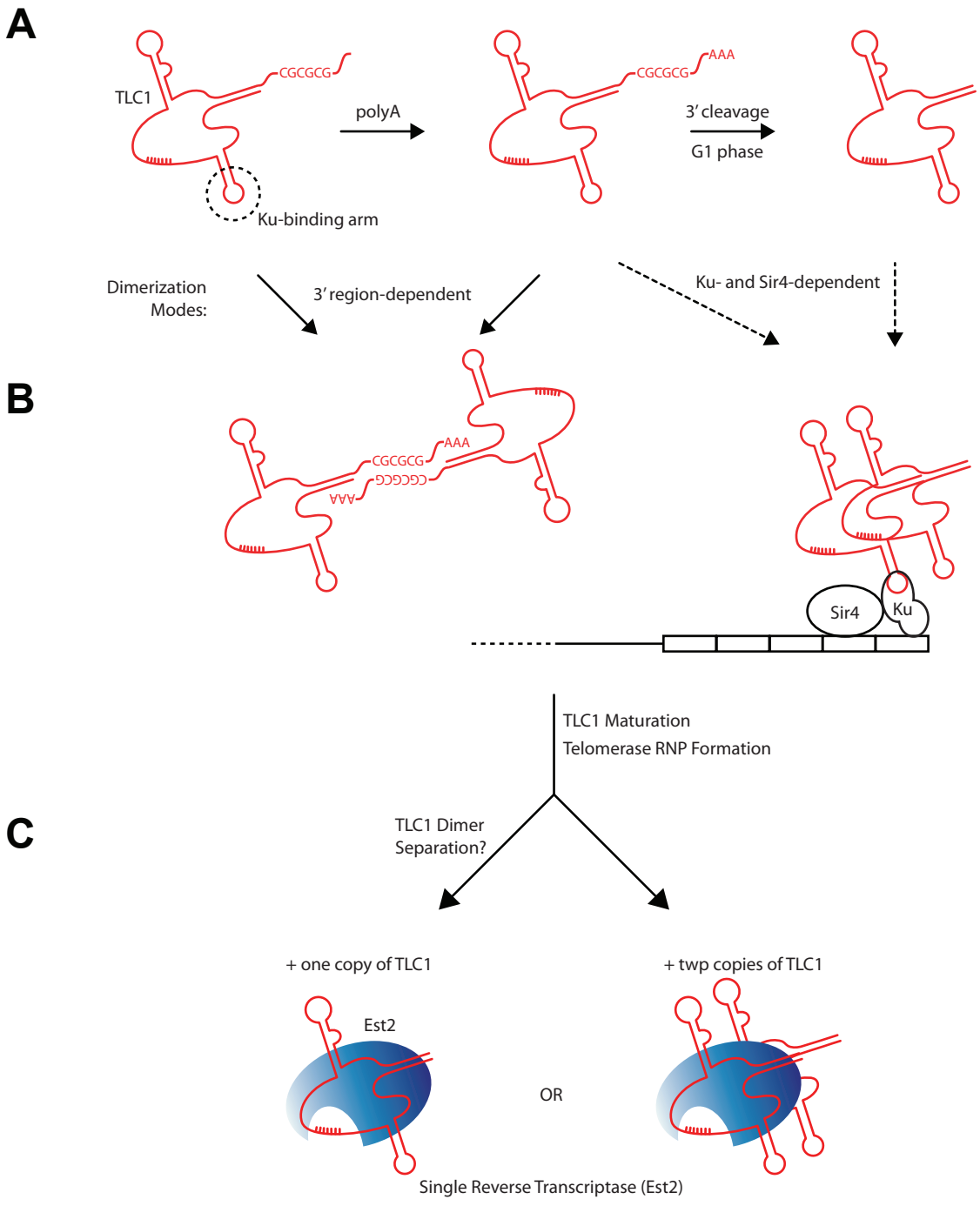
A
TLC1
CGCGCG
polyA
AAA
CGCGCG
3′ cleavage
G1 phase
Ku-binding arm
Dimerization
Modes:
3′ region-dependent
Ku- and Sir4-dependent
B
CGCGCG
AAA
CGCGCG
AAA
Sir4
Ku
C
TLC1 Maturation
Telomerase RNP Formation
TLC1 Dimer
Separation?
+ one copy of TLC1
+ twp copies of TLC1
Est2
OR
Single Reverse Transcriptase (Est2)

Chapter 3: Est1 and Est3 Modulate Telomerase Template Access

Tetsuya Matsuguchi and Elizabeth H. Blackburn

Department of Biochemistry and Biophysics

University of California, San Francisco

San Francisco, CA 94158

Results

Telomerase containing tlc1-476gug is active

To detect the *in vivo* usage of the template mutant, *tlc1-476gug*, a quantitative PCR (qPCR) method was developed to measure the number of mutant telomeric repeats incorporated into telomeres as a result of copying of the 476gug template. The 476gug mutant template-specific oligonucleotide (see Materials and Methods) was designed such that the GTG sequence unique to the mutant telomeric repeats is near the 3' end of the reverse primer (Figure 3-1A). The forward primer was designed to anneal to the most common 22-mer sequence present in the wild-type telomeres (Figure 3-1A). The PCR products were specific to GTG containing telomeres and the assay showed linearity of signal over four orders of magnitudes (Figure 3-1B).

Wild-type TLC1 was expressed from its endogenous locus, and *tlc1-476gug* gene was introduced on a CEN-ARS plasmid. A colony carrying this plasmid was picked from a selective medium plate and patched before DNA extraction (at a time point corresponding to ~40 generations of carrying *tlc1-476gug*). To determine the specificity

of the qPCR method in detecting 476gug repeats incorporated into telomeres, the experiment was also carried out in *est1Δ*, *est2Δ*, *est3Δ*, and *tlc1Δ* survivor strains. In these strains telomeres are maintained by recombination and not by telomerase, and these strains therefore served as negative controls for detection of mutant 476gug-directed repeat incorporation. As expected, there was a robust 476gug incorporation in the wild-type strain co-expressing chromosomal *TLC1* and the CEN-ARS-plasmid-borne *tlc1-476gug* gene, while there were no detectable 476gug repeats incorporated into DNA in *est1Δ*, *est2Δ*, or *est3Δ* strains (Figure 3-1C). Surprisingly, in *tlc1Δ* cells expressing only *tlc1-476gug* and no other telomerase RNA, 476gug telomeric repeats were detected in small amounts, but significantly above background (Figure 3-1C).

This was the first finding that suggests that *tlc1-476gug* telomerase is not completely catalytically inactive, as formerly reported. Previously, the telomerase enzyme containing the mutant template 476gug was reported to be catalytically inactive, based on two main criteria: the *in vitro* telomerase telomeric DNA polymerization assay using a non-PCR-based method, and its classic senescence phenotype, which showed progressive telomeric DNA shortening and senescence rates indistinguishable from those of telomerase deletion mutants (Prescott and Blackburn 1997a).

Rescue of 476gug mutant repeat incorporation is dependent on the template sequence of the co-expressed *tlc1* allele

The senescence phenotype of the template mutation *tlc1-476gug* is quite unusual for telomerase RNA template mutants, and in order to determine what aspect of the template

mutation leads to senescence, a previous study in this laboratory introduced all 64 possible sequences (including wild-type) at the 474-476 positions, which are within the template sequence of the *TLC1* gene (Lin *et al*. 2004a). These template mutations led to different classes of telomere phenotypes: short-and-stable, elongated, degraded, and mixed lengths. Notably, however, only *tlc1-476gug* was senescent, giving no further clue as to the nature of this seemingly inactive telomerase.

The other interesting aspect of the *tlc1-476gug* mutation is that the mutant template can be used by telomerase to incorporate mutant telomeric repeats in the presence of co-expressed wild-type *TLC1*. To determine the role of the wild-type template in rescuing the 476gug template, the same 64 template mutants described above were each in turn co-expressed with *tlc1-476gug*. Genomic DNA from each of the 58 strains (some of the previously constructed mutations were re-sequenced and found to be incorrect) was extracted, and the amount of 476gug repeats incorporation was measured as described above (Figure 3-2A). First, 12 template mutations were able to allow up to an order of magnitude of higher levels of 476gug mutant repeat incorporation than co-expressed wild-type template *TLC1*. However, most of the 58 mutations were less capable of rescuing the 476gug template usage. The top three 476gug mutant template rescuers had the wild-type sequence except at template nucleotide position 476 (AC*t*, AC*a*, AC*g*). Surprisingly, there were a few templates that slightly inhibited 476gug template usage; in those cases, lower levels of 476gug mutant repeats were incorporated into telomeres than when *tlc1-476gug* was expressed alone. The class of telomere phenotype of the co-expressed template mutations (short-and-stable, elongated, degraded,

etc.) had no strict correlation with how well the 476gug template was used, although there was a trend toward short-and-stable telomere phenotype template mutants being less efficient, and degraded-telomere phenotype template mutants being more efficient, at stimulating 476gug repeat incorporation. Strikingly, when the levels of 476gug incorporations were log normalized to the wild-type level, they showed a fairly uniform distribution across all 58 template sequences (Figure 3-2B).

Next, we looked at whether a particular nucleotide at each of the 3 positions mutated (474-476) was preferred for the ability to rescue 476gug mutant template. In overview, first, regardless of how the calculation was performed, the overall pattern was that G residues at any of positions 474, 475 or 476 were strongly disfavored for the *trans* rescue of co-expressed 476gug template usage as measured by the GTG sequence incorporation into telomeric DNA. For each template, the log of relative efficiency at rescuing 476gug mutant template usage was calculated. These values were totaled for each nucleotide at each of the 3 positions. Finally, relative contribution of each nucleotide at each position was expressed as the percent of total at each position (Figure 3-2C). This analysis showed that C and A nucleotides are generally preferred at each position for *trans* 476gug template rescue; these are the nucleotides that are present in the wild-type template. The result was comparable to the result of a screen searching for templates that can support cell growth (Förstemann *et al*. 2003). Both results show that telomerase prefers C's and A's. The same analysis was done without the log normalization (Figure 3-2D). This analysis showed strong preference for A at position 474 and C at position 475, while there was no preference at position 476, and G's were

strongly disfavored at all positions. This non-log normalized effect was largely driven by the best three template mutations that rescued 476gug template usage, because when these three were eliminated, no specific preference remained, except that G's were still disfavored (Figure 3-2E).

We tested whether the palindromic nature of *tlc1-476gug* (CACgugCAC) might make this template inactive. According to this model, two copies of the 476gug mutant template on two separate *TLC1* telomerase RNA molecules can anneal to each other and thereby prevent access to the template by the telomerase catalytic site (Figure 3-3A). In this model, this hybridization can be prevented in presence of wild-type template, because wild-type and 476gug templates do not have a significant complementarity. A prediction of this model is that the complementarity of the other, co-expressed template mutations would correlate with how well they rescue 476gug template usage. Specifically, the observed disfavoring of G residue(s) in the co-expressed mutant template telomerase RNA for conferring rescue of 476gug template usage, as described above, might similarly be predicted from this model, because such G residue(s) would allow some base-pairing of that template with the C- and A-rich 476gug template. The hybridization potential of each mutant template to 476gug template was calculated using a simple RNA folding program and given as ΔG (kcal / mol). These values were plotted against the ability of each template to rescue 476gug template usage (Figure 3-3B).

A subset of the mutants seems to fit the proposed model. A Boolean distribution was seen as follows: Of all the 58 mutants examined, 41 mutants (including 476gug) produced GTG/PGK1 incorporation of less than 0.7. In contrast, for the remaining 17

mutants GTG/PGK1 ratios of over 0.7 were seen for all 15 mutants with predicted ΔG values of -3.4 kcal / mol (including wild-type), but only two template mutants with a lower predicted ΔG value (-8.2 kcal / mol) fell into this category of a greater than 0.7 GTG/PGK1 incorporation level. A good number of mutations, that show little or no complementarity, still spanned the entire range of ability to rescue 476gug template usage. However, interpretation of this set of data is confounded by at least two factors: 1. Each of the mutant templates may have very different levels of overall telomerase activity, such that it cannot be excluded that apparent low rescue could have resulted from a bias in the telomerase activity readout caused by expression of the mutant template; although this would not be expected to affect the incorporation of GTG repeats by the 476gug telomerase itself, there could have been indirect or unknown effects of interaction of the co-expressed mutant template with the 476gug telomerase; and 2. The resulting mutant telomeric repeats often disrupt other telomere binding proteins and hence would be selected against in cells, leading to their under-representation in the DNA extracted for analysis of 476gug repeat DNA incorporation. This effect could lead to unpredictable biases in the quantity of GTG template incorporation that was measured against the normalizing PGK1 level.

Effect of mutations in telomerase subunit *EST1* on 476gug template utilization

Est1 binds directly to both telomerase RNA, TLC1, and to the telomeric single-strand DNA binding protein Cdc13, and through these interactions, Est1 recruits the telomerase enzyme complex to telomeres (Zhou *et al*. 2000; Qi and Zakian 2000; Pennock *et al*.

2001). In addition, it has been suggested that Est1 also has a role in the "activation" of telomerase activity: In strains expressing Cdc13-Est2 fusions, which bypass Est1's role in telomerase recruitment, the presence of Est1 significantly increases telomere lengths (Evans and Lundblad 1999). A series of mutations separating the recruitment versus "activation" functions of Est1 supported this interpretation of the roles of Est1 in telomerase activity *in vivo* (Evans and Lundblad 2002). A recent publication has suggested that this "activation" function may relate to Est1's ability to promote formation of a DNA G-quartet structure (Zhang *et al*. 2010). Est1 has been shown to promote telomeric single-stranded DNA into a G-quartet structure *in vitro*; the same point mutations that disrupted Est1's ability to form a G-quartet *in vitro* resulted in shortening of telomeres *in vivo*. In addition, the same residues required for G-quartet formation also were required for separating telomeric DNA hybridized to RNA *in vitro* (Zhang *et al*. 2010). This inferred helix-destabilizing function of Est1 could, therefore, also be important for separating potential template-template interactions between 476gug mutant templates.

To test the possibility that Est1 plays a role in 476gug template usage rescue, a library of *est1* mutations was assayed for their ability to affect incorporation of 476gug mutant repeats into telomeres, in the genetic setting of co-expressed wild-type *TLC1* and *tlc1-476gug* (Evans and Lundblad 2002 and see Table 3-1). First, when these *est1* mutants were introduced into either an *est1Δ* strain or an *est1Δ* strain expressing a Cdc13-Est2 fusion, the amount of 476gug mutant repeats in telomeres correlated perfectly well with the overall telomere length (*i.e*. with the level of telomerase activity; Figure 3-4 A

and B). Hence this finding also provided an independent validation of the quantification method developed to measure *in vivo* incorporation of 476gug mutant repeats.

In order to measure the ability of each *est1* mutant to rescue 476gug template usage specifically, an additional template mutation, *tlc1-476ucu*, was employed. Independent experiments were first done to show that this template mutation does not require a wild-type template for incorporation of its specified telomeric DNA repeats and that it can rescue 476gug template usage just as well as wild-type (Figure 3-2A, "TCT"; and data not shown). The main advantage of introducing another template mutation is to be able to measure its incorporation in the sea of pre-existing and other wild-type telomeric sequences. The amount of 476ucu repeat incorporation, which occurs under the influence of a specific *est1* mutant in this case, therefore, serves to normalize for telomerase activity. After the amount of 476gug mutant repeat incorporation was normalized to the amount of 476ucu mutant repeat incorporation, five *est1* mutations showed levels of 476gug incorporation similar to vector control (indicating that these *est1* mutants could not support rescue of 476gug incorporation), while others were similar to the wild-type *EST1* level. The "activation" function has been shown to be defective in *est1-42*, *est1-52*, and *est1-Δ19*. Those *est1* mutations that could not support 476gug mutant template rescue included *est1-42*, *est1-52*, and *est1-Δ19*. In addition, the remaining two *est1* mutations that could not support 476gug mutant template rescue were *est1-7* and *est1-47*. The *est1-7* and *est-47* mutations are located in the same region of Est1 as *est1-42* and *est1-Δ19*. The 476gug incorporation level in *est1-7*, *est1-47* and *est1-52* showed similar levels to the wild-type level before the normalization (that was done

using 476ucu mutant incorporation level), emphasizing the specificity of the "activation" defect in 476gug rescue, as opposed to a telomerase recruitment defect. We note that the G-quartet formation *in vitro* assay has also been reported to be impaired in *est1-52*. Other *est1* mutants have not been described for this *in vitro* phenotype.

Effect of mutations in telomerase subunit *EST3* on 476gug template utilization

The exact role of Est3 in telomerase activity remains elusive. Some of the suggested functions for Est3 have included facilitating telomerase processivity, an intrinsic telomeric RNA-DNA hybrid helicase activity, and a GTPase activity (Lee *et al*. 2010; Sharanov *et al*. 2006; Shubernetskaya *et al*. 2011). The potential RNA-DNA helicase activity of Est3 is intriguing in that a similar role has been proposed for Est1, and as described above, Est1 has specific effects on 476gug template usage. In turn, our present findings and previous findings suggest the possibility of 476gug template-template hybridization interactions that are intermolecular, which might be affected by these putative roles for Est1 and Est3, or be competed out by template-DNA hybridization. In addition, at high concentrations, Est3 has been reported to have an ability to dimerize *in vitro*. While this dimerization may not be relevant physiologically *in vivo*, some mutations at conserved residues have been found to disrupt this reported ability of Est3 to dimerize *in vitro* (Yang *et al*. 2006).

To test the role of Est3 in 476gug template usage rescue, we carried out the same sets of experiments as done for *est1* mutations. In each *est3* mutant background, the levels of 476gug and 476ucu mutant repeat incorporations were measured (Figure 3-5).

This analysis showed that in addition to those mutations reported to disrupt Est3 dimerization (at high Est3 concentrations *in vitro*), several of the *est3* mutations that cause short telomere phenotypes had defects in rescue of 476gug repeat incorporation. However, the degrees of telomere shortness caused by the various *est3* mutants did not correlate well with the extents of 476gug incorporation rescue. Also, the extents of 476gug rescue did not correlate well with the reported effects of the *est3* mutations on *in vitro* Est3 dimerization. Together, these findings indicate that the effects of *est3* mutations on 476gug rescue in the presence of co-expressed wild type TLC1 are not simply accounted for by effects on Est3's known functions in activating telomerase. Furthermore, they were not correlated with the putative effects reported on Est3 dimerization.

Effects of Sir4 and Ku complexes on 476gug template utilization

Sir4- and Ku-containing complexes are important for the physical interaction between two *TLC1* RNAs (see Chapter 2 of this thesis). Furthermore, as described in Chapter 2, epistasis experiments, suggested that Ku and Sir4 act in the same pathway to cause interaction between two different, co-expressed, TLC1 molecules, as was measured by their pull-down in the same complex from lysed cell extracts. To test whether this physical association between TLC1 molecules *in vivo* (TLC1 dimerization) plays a role in the functional interaction between different mutant templates manifested in 476gug template rescue, the level of 476gug mutant repeat incorporation was measured in *sir4Δ*, *yku70Δ* and *yku80Δ* cells. In addition, *sir2Δ* strains were tested. Sir2 is not required for

TLC1 dimerization (see Chapter 2 of this thesis). In contrast, most known other functions of Sir4 (notably, in silencing) require Sir2.

Similarly to the experiments described above, *tlc1-476gug* and *tlc1-476cuu* template mutants were co-expressed along with the wild-type TLC1. When the level of 476gug mutant repeat incorporation was normalized to the level of 476cuu mutant repeat incorporation, *sir2Δ* and *sir4Δ* strains showed increased levels of 476gug repeats compared to wild-type. However, *yku70Δ* and *yku80Δ* cells showed decreased levels of 476gug repeat compared to wild-type (Figure 3-6, A and B). The disparity in the measured level of 476gug mutant repeat incorporation between the Sir complex and the Ku complex suggests that physical dimerization of TLC1 is not the only contributing factor in the rescue of 476gug template usage. However, confounding the interpretation of these results, in *sir2Δ* and *sir4Δ* cells the amount of 476gug incorporation was quite variable from colony to colony (Figure 3-6A), possibly due to increased level of recombination at telomeres in absence of the Sir complex.

Telomerase complex pull-down with telomeric substrate DNA oligonucleotides

A previous study concluded that a dimeric telomerase complex containing two *tlc1-476gug* RNAs does not have any detectable telomerase activity *in vitro*, while a heterodimeric complex from a DEAE-agarose column fractionated cell lysate containing co-expressed wild-type *TLC1* and *tlc1-476gug* RNAs can extend two primer substrates that separately use the wild-type and 476gug templates (Prescott and Blackburn 1997b). These previous experiments took advantage of the stable interaction between telomerase

and its elongation reaction product, the extended telomeric oligonucleotide substrate. In brief, it was found that in incubations using extracts of cells co-expressing *tlc1-476gug* and wild type *TLC1* RNAs, biotinylated 476gug mutant template-specific reaction products, following elongation of the DNA oligonucleotide substrates using dNTPs supplied *in vitro*, specifically associated with the product of simultaneously added wild-type specific substrate, but not with a simultaneously added, 476gug-specific DNA oligonucleotide elongated substrate.

To test whether un-elongated substrate-dependent pull-down of telomerase complex can occur, biotinylated DNA oligonucleotide substrates were added to a final concentration of ~1 uM to S100 cell lysates and incubated in the telomerase activity assay buffer with or without 100 uM dNTPs (see Materials and Methods). To assess the level of telomerase associated with the biotinylated DNA substrate/elongation product, TLC1 amount in the substrate/elongation product-bound fraction was quantified. TLC1 was enriched at similar levels regardless of dNTP addition (Figure 3-7A). To eliminate the possibility that there were enough dNTPs for telomerase reaction already present in the S100 lysates, 3' amino-labeled telomeric substrates, which do not allow any addition of nucleotides, were used to pull-down telomerase in presence of dNTPs. Consistent with the experiment above, both extendable and non-extendable substrates were able to pull down TLC1 at similar levels (Figure 3-7B).

To ensure the TLC1 pull-down was representative of telomerase complex pull-down and not just TLC1, the same assay with dNTPs was performed on extracts prepared from wild-type *EST2*, *est2Δ*, and *est2-530A* (catalytically dead telomerase) strains. This

experiment showed not only that TLC1 pull-down by telomeric substrate is Est2-dependent, but also the substrate was able to pull down catalytically dead telomerase significantly more than wild-type telomerase (Figure 3-7C). These sets of experiments provided strong evidence that in the conditions tested here -- namely, in the S100 fraction of cell extracts -- an un-extended telomeric DNA substrate can bind tightly to telomerase complex *in vitro*.

Discussion

The *tlc1-476gug* telomerase has low but measurable activity

The new quantitative method developed for measuring *tlc1-476gug* template usage, by assessing 476gug template-directed DNA repeat incorporation into telomeres *in vivo*, allowed detection of small but detectable amount of telomerase activity of this mutant. Previously, the telomerase enzyme containing the mutant template *tlc1-476gug* was reported to be catalytically inactive, based on two main criteria: the *in vitro* assay, and its classic senescence phenotype, with a telomere shortening rate indistinguishable from that of telomerase deletion mutants. Those former reports had been based on the combined phenotypes of failure to detect *in vitro* activity of the *tlc1-476gug* telomerase using a conventional (non-PCR-based) assay, and the observed progressive telomere shortening (EST or Ever Shortening Telomeres phenotype) and senescence phenotype of *tlc1-476gug* cells. Furthermore, like a classic telomerase gene deletion strain, following the senescent stage the *tlc1-476gug* cells also showed the emergence of survivors, which have recombination-maintained telomeres, at rates similar to telomerase deletion strains.

The other previous method for detecting the mutant repeat incorporation was based on the palindromic DNA sequence, CACGTGCAC, created by the 476gug template. This sequence is recognized by ApaLI and PmlI restriction digest enzymes; therefore, the presence of the palindromic sequence can be detected by the size change on telomere Southern blot (teloblot) when DNA is digested by mutant-specific restriction enzymes (Prescott and Blackburn 1997a). This method was limited to detecting whether there is none or at least one incorporated mutant telomeric repeat per telomere. The small number of 476gug repeats detected and the continuous shortening of telomeres in *tlc1-476gug* strains suggest that 476gug repeats are likely to be present only at near the distal end of telomeres, which would make the size difference discrimination on a teloblot difficult, and a low level of incorporation could have been missed. It also cannot be excluded that in addition to the significantly decreased inherent *in vitro* enzymatic activity of *tlc1-476gug* telomerase, the predicted inability of the 476gug-specified terminally-incorporated telomeric repeat sequences to bind Rap1, which was demonstrated directly *in vitro* (Prescott and Blackburn 2000), may also have further contributed to the previously observed eventual senescent or delayed cell inviability phenotype of *tlc1-476gug* cells. However, arguing against this possibility, *tlc1* mutant strains that caused incorporation of telomeric DNA repeats with even more diminished Rap1 binding ability *in vitro* than 476gug did not show senescence (Prescott and Blackburn 2000). Taken together, the current and previous findings indicate that although *tlc1-476gug* telomerase indeed has a low inherent telomerase activity *in vivo*, this

minimal level of *tlc1-476gug* enzymatic activity is not sufficient to prevent a classic Ever Shortening Telomeres (EST) and senescence phenotype.

Template interactions *in vivo*

Surprisingly, the ability to rescue *tlc1-476gug* template usage depended strongly on the template sequence of a *tlc1* allele co-expressed in *trans* and ranged nearly three orders of magnitude. Additionally, there was no particular sequence trait unambiguously identified that was critical for the rescue, as evidenced by the distribution of the ability to recue 476gug template usage across 58 different templates mutated at positions 474, 475 and 476, with different sequence properties. Notably however, a trend was seen, as there was the following Boolean distribution of abilities of the different template mutants to rescue 476gug template function: out of the entire group of 58 templates tested, 15 (including the wild-type template sequence) out of the 17 sequences that rescued (with a level of relative 476gug incorporation above a 0.7 threshold value) all shared in common the lowest predicted template-template hybridization ability (*i.e.* a ΔG value of -3.5 kcal / mole). However, further analyses will be required to interpret these findings.

The rudimentary analysis of the position and nucleotide effects on rescue showed that C and A nucleotides in the rescuing template sequence at positions 474-476 are preferred; across the whole template, C and A preference is a known preference for *in vivo* yeast telomerase activity in general (Förstemann *et al*. 2003). However, several factors limit the interpretation of the C and A bias, and the disfavoring of G residues, in the 476gug template rescue *in vivo*.

First, because many of the telomere binding proteins are sequence-specific, different *tlc1* template sequences *in vivo* are known to affect telomere structures differentially. For example, an *in vitro* analysis of a set of 6 different template mutants in the 474-476 template region (included among the 58 analyzed in the present work) showed that the mutant telomeric DNA sequences predicted to be specified by these mutant templates had a wide range of reductions in ability to bind Rap1 protein (Prescott and Blackburn 2000). The C and A preference may therefore reflect the preferred telomeric sequences that are protected by sequence-specific proteins at yeast telomeres such as Rap1 and Cdc13, because such incorporated sequences will be selected for, and therefore enriched in DNA preparations from cell populations. As previously reported, the library of 64 template mutations (including wild-type) result in many different lengths and forms of telomeres, and some of these template mutations cause misincorporation of non-templated residues into the telomeric DNA *in vivo* (Lin *et al*. 2004b). These differently regulated telomeres are likely also to have some effect on how well telomerase can act on the telomeres, and also on how well the 476gug mutant repeats remain in the telomere without degrading.

Second, the C and A preference may also reflect effects of template mutations on intrinsic telomerase activity. Some of the 64 template mutations covering positions 464-476 caused misincorporation of non-templated residues into the telomeric DNA *in vivo* (Lin *et al*. 2004b). To further test for these and other positional effects, a systematic pairwise analysis of different template mutations may show some useful information. For

example, the ability to rescue may depend on the position 476 if and only if position 475 is a C.

Thirdly, a limitation in interpreting the results is that the complementarity calculation was based on the hybridization energy if two free RNA sequences were mixed together. However, the template is a small region in a highly structured RNA scaffold that has several proteins bound *in vivo*, and steric effects are also likely to be a contributing factor, which were not accounted for in the analysis.

In summary, despite all these confounding factors, it is still possible to identify strong effects. For example, the templates that allowed the most amount of 476gug mutant repeat incorporated into the telomeres had the least complementarity to the 476gug template, and the least favorable templates (including 476gug) had the most complementarity to 476gug template.

The Est1 "activation" function is required for 476gug template rescue

Est1's best-understood essential role in telomerase activity is the recruitment of telomerase to telomeres. Bypassing this essential function has allowed the uncovering of another function of Est1, namely, its "activation" function (Evans and Lundblad 1999). Three known mutations reduce the "activation" function: *est1-42*, *est1-52*, and *est1-Δ19*. All of these mutations also affected the ability of the wild-type template to rescue the usage of 476gug mutant template, suggesting that the "activation" function and the 476gug rescue are part of the same process. In addition, *est-7* and *est1-47* were also defective in 476gug rescue. Although these mutations were not specifically impaired in

the "activation" function, the mutation lies in the same domain as *est1-52* and *est1-Δ19*. Hence, the 476gug rescue function may require, and be related to, the classic "activation" function, but also require an Est1 function over and above its activation function. Recently, *est1-52* has been shown to be defective for promoting G-quartet formation and separating a telomeric RNA-DNA duplex *in vitro* (Zhang *et al*. 2010).

It is intriguing that Est1 is capable of separating a telomeric RNA-DNA duplex *in vitro* (Zhang *et al*. 2010). We propose a model from these combined observations: that TLC1 dimerization may require such a helicase-like activity of Est1 to form the mature monomeric telomerase complex. While extra base pairing between the two 476gug templates may impose an extra challenge *in vivo* for the unraveling of a TLC1 dimer, Est1 may be sufficient to separate the wild-type/476gug heterodimeric templates, which is predicted to be less stable than a 476gug/476gug homodimer (Figure 3-8).

An alternative model is for a requirement for Est1's ability to promote G-quartet in rescuing the 476gug template usage. In this hypothetical model, the main defect in 476gug template mutation is not that telomerase enzyme with the mutant template is less active, but that the mutant repeats incorporated into telomeres are incapable of forming a G-quartet. If the 476gug mutant repeats are incapable of forming a G-quartet, which in this model may be required to promote telomerase activity, then telomerase will have difficulty extending 476gug repeat-containing telomeres, just as *est1* mutants that cannot promote G-quartet formation have difficulty promoting telomerase activity *in vivo*. According to this model, the co-expression of wild-type template would rescue this defect by incorporating enough wild-type repeats to form a G-quartet. However,

countering this potential model is the evidence that a 476gug/476gug-containing telomerase homodimer is inactive but the 476gug/wild-type telomerase heterodimer is active. This will be further discussed later.

Est3 is important in 476gug template rescue

It was possible to show specific effects of Est3 mutations on 476gug incorporation rescue *in vivo*, and these effects did not simply mirror effects of the Est3 mutations on telomerase activity *in vivo*. The evidence for this interpretation was that, for the set of *est3* mutants examined, the extent of 476gug rescue by each *est3* mutant did not correlate with the degree of telomere shortening effect caused by the *est3* mutant alone. There has been some suggested evidence for Est3's functioning variously in telomerase processivity, RNA-DNA hybrid separation, and having GTPase activity; however, the evidence for each of these is limited, and the full picture of Est3 functions remains unresolved (Lee *et al*. 2010; Shubernetskaya *et al*. 2011; Yang *et al*. 2006; Malyavko *et al*. 2010). As such, it is difficult to speculate on the exact role of Est3 in rescuing 476gug template usage. As discussed for Est1, Est3 might also have some activity related to the separation of the TLC1 dimer (Figure 3-8).

Roles of Sir complexes and Ku complexes

The Sir complex and Ku complex are both important factors in maintaining telomeres; their functions include forming silent chromatin at telomeres and recruiting telomeres to nuclear periphery (Boulton and Jackson 1998; Taddei *et al*. 2004). In addition, Sir4 and

the Ku complex, but not Sir2, were required for TLC1 physical dimerization, and apparently act in the same pathway for physical dimerization (see Chapter 2). Given the idea that the wild-type *TLC1* and *tlc1-476gug* RNAs functionally interact in order to rescue 476gug template usage, these complexes were naturally good candidates for testing their roles in *tlc1-476gug*. The results, however, are more puzzling than expected. While Sir complex seems to promote the recue of 476gug template usage, the Ku complex has reduced ability to rescue 476gug template. The fact that both Sir2 and Sir4 are important in this 476gug template rescue suggest that the role of Sir complex in the 476gug rescue is not through the TLC1 dimerization pathway, but may be through its role in telomere chromatin formation.

Stable interaction of unreacted substrate and telomerase *in vitro*

A previous study on pulling down telomerase complex and any products that are stably associated with telomerase complex suggested that there are at least two catalytic sites on a single telomerase complex (Prescott and Blackburn 1997b). However, this interpretation relies on the biotinylated substrate being stably bound to a telomerase complex only when it has reacted. Evidence supporting this assumption included the finding that, while all elongation products remained stably bound to the telomerase complex for at least 15 minutes, only the longer elongation products (five or more nucleotide added) remained bound after 1-2 hour incubations. In the S100 fractions tested here, the pull-down assay on est2-D530A and by a non-extendable substrate showed that this is not true. However, the previous results were obtained using DEAE-agarose

fractions that had been further purified from S100 extracts. Therefore, we cannot eliminate the possibility that other factors in the extracts besides telomerase may have influenced these different results.

The previous pull-down studies were only able to detect extended products, because ^{32}P-labeled radioactive nucleotides were used to follow reaction product oligonucleotides, and non-extended products were not probed in any way. The previous experiments, by following only the elongation reaction DNA products themselves (which were only those DNA oligonucleotides that became ^{32}P-radioactively labeled, because the only radioactive entities added to the incubation were the added ^{32}P-labeled dNTP substrates), by definition followed the properties of complexes that were enzymatically active in the extracts, and did not track or analyze any enzymatically inactive telomerase complexes, or any (partially) denatured enzyme complexes that were able to bind DNA primer but not able to extend it *in vitro*. In the present experiments, we note that non-extended DNA primers in the incubations with S100 cell extracts are likely to be present in vast excess over active telomerase complexes, which in cell extracts will typically be in picomolar concentrations (based on Mozdy and Cech 2006 and see Materials and Methods). The fraction of telomerase complexes in the S100 extracts that were enzymatically active and extended a bound DNA primer in the incubation, versus those that bound the primer, but were enzymatically inactive, during the incubation is unknown. However, typically, in *in vitro* enzyme reactions, the fraction of molecules of that are enzymatically active can be quite low compared with the total number of enzyme molecules biochemically present in an incubation, because of various contributions to

denaturation and unfolding of the enzyme that occur during preparation and during incubation.

With the above caveats noted, in the new experiments, the specificity and telomerase dependence of the association of *TLC1* RNA with the biotinylated DNA oligonucleotide substrate were shown by the *est2* deletion strain negative control experiment, in which essentially no *TLC1* RNA was pulled down by the biotinylated DNA oligonucleotide substrate. From this experiment, and from the pull-down of a 3'-amino-modified un-extendable DNA primer, the present new experiments showed that not only any extended DNA oligonucleotide products, but also un-extendable DNA primers, were stably bound to telomerase RNA in an Est2-dependent manner. However, the fraction of telomerase-bound DNA primers that actually underwent extension was not measured in these assays, but based on typical precedents for other enzyme reactions, it may have been quite low. Hence, these TLC1-associated biotinylated DNA oligonucleotides are likely to have been bound to a mixture consisting of an unknown proportion of enzymatically-competent telomerase complexes, present together with telomerase complexes that were competent to bind the DNA substrates, but not to extend them enzymatically.

Interestingly, these new experiments showed that the pull-down of TLC1 by biotinylated DNA oligonucleotide substrates was not only Est2 protein-dependent, but also that the recovery of TLC1 pulled down onto the immobilized, bead-borne DNA oligonucleotide substrates was greater if the cell extracts were prepared either with no dNTPs present in the S100 incubation mix, compared with when dTNPs were added to

the extract, or if the cell extract was prepared from a strain that expressed only the catalytically dead Est2 point mutant (*est2-D530A*), compared with wild type *EST2* cells. The latter difference was especially strong. The greater recovery of TLC1 in both these situations suggests that a telomerase complex in an inactive conformation (*est2-D530A* or no dNTPs added to the incubation) binds tighter to the bulk of the biotinylated DNA primer present on the beads than a telomerase that is capable of extending (or that has extended) that DNA primer. The results showed that primer elongation was clearly not required for this Est2-dependent TLC1 association with DNA primer; strikingly rather, this association was improved if the primers were un-extendable, or the telomerase contained catalytically-incompetent Est2, which is still competent for TLC1 assembly and DNA primer binding. These results may define a new situation, in which tight binding of telomerase with a DNA primer results if the primer cannot be extended.

The previous study proposed a model that there are two catalytic sites in an active telomerase complex *in vitro* based on these facts (Prescott and Blackburn 1997b): 1. Oligonucleotide elongation products (^{32}P-labeled) remain stably bound to telomerase after they are elongated. 2. Biotinylated oligonucleotides that are stably bound to telomerase can pull down un-biotinylated oligonucleotides that have been extended to incorporate ^{32}P-labeled nucleotides. If the substrate must be elongated in order to remain stably bound to the telomerase complex, then both the biotinylated and un-biotinylated oligonucleotides must have been extended and remained bound in a single complex; this complex would have to contain at least two catalytic sites. However, the present study showed that substrates can remain stably bound to an Est2-and-TLC1-containing

complex (that may or may not be active), albeit under a different reaction condition. This allows an alternative explanation for the results from the previous study: that it is possible for an un-elongated, biotinylated oligonucleotide stably bound to telomerase complex not at the catalytic site to co-purify an un-biotinylated, extended oligonucleotide stably bound to the catalytic site. This model would require that there are at least two copies of TLC1 but only one catalytic subunit per telomerase complex. This latter model is more consistent with the results from Chapter 2, which failed to find any Est2-Est2 interactions *in vitro*.

In the same previous study, 476gug-476gug telomerase dimer was shown to be inactive while 476gug-WT-template telomerase complex is active, using the similar setup described above, in which biotinylated 476gug-specific substrate was able to co-purify with wild-type product but not with 476gug product (Prescott and Blackburn 1997b). That result is consistent with the current working model, in which the template-template interaction in *tlc1-476gug* prevents access by the biotinylated oligonucleotides in the 476gug homodimer; the wild-type/476gug heterodimer allows 476gug template access and co-purifies with the wild-type product as described above. This predicts that from cell lysates containing only the *tlc1-476gug* telomerase would have much reduced *TLC1* RNA bind to biotinylated oligonucleotides in a pull-down assay compared to cell lysates containing wild-type and *tlc1-476gug* telomerase.

Current working model

The mechanism by which the rescue of 476gug template usage by the wild-type template still remains elusive; however, based on the results from both Chapter 2 and 3, we propose the following model (Figure 3-8): (A) There are at least two mechanisms by which TLC1 dimerizes (see Chapter 2), during which the templates are brought together in proximity, allowing base-pairing in *tlc1-476gug*. (B) Est1 and Est3, through their "activation" function, separate the dimeric TLC1 or make the template region accessible. The extensive base pairing in *tlc1-476gug* templates, however, prevents the template region from becoming accessible. This model raises the possibility that dimerization of telomerase RNA can act as a regulatory step, in which the access to the template region limits the telomerase activity and require an activation step.

Future Directions

The main feature of the proposed model is the accessibility of the template region of TLC1. An attempt was made without success to assess the accessibility using a DMS chemical protection assay, in which bases not participating in base pairing are modified. Further development of this method may be fruitful. The biotinylated oligonucleotide pull-down of telomerase complexes in various states of activity also can also be used to test the accessibility, as we have shown here that extension is not required for the stable interaction of DNA oligonucleotides added at high concentration to cell extracts. The template accessibility assays should be carried out in *est1Δ* and *est3*Δ to assess their roles.

A major caveat in studying the 476gug mutant template and any other template mutations *in vivo* is that mutant repeats change the nature of telomeres. Many of the telomere length regulators, such as Rap1 and Cdc13, depend on the telomere sequences. Studying *tlc1-476gug* telomerase *in vitro* also is difficult as Est1, Est3, and other cofactors are not required, and hence their roles cannot readily be studied.

One of the challenges in studying the 476gug incorporation into telomeres is the low incidence of telomeres containing these mutant repeats. Although the qPCR method has allowed quantitative measurement of the number of these repeats, it is not possible to determine the distribution of these mutant repeats, where surely a lot of information is hidden. This challenge, however, can be overcome with the recent breakthrough in the next-generation sequencing technologies. Specifically, the 454 sequencing technology, which allows sequencing of up to 500 base-pairs, is ideal for this, because the bulk of wild type *S. cerevisiae* terminal telomeric TG repeat tracts are 250-350 base pairs in length.

Materials and Methods

Plasmids

TLC1 template mutations on HIS3-marked CEN-ARS plasmids were provided by Jue Lin (Lin *et al*. 2004b). Est1 mutations on TRP1-marked CEN-ARS plasmids were generously provided by Vicki Lundblad (Evans and Lundblad 2002). Est3 mutations were cloned using site-specific mutagenesis PCR. Cdc13-Est2 fusion plasmid was provided by Sveta Makovets. The plasmids are listed in Table 3-1.

Yeast strains, media, and genomic DNA extractions

All yeast strains used were derived from S288c BY4746 (Table 3-2). Standard protocols were used for growth and genetic manipulations. Genomic DNA was purified using Zymo-Spin I columns (Zymo Research). Yeast cells were lysed in 500 uL Lysis Buffer (20 mM phosphate buffer pH7.0, 10 mM EDTA, 100 mM NaCl, 1% SDS, 0.1% Sodium Deoxycholate, 1% 2-mercaptoethanol) at 65 °C for 15 minutes. After incubation 350 uL of 6.5 M Guanidine HCl was added, and the cleared supernatant was loaded on the Zymo-Spin I column. The column was washed twice with Wash Buffer (80% ethanol, 10 mM Tris pH7.5, 1 mM EDTA, 100 mM NaCl). The DNA was eluted in 100 uL of water.

Quantitative PCR

LightCycler 480 (Roche) with 386-well module was used for all quantitative PCR reactions. All reactions were run as triplicates, and the standard curve was run for each amplicon on the same run as the experimental reactions. PCR reactions were carried out in a 10 uL using the LightCycler® 480 SYBR Green I Master, with the final primer concentrations of 200 nM. The reverse primers for the mutant-specific telomeric repeat detection for 476gug, 476ucu, and 476cuu, T5-CA15-gug-qPCR (tttttCACACCCACACACCACgtg), T5-CA15-ucu-qPCR (tttttCACACCCACACACCACtct), T5-CA15-cuu-qPCR (tttttCACACCCACACACCACctt). The same forward primer used for all mutant repeat quantitation was T5-TG18-qPCR (tttttGTGTGTGGGTGTGGTGTG). Five extra T's were added to the 5' end of each primer to prevent run off amplification. LightCycler

software was used to fit the standard curve and to calculate the concentrations for each sample.

Calculation of sequence preference for 476gug template rescue

The level of 476gug mutant repeat incorporated into telomeres in cells expressing different template mutations was normalized to the level of 476gug mutant repeat expressing the wild-type *TLC1*. For each position, 474-476, four bins representing A, C, G, and T nucleotides were created. The value of the normalized level for each template was added to the appropriate nucleotide bin representing the template mutation at each position. The sum of these values for each bin at each position were calculated and represented in the figure as percentage of total in each bin. The log normalized values were calculated by normalizing to the minimum value, rather than the wild-type level.

Free energy calculation for template-template hybridization

Free energy of hybridization between the 64 mutant templates and the 476gug template mutation was calculated using "hybrid-2s.pl" program, which is a part of the UNAFold 3.6 software package (Markham and Zuker 2008). The full template region was used in this analysis. The temperature at which the hybridization was simulated was 30 °C.

Telomerase complex pull-down with telomerase substrates

Tel15 (TGTGTGGTGTGTGGG), Tel24 (TGTGTGGGTGTGTGGGTGTGTGGG), and CA24 (CCCACACACCCACACACCCACACA) sequences were used as telomerase

substrates. The 5'-biotinylated versions of Tel15, Tel24, and CA24, as well as 5'-biotinylated and 3'-amino-modified versions of Tel15 and Tel24 were purchased from IDT. Streptavidin magnetic beads were composed of equal volumes of M280, M270, C1, and T1 (Invitrogen). The beads were washed and prepared as instructed in the manual. For each reaction, 1 mg of magnetic beads, which has the capacity to bind ~200 pmol of oligonucleotides, were mixed with 500 pmol each of biotinylated Tel15 and Tel24 and washed. Yeast whole lysate was incubated with TG15 and TG24 bound magnetic beads in Telomerase Assay Buffer (50 mM Tris pH 7.9, 1 mM spermidine, 1 mM DTT, 100 uM dNTPs) in a final volume of 200 uL with ~1 uM of bound substrate. The reaction mixture was incubated for 30 minutes at 30 °C. The beads were washed in the TMG buffer twice, and RNA bound to beads was extracted using RNeasy Mini Kit (Qiagen).

Acknowledgements

We thank Jue Lin, Sveta Makovets, Vicki Lundblad for generously providing us with the plasmids used in this study.

References

Boulton, S.J. and Jackson, S.P., 1998. Components of the Ku-dependent non-homologous end-joining pathway are involved in telomeric length maintenance and telomeric silencing. *The EMBO Journal*, 17(6), pp.1819-1828.

Evans, S.K. and Lundblad, V., 1999. Est1 and Cdc13 as Comediators of Telomerase Access. *Science*, 286(5437), pp.117 -120.

Evans, S.K. and Lundblad, V., 2002. The Est1 Subunit of Saccharomyces cerevisiae Telomerase Makes Multiple Contributions to Telomere Length Maintenance. *Genetics*, 162(3), pp.1101 -1115.

Förstemann, K., Zaug, A.J., Cech, T.R. and Lingner, J., 2003. Yeast telomerase is specialized for C/A-rich RNA templates. *Nucleic Acids Research*, 31(6), pp.1646 -1655.

Lee, J., Mandell, E.K., Rao, T., Wuttke, D.S. and Lundblad, V., 2010. Investigating the role of the Est3 protein in yeast telomere replication. *Nucleic Acids Research*, 38(7), pp.2279 -2290.

Lin, J., Smith, D.L. and Blackburn, E.H., 2004a. Mutant telomere sequences lead to impaired chromosome separation and a unique checkpoint response. *Molecular Biology of the Cell*, 15(4), pp.1623-1634.

Lin, J., Smith, D.L. and Blackburn, E.H., 2004b. Mutant Telomere Sequences Lead to Impaired Chromosome Separation and a Unique Checkpoint Response. *Molecular Biology of the Cell*, 15(4), pp.1623-1634.

Malyavko, A.G., Logvina, N.A., Zvereva, M.E. and Dontsova, O.A., 2010. *In vitro* dimerization of telomerase protein Est3p is stimulated by magnesium cations. *Doklady Biochemistry and Biophysics*, 433(1), pp.152-154.

Markham, N.R. and Zuker, M., 2008. UNAFold: software for nucleic acid folding and hybridization. *Methods in Molecular Biology (Clifton, N.J.)*, 453, pp.3-31.

Mozdy, A.D. and Cech, T.R., 2006. Low abundance of telomerase in yeast: Implications for telomerase haploinsufficiency. *RNA*, 12(9), pp.1721 -1737.

Pennock, E., Buckley, K. and Lundblad, V., 2001. Cdc13 Delivers Separate Complexes to the Telomere for End Protection and Replication. *Cell*, 104(3), pp.387-396.

Prescott, J. and Blackburn, E.H., 1997a. Telomerase RNA mutations in Saccharomyces cerevisiae alter telomerase action and reveal nonprocessivity *in vivo* and *in vitro*. *Genes & Development*, 11(4), pp.528 -540.

Prescott, J. and Blackburn, E.H., 1997b. Functionally interacting telomerase RNAs in the yeast telomerase complex. *Genes & Development*, 11(21), pp.2790 -2800.

Prescott, J. and Blackburn, E.H., 2000. Telomerase RNA Template Mutations Reveal Sequence-Specific Requirements for the Activation and Repression of Telomerase Action at Telomeres. *Mol. Cell. Biol.*, 20(8), pp.2941-2948.

Qi, H. and Zakian, V.A., 2000. The Saccharomyces telomere-binding protein Cdc13p interacts with both the catalytic subunit of DNA polymerase α and the telomerase-associated Est1 protein. *Genes & Development*, 14(14), pp.1777 -1788.

Sharanov, Y.S., Zvereva, M.I. and Dontsova, O.A., 2006. Saccharomyces cerevisiae telomerase subunit Est3p binds DNA and RNA and stimulates unwinding of RNA/DNA heteroduplexes. *FEBS Letters*, 580(19), pp.4683-4690.

Shubernetskaya, O., Logvina, N., Sharanov, Y. and Zvereva, M., 2011. Yeast telomerase protein Est3 is a novel type of GTPase. *Biochimie*, 93(2), pp.202-206.

Taddei, A., Hediger, F., Neumann, F.R., Bauer, C. and Gasser, S.M., 2004. Separation of silencing from perinuclear anchoring functions in yeast Ku80, Sir4 and Esc1 proteins. *EMBO J*, 23(6), pp.1301-1312.

Yang, C.-P., Chen, Y.-B., Meng, F.-L. and Zhou, J.-Q., 2006. Saccharomyces cerevisiae Est3p dimerizes *in vitro* and dimerization contributes to efficient telomere replication *in vivo*. *Nucleic Acids Research*, 34(2), pp.407 -416.

Zhang, M.-L., Tong, X.-J., Fu, X.-H., Zhou, B.O., Wang, J., Liao, X.-H., Li, Q.-J., Shen, N., Ding, J. and Zhou, J.-Q., 2010. Yeast telomerase subunit Est1p has guanine quadruplex-promoting activity that is required for telomere elongation. *Nat Struct Mol Biol*, 17(2), pp.202-209.

Zhou, J., Hidaka, K. and Futcher, B., 2000. The Est1 Subunit of Yeast Telomerase Binds the Tlc1 Telomerase RNA. *Mol. Cell. Biol.*, 20(6), pp.1947-1955.

Figure Legends

Figure 3-1. Quantitative PCR method to detect 476gug mutant template.

A minute number of 476gug mutant repeat incorporated into telomeres can be detected by a qPCR method. (A) A schematic of a telomere, where the wild-type TG_{1-3} telomeric repeats are represented by white squares and the gray squares represent 476gug mutant repeats. The forward TG_{1-3} primer can anneal to multiple locations within the wild-type repeats. The reverse, GTG-specific primer can only anneal to a 476gug mutant repeat at the 3' end, while the 5' end of the primer can anneal non-specifically to TG_{1-3} sequences. (B) The standard curve for the qPCR linearity test was made by serially diluting the genomic DNA sample containing 476gug mutant repeats. (C) Strains deleted for essential telomerase components were transformed with *tlc1-476gug*, and the amount of 476gug mutant repeats were quantified in the genomic DNA extracted from these strains. The level of 476gug mutant repeat incorporation was normalized to the level of *PGK1* locus in the sample, and this was normalized to the wild-type samples. The error bars indicate the standard deviation among three measurements.

Figure 3-2. Rescue of 476gug template usage by other template mutants.

The library of 58 template mutations were co-expressed with *tlc1-476gug* in *tlc1Δ* cells, and the 476gug mutant repeat incorporation was measured. (A) shows the level of 476gug mutant repeats normalized to *PGK1* locus, which is then normalized to the level of incorporation in the wild-type. The same set of data is shown in log scale in (B). The preference for a particular nucleotide at each position in the rescuing template sequence

was calculated (see Materials and Methods) using (C) log normalized values, (D) linearly normalized values, and (E) linearly normalized values with the top three mutant templates omitted.

Figure 3-3. Template-template interactions by base pairing.

The 476gug template mutation results in a palindromic sequence, allowing for inter-template base pairing. (A) The figure shows two alternative alignments of the two templates in *trans*, in which six bases are complementary between the interacting templates. (B) For each of the mutant templates, the hybridization energy to the 476gug template was calculated using UNafold software, and ΔG (kcal / mole) was plotted against the amount of 476gug incorporation from Figure 3-2B. The wild-type (WT) and *tlc1-476gug* (GTG) data are indicated with a line.

Figure 3-4. Est1 contributes to 476gug mutant template rescue.

Each *est1* mutant carried on a plasmid was co-transformed with *tlc1-476gug* also on a plasmid into (A) *est1Δ* and (B) *est1Δ CDC13-EST2* strains. The amounts of 476gug mutant repeats were quantified and normalized to *PGK1* locus. (C) Each *est1* mutant was co-transformed with *tlc1-476gug* and *tlc1-476ucu* into *est1Δ CDC13-EST2* strain. The amounts of incorporated 476gug and 476ucu mutant repeats were quantified, and the ratio of 476gug to 476ucu is plotted. The error bars represent standard deviation, and the asterisks indicate samples in which one-sample t-test showed $p < 0.05$.

Figure 3-5. Est3 plays an important role in 476gug mutant template rescue.
Each *est3* mutant was co-transformed with *tlc1-476gug* and *tlc1-476ucu* into *est3Δ*. The amounts of incorporated 476gug and 476ucu mutant repeats were quantified, and the ratio of 476gug to 476ucu is plotted. The mutations are denoted by the amino acid residue change. The error bars represent standard deviation between two experiments.

Figure 3-6. Rescue of 476gug mutant template in TLC1 dimerization mutants.
Plasmids containing *tlc1-476gug* and *tlc1-476ucu* are co-transformed into the strains indicated. The amounts of incorporated 476gug and 476ucu mutant repeats were quantified, and the ratio of 476gug to 476ucu is plotted. (A) Six independent transformants were tested, and the error bars indicate the triplicate measurements of the same sample. (B) The averages of six data point from (A) are plotted with the error bars representing the standard error among the six samples. The one-sample t-test values for the comparison with the wild-type are indicated.

Figure 3-7. Un-elongated telomerase substrates are stably bound to telomerase complex.
An equal mixture of biotinylated telomeric oligonucleotides TG24 and TG15 were bound to streptavidin magnetic beads and incubated with lysates in telomerase activity assay buffer. The percentages of RNAs indicated that remained bound to the magnetic beads are plotted. (A) The S100 lysates from wild-type strains were incubated in telomerase assay buffer with or without dNTPs. (B) The whole lysates from wild-type strains were incubated with extendable TG24/15 oligonucleotides; un-extendable, 3' amino-modified

TG24/15-AM oligonucleotides; or extendable CA24 oligonucleotides. (C) The whole lysates from indicated strains were incubated with extendable TG24/15 oligonucleotides. The error bars represent the standard deviation between the results from two experiments.

Figure 3-8. The model for template-template interaction.

(A) The model shows the template-template interactions between the wild-type and 476gug template mutation. The number of base-pairs indicates the maximum number of Watson-Crick base-pairing that may form between the templates. (B) The disruption of the template-template interaction and the separation of TLC1 dimer are facilitated by Est1 and Est3. The extensive base-pairing between 476gug mutants prevents this step. (C) Telomerase is competent for activity once the template region is accessible.

Table 3-1. Plasmids used in Chapter 3

Plasmid number	Descriptive name	Reference
pEHB22,256	pRS416-TLC1	This study.
pEHB22,257	pRS416-tlc1-476gug	This study.
pEHB22,254	pRS415-TLC1	This study.
pEHB22,255	pRS415-tlc1-476gug	This study.
pEHB22,456	pRS415-tlc1-476uCu	This study.
pEHB22,457	pRS415-tlc1-476uuc	This study.
-	pRS313-tlc1-476aaA	Lin *et al*. 2004.
-	pRS313-tlc1-476aac	Lin *et al*. 2004.
-	pRS313-tlc1-476aag	Lin *et al*. 2004.
-	pRS313-tlc1-476aau	Lin *et al*. 2004.
-	pRS313-tlc1-476aCA	Lin *et al*. 2004.
-	pRS313-tlc1-476aCg	Lin *et al*. 2004.
-	pRS313-tlc1-476agA	Lin *et al*. 2004.
-	pRS313-tlc1-476agc	Lin *et al*. 2004.
-	pRS313-tlc1-476agg	Lin *et al*. 2004.
-	pRS313-tlc1-476agu	Lin *et al*. 2004.
-	pRS313-tlc1-476auA	Lin *et al*. 2004.
-	pRS313-tlc1-476auc	Lin *et al*. 2004.
-	pRS313-tlc1-476aug	Lin *et al*. 2004.
-	pRS313-tlc1-476auu	Lin *et al*. 2004.
-	pRS313-tlc1-476CaA	Lin *et al*. 2004.
-	pRS313-tlc1-476Cac	Lin *et al*. 2004.
-	pRS313-tlc1-476Cau	Lin *et al*. 2004.
-	pRS313-tlc1-476CCA	Lin *et al*. 2004.
-	pRS313-tlc1-476CCc	Lin *et al*. 2004.
-	pRS313-tlc1-476CCg	Lin *et al*. 2004.
-	pRS313-tlc1-476CCu	Lin *et al*. 2004.
-	pRS313-tlc1-476CgA	Lin *et al*. 2004.
-	pRS313-tlc1-476Cgc	Lin *et al*. 2004.
-	pRS313-tlc1-476Cgg	Lin *et al*. 2004.
-	pRS313-tlc1-476Cgu	Lin *et al*. 2004.
-	pRS313-tlc1-476CuA	Lin *et al*. 2004.
-	pRS313-tlc1-476Cuc	Lin *et al*. 2004.
-	pRS313-tlc1-476Cug	Lin *et al*. 2004.
-	pRS313-tlc1-476Cuu	Lin *et al*. 2004.
-	pRS313-tlc1-476gaA	Lin *et al*. 2004.
-	pRS313-tlc1-476gag	Lin *et al*. 2004.

-	pRS313-tlc1-476gau	Lin *et al*. 2004.
-	pRS313-tlc1-476gCA	Lin *et al*. 2004.
-	pRS313-tlc1-476gCc	Lin *et al*. 2004.
-	pRS313-tlc1-476gCg	Lin *et al*. 2004.
-	pRS313-tlc1-476gCu	Lin *et al*. 2004.
-	pRS313-tlc1-476ggA	Lin *et al*. 2004.
-	pRS313-tlc1-476ggc	Lin *et al*. 2004.
-	pRS313-tlc1-476ggg	Lin *et al*. 2004.
-	pRS313-tlc1-476guA	Lin *et al*. 2004.
-	pRS313-tlc1-476guc	Lin *et al*. 2004.
-	pRS313-tlc1-476gug	Lin *et al*. 2004.
-	pRS313-tlc1-476guu	Lin *et al*. 2004.
-	pRS313-tlc1-476uaA	Lin *et al*. 2004.
-	pRS313-tlc1-476uac	Lin *et al*. 2004.
-	pRS313-tlc1-476uag	Lin *et al*. 2004.
-	pRS313-tlc1-476uau	Lin *et al*. 2004.
-	pRS313-tlc1-476uCA	Lin *et al*. 2004.
-	pRS313-tlc1-476uCc	Lin *et al*. 2004.
-	pRS313-tlc1-476uCg	Lin *et al*. 2004.
-	pRS313-tlc1-476uCu	Lin *et al*. 2004.
-	pRS313-tlc1-476ugc	Lin *et al*. 2004.
-	pRS313-tlc1-476ugg	Lin *et al*. 2004.
-	pRS313-tlc1-476ugu	Lin *et al*. 2004.
-	pRS313-tlc1-476uuA	Lin *et al*. 2004.
-	pRS313-tlc1-476uuc	Lin *et al*. 2004.
-	pRS313-tlc1-476uug	Lin *et al*. 2004.
-	pRS313-tlc1-476uuu	Lin *et al*. 2004.
pEHB22,304	pRS414-EST1	This study.
pEHB22,283	pVL-est1-06-18myc (pVL1612)	Evans and Lundblad 2002.
pEHB22,284	pVL-est1-07-18myc (pVL1613)	Evans and Lundblad 2002.
pEHB22,285	pVL-est1-38-18myc (pVL1616)	Evans and Lundblad 2002.
pEHB22,286	pVL-est1-39-18myc (pVL1617)	Evans and Lundblad 2002.
pEHB22,287	pVL-est1-41-18myc (pVL1618)	Evans and Lundblad 2002.
pEHB22,288	pVL-est1-42-18myc (pVL1619)	Evans and Lundblad 2002.
pEHB22,289	pVL-est1-46-18myc (pVL1621)	Evans and Lundblad 2002.
pEHB22,290	pVL-est1-47-18myc (pVL1622)	Evans and Lundblad 2002.
pEHB22,291	pVL-est1-49-18myc (pVL1624)	Evans and Lundblad 2002.
pEHB22,292	pVL-est1-50-18myc (pVL1625)	Evans and Lundblad 2002.
pEHB22,293	pVL-est1-51-18myc (pVL1626)	Evans and Lundblad 2002.
pEHB22,294	pVL-est1-52-18myc (pVL1627)	Evans and Lundblad 2002.

pEHB22,295	pVL-est1-54-18myc (pVL1629)	Evans and Lundblad 2002.
pEHB22,296	pVL-est1-55-18myc (pVL1630)	Evans and Lundblad 2002.
pEHB22,297	pVL-est1-19-18myc (pVL1633)	Evans and Lundblad 2002.
pEHB22,298	pRS316-EST3	This study.
pEHB22,406	pRS316-est3-K3A	This study.
pEHB22,407	pRS316-est3-D49A	This study.
pEHB22,408	pRS316-est3-D49K	This study.
pEHB22,409	pRS316-est3-D49R	This study.
pEHB22,410	pRS316-est3-K68A	This study.
pEHB22,411	pRS316-est3-K68D	This study.
pEHB22,412	pRS316-est3-K68E	This study.
pEHB22,413	pRS316-est3-K71A	This study.
pEHB22,414	pRS316-est3-F72A	This study.
pEHB22,415	pRS316-est3-A82E	This study.
pEHB22,416	pRS316-est3-D86A	This study.
pEHB22,417	pRS316-est3-S87A	This study.
pEHB22,418	pRS316-est3-F95A	This study.
pEHB22,419	pRS316-est3-F103A	This study.
pEHB22,420	pRS316-est3-E104A	This study.
pEHB22,421	pRS316-est3-T115A	This study.
pEHB22,422	pRS316-est3-D166A	This study.
pEHB22,423	pRS316-est3-D166K	This study.
pEHB22,424	pRS316-est3-D166R	This study.
pEHB22,425	pRS316-est3-D49K-K68D	This study.
pEHB22,426	pRS316-est3-D49K-K68E	This study.
pEHB22,427	pRS316-est3-D49R-K68D	This study.
pEHB22,428	pRS316-est3-D49R-K68E	This study.
pEHB22,431	pRS316-est3-K68D-D166K	This study.
pEHB22,432	pRS316-est3-K68D-D166R	This study.
pEHB22,433	pRS316-est3-K68E-D166K	This study.
pEHB22,434	pRS316-est3-K68E-D166R	This study.
pEHB22,435	pRS316-est3-D49K-K68D-D166K	This study.
pEHB22,436	pRS316-est3-D49K-K68D-D166R	This study.
pEHB22,437	pRS316-est3-D49K-K68E-D166K	This study.
pEHB22,438	pRS316-est3-D49K-K68E-D166R	This study.
pEHB22,439	pRS316-est3-D49R-K68D-D166K	This study.
pEHB22,440	pRS316-est3-D49R-K68D-D166R	This study.
pEHB22,441	pRS316-est3-D49R-K68E-D166K	This study.
pEHB22,442	pRS316-est3-D49R-K68E-D166R	This study.

Table 3-2. Strains used in Chapter 3

All strains are in the S288c strain background and are isogenic, except as noted below.

Strain number	Relevant genotype
yEHB22,321	*ADE2 his3Δ1 leu2Δ0 lys2Δ0 met15Δ0 trp1Δ63 ura3Δ0 bar1Δ0 MATa*
yEHB22,465	*ADE2 his3Δ1 leu2Δ0 lys2Δ0 met15Δ0 trp1Δ63 ura3Δ0 bar1Δ0 MATa*
yEHB22,692	yEHB22,321 but *est1Δ::KanMX6*
yEHB22,693	yEHB22,465 but *est1Δ::KanMX6*
yEHB22,606	yEHB22,321 but *est2Δ::KanMX6*
yEHB22,607	yEHB22,465 but *est2Δ::KanMX6*
yEHB22,694	yEHB22,321 but *est3Δ::KanMX6*
yEHB22,695	yEHB22,465 but *est3Δ::KanMX6*
yEHB22,696	yEHB22,321 but *tlc1Δ::KanMX6*
yEHB22,697	yEHB22,465 but *tlc1Δ::KanMX6*
yEHB22,710	yEHB22,321 but *CDC13-EST2::HIS3 est1Δ::KanMX6*
yEHB22,711	yEHB22,321 but *CDC13-EST2::HIS3 est1Δ::KanMX6*
yEHB22,682	*HIS3-CYC1$_P$-CP-3xMyc TLC1-URA3-TLC1-MS2 yku70Δ::KanMX6 MATa*
yEHB22,683	*HIS3-CYC1$_P$-CP-3xMyc TLC1-URA3-TLC1-MS2 yku70Δ::KanMX6 MATa*
yEHB22,686	*HIS3-CYC1$_P$-CP-3xMyc TLC1-URA3-TLC1-MS2 yku80Δ::KanMX6 MATa*
yEHB22,687	*HIS3-CYC1$_P$-CP-3xMyc TLC1-URA3-TLC1-MS2 yku80Δ::KanMX6 MATa*
yEHB22,728	*HIS3-CYC1$_P$-CP-3xMyc TLC1-URA3-TLC1-MS2 sir2Δ::KanMX6 MATa*
yEHB22,729	*HIS3-CYC1$_P$-CP-3xMyc TLC1-URA3-TLC1-MS2 sir2Δ::KanMX6 MATa*
yEHB22,730	*HIS3-CYC1$_P$-CP-3xMyc TLC1-URA3-TLC1-MS2 sir4Δ::KanMX6 MATa*
yEHB22,731	*HIS3-CYC1$_P$-CP-3xMyc TLC1-URA3-TLC1-MS2 sir4Δ::KanMX6 MATa*
yEHB22,600	*can1Δ::STE2$_P$-HIS5 lyp1Δ::STE3$_P$-LEU2 EST2-ADH1T::natMX6 MATα*
yEHB22,602	*can1Δ::STE2$_P$-HIS5 lyp1Δ::STE3$_P$-LEU2 est2Δ::natMX6 MATα*
yEHB22,605	*can1Δ::STE2$_P$-HIS5 lyp1Δ::STE3$_P$-LEU2 est2-D530A::natMX6 MATα*

Figure 3-1

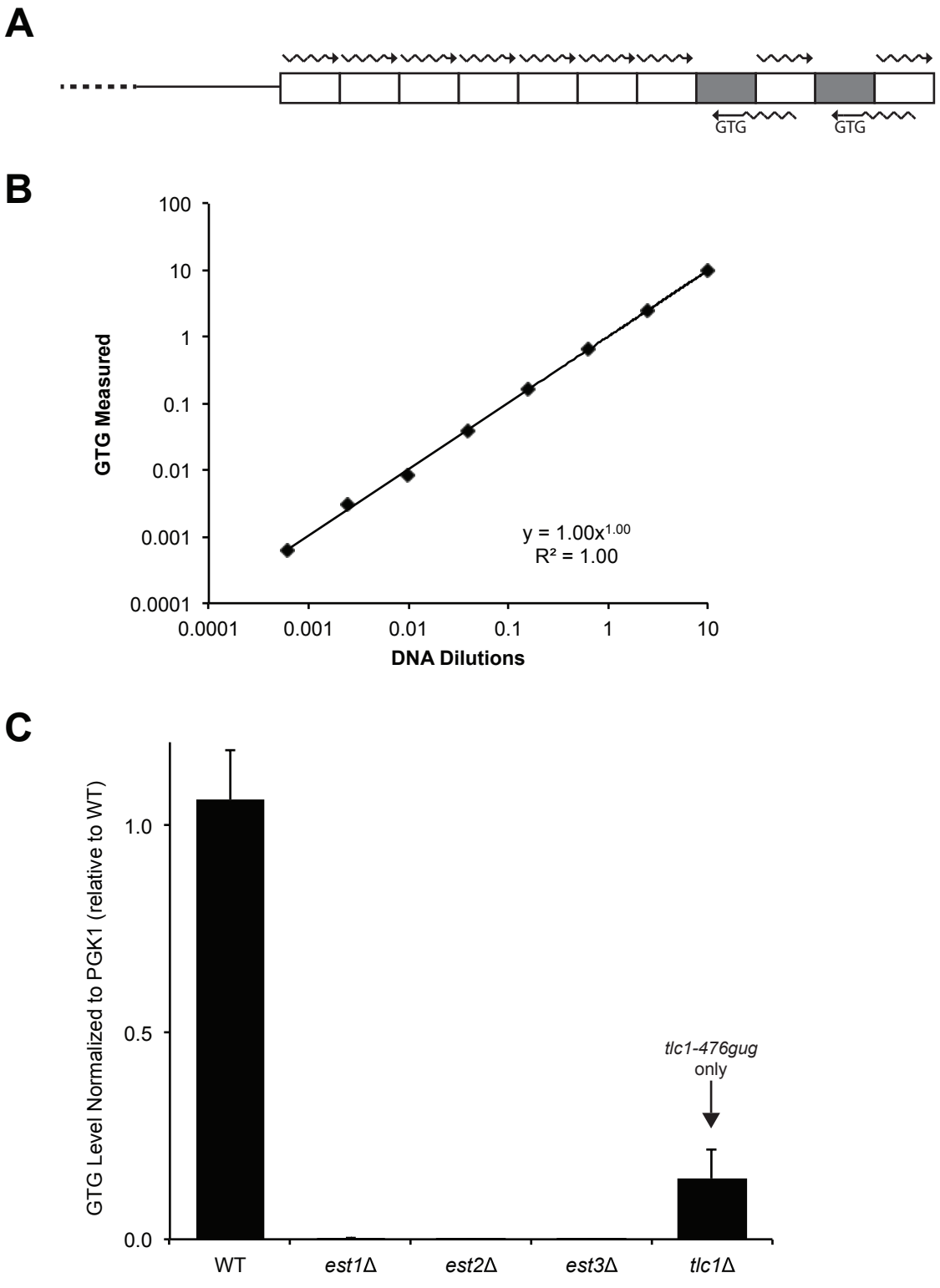
A
GTG
GTG
B
GTG Measured
100
10
1
0.1
0.01
0.001
0.0001
y = 1.00x^1.00
R² = 1.00
0.0001
0.001
0.01
0.1
1
10
DNA Dilutions
C
GTG Level Normalized to PGK1 (relative to WT)
1.0
0.5
0.0
tlc1-476gug
only
WT
est1Δ
est2Δ
est3Δ
tlc1Δ

Figure 3-2

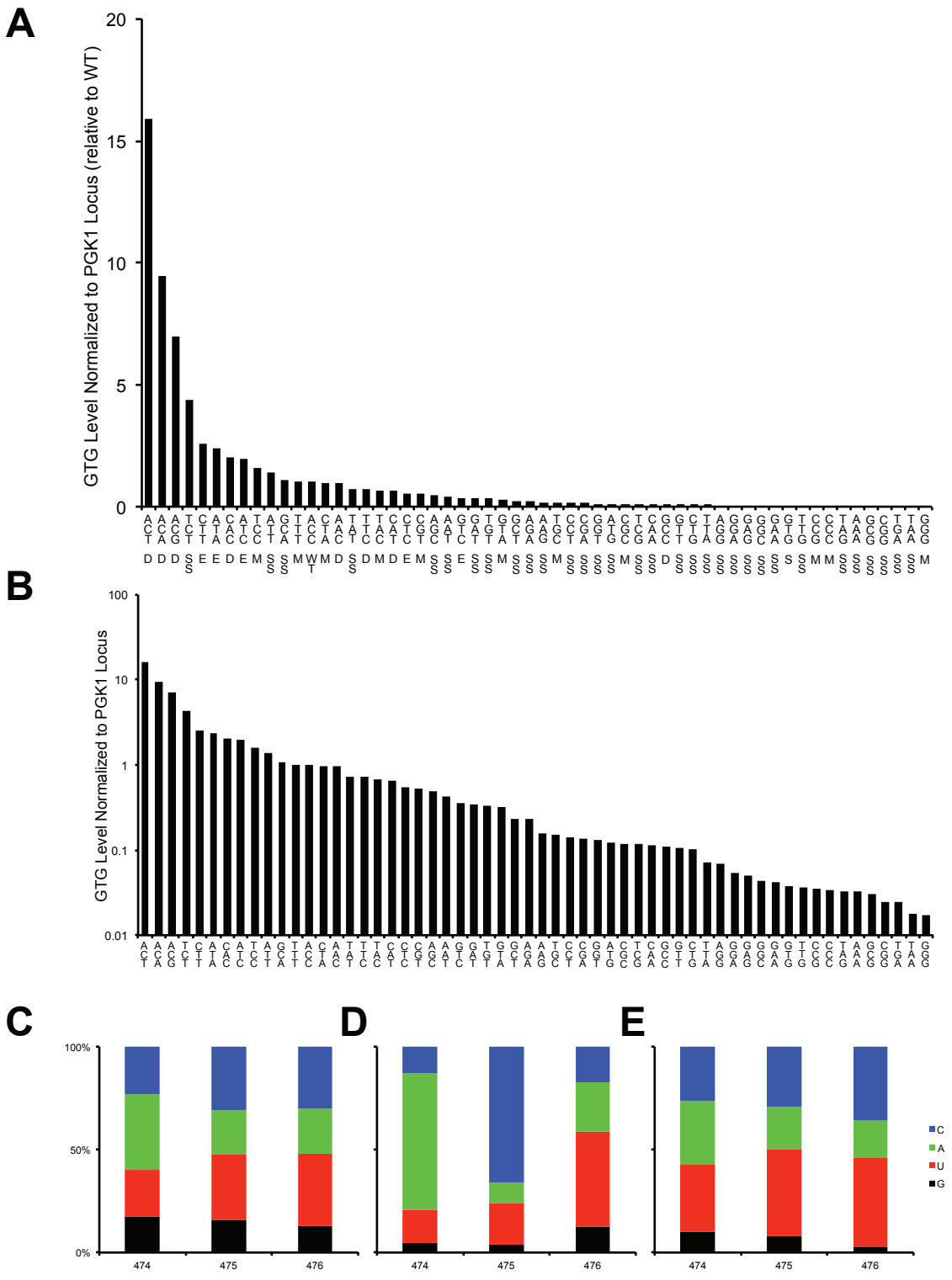
A
GTG Level Normalized to PGK1 Locus (relative to WT)
20
15
10
5
0
B
GTG Level Normalized to PGK1 Locus
100
10
1
0.1
0.01
C
D
E
100%
50%
0%
474
475
476
C
A
U
G

Figure 3-3

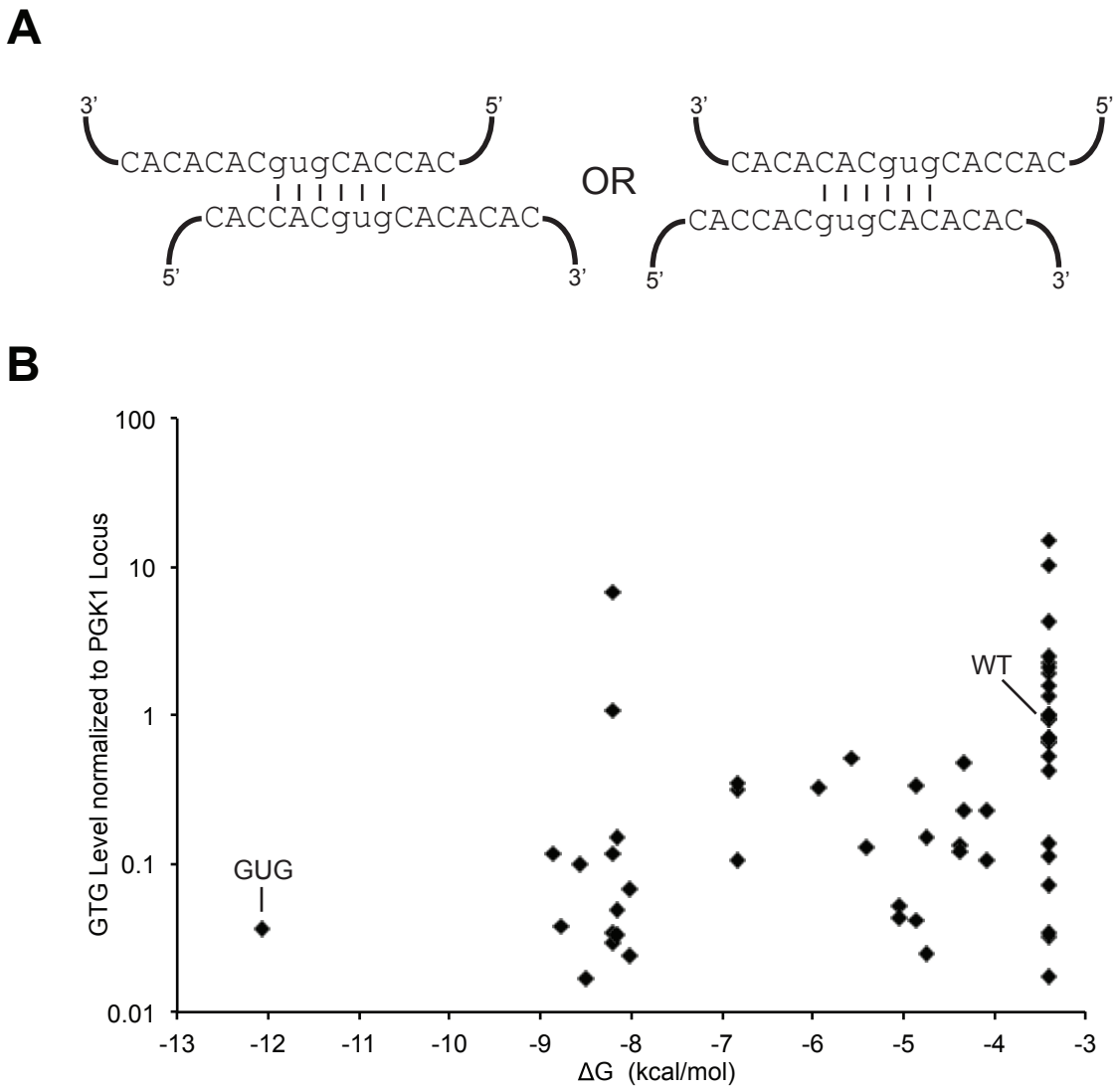
A
3'
5'
CACACACgugCACCAC
CACCACgugCACACAC
5'
3'
OR
3'
5'
CACACACgugCACCAC
CACCACgugCACACAC
5'
3'
B
GTG Level normalized to PGK1 Locus
100
10
1
0.1
0.01
GUG
WT
-13
-12
-11
-10
-9
-8
-7
-6
-5
-4
-3
ΔG (kcal/mol)

Figure 3-4

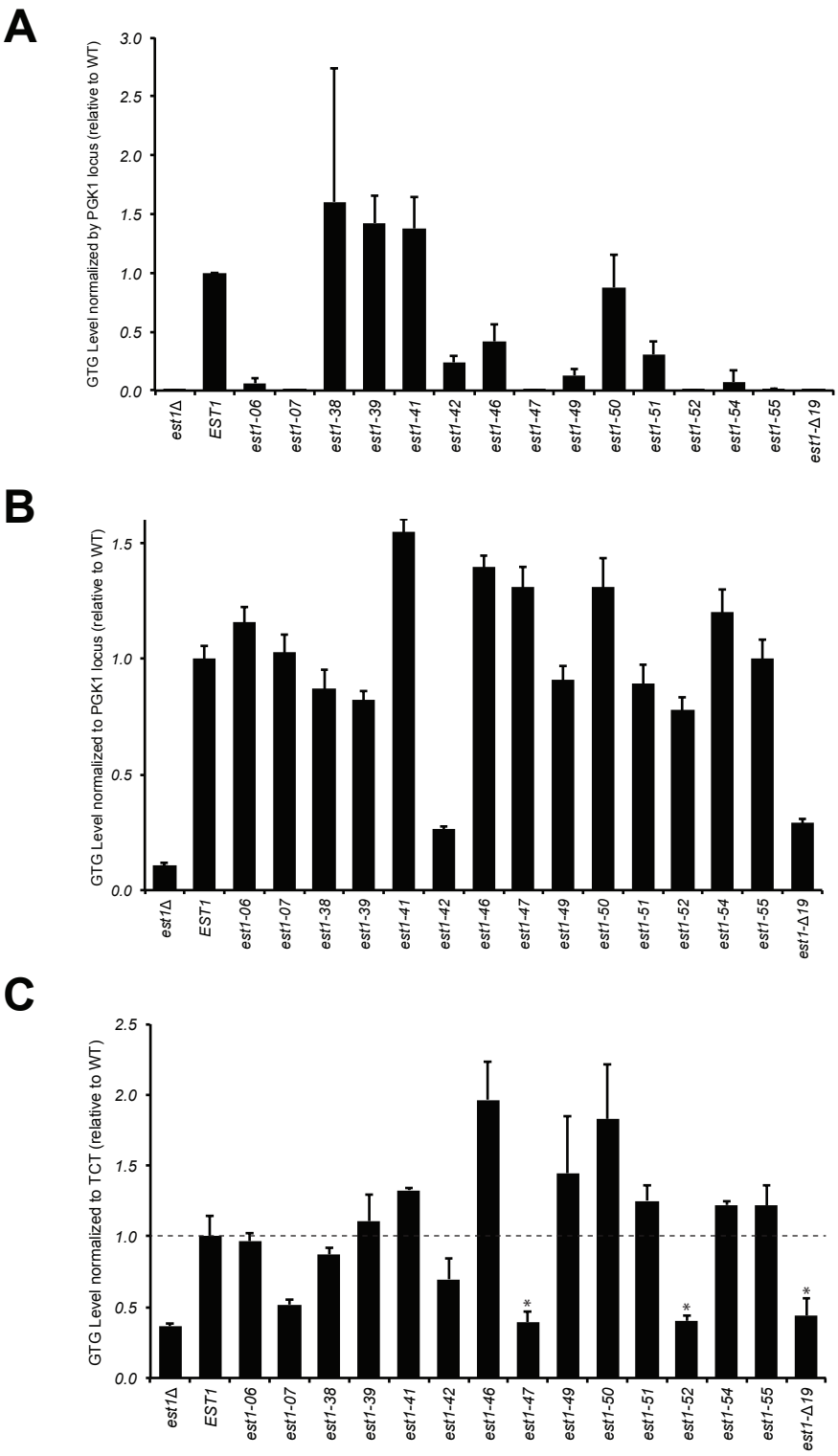
A
GTG Level normalized by PGK1 locus (relative to WT)
3.0
2.5
2.0
1.5
1.0
0.5
0.0
est1Δ
EST1
est1-06
est1-07
est1-38
est1-39
est1-41
est1-42
est1-46
est1-47
est1-49
est1-50
est1-51
est1-52
est1-54
est1-55
est1-Δ19
B
GTG Level normalized to PGK1 locus (relative to WT)
1.5
1.0
0.5
0.0
est1Δ
EST1
est1-06
est1-07
est1-38
est1-39
est1-41
est1-42
est1-46
est1-47
est1-49
est1-50
est1-51
est1-52
est1-54
est1-55
est1-Δ19
C
GTG Level normalized to TCT (relative to WT)
2.5
2.0
1.5
1.0
0.5
0.0
*
*
*
est1Δ
EST1
est1-06
est1-07
est1-38
est1-39
est1-41
est1-42
est1-46
est1-47
est1-49
est1-50
est1-51
est1-52
est1-54
est1-55
est1-Δ19

Figure 3-5

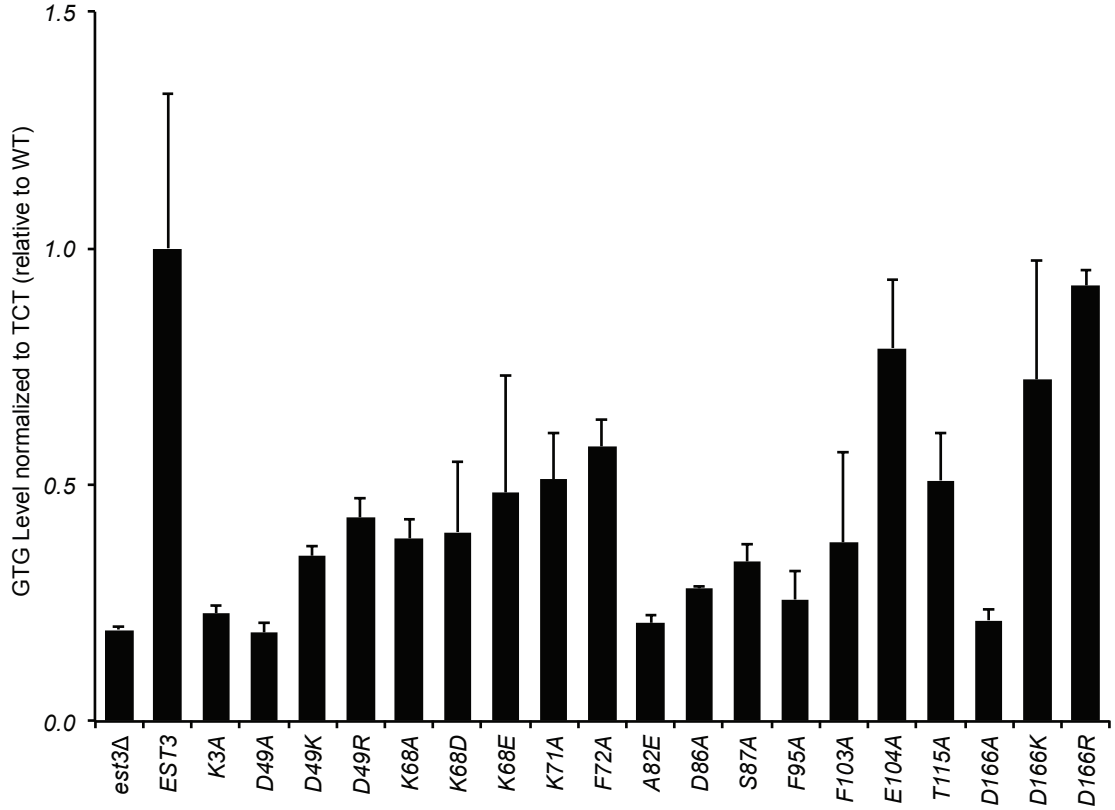
GTG Level normalized to TCT (relative to WT)
1.5
1.0
0.5
0.0
est3Δ
EST3
K3A
D49A
D49K
D49R
K68A
K68D
K68E
K71A
F72A
A82E
D86A
S87A
F95A
F103A
E104A
T115A
D166A
D166K
D166R

Figure 3-6

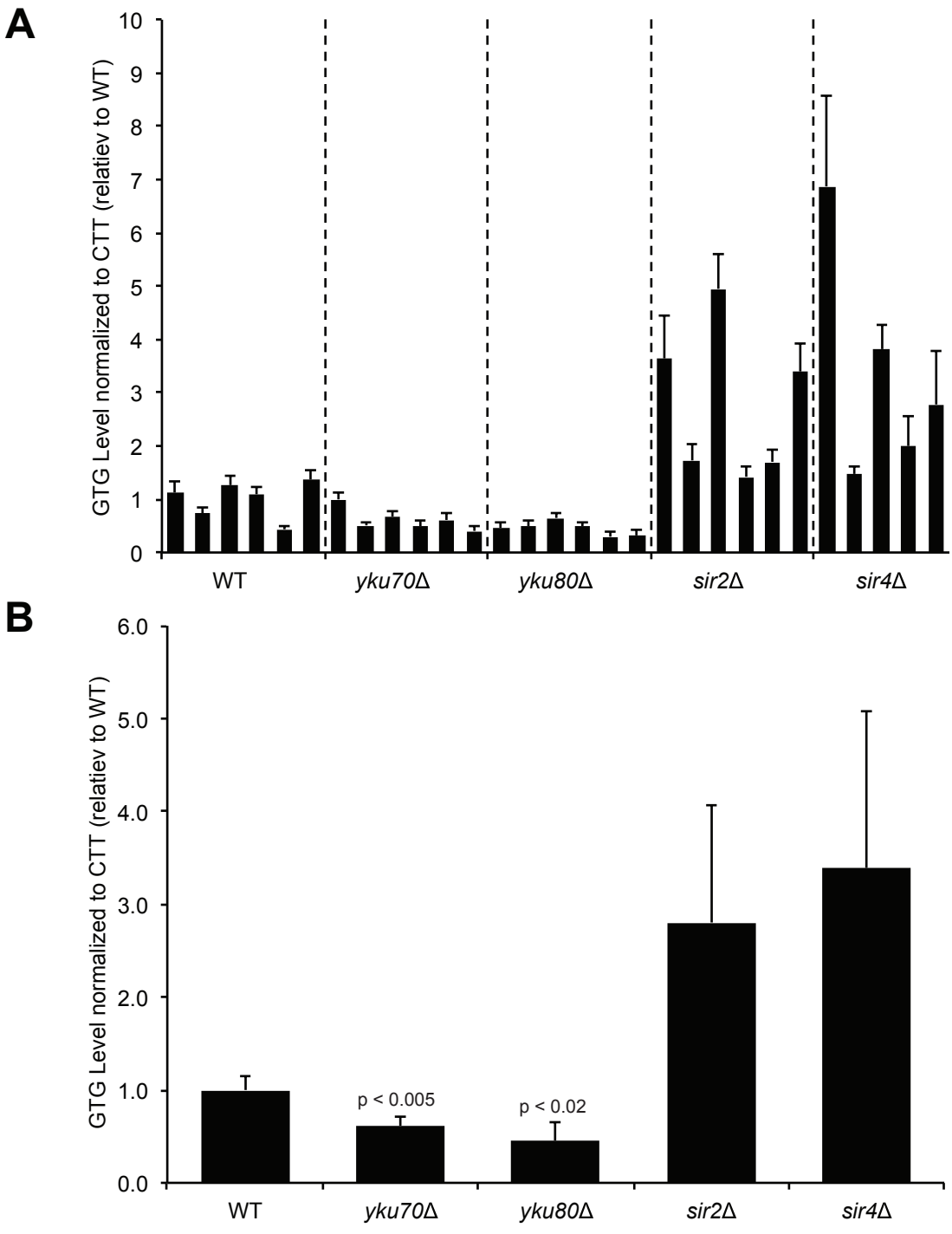
A
GTG Level normalized to CTT (relatiev to WT)
10
9
8
7
6
5
4
3
2
1
0
WT
yku70Δ
yku80Δ
sir2Δ
sir4Δ
B
GTG Level normalized to CTT (relatiev to WT)
6.0
5.0
4.0
3.0
2.0
1.0
0.0
p < 0.005
p < 0.02
WT
yku70Δ
yku80Δ
sir2Δ
sir4Δ

Figure 3-7

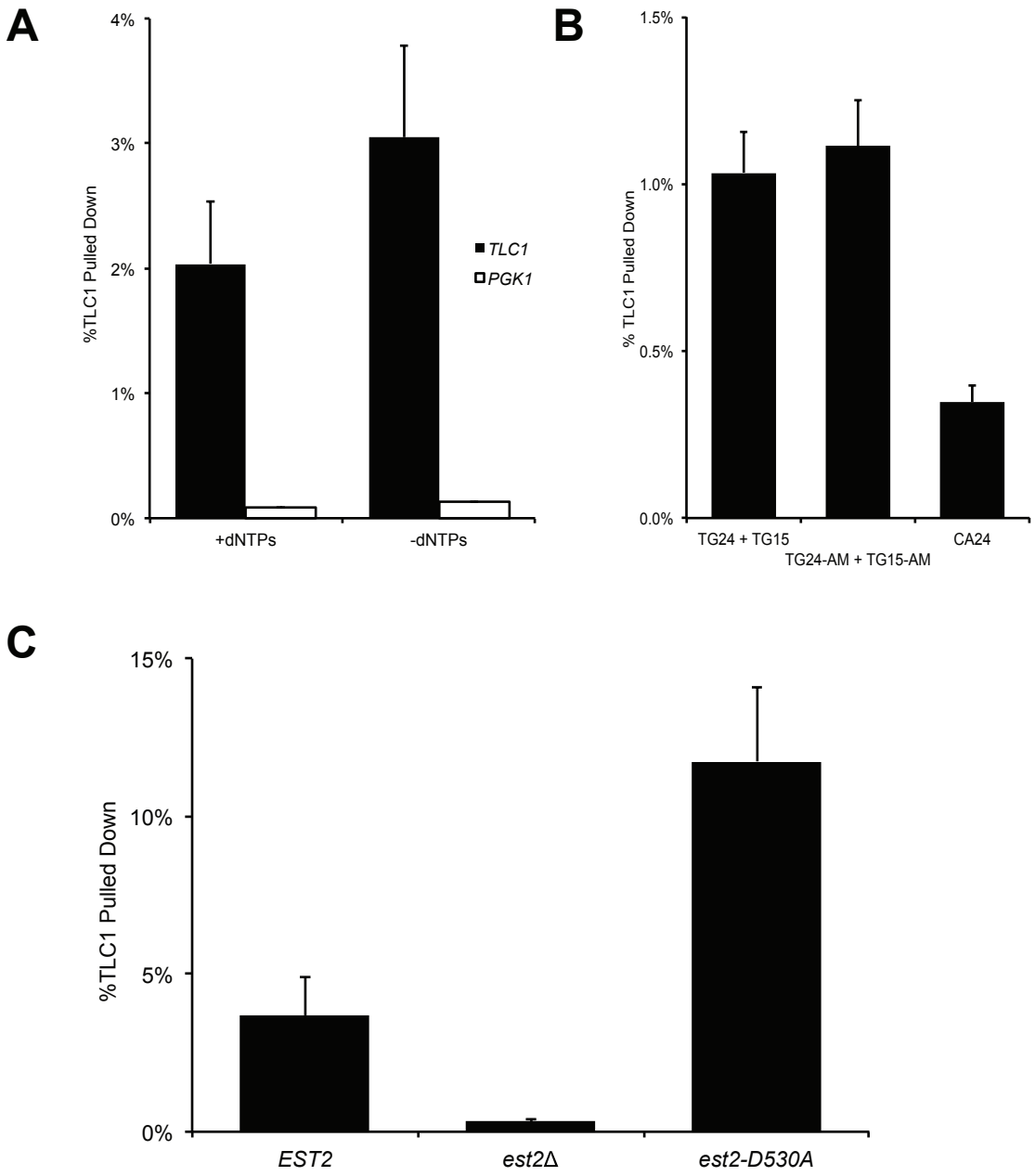
A
4%
3%
2%
1%
0%
%TLC1 Pulled Down
TLC1
PGK1
+dNTPs
-dNTPs
B
1.5%
1.0%
0.5%
0.0%
% TLC1 Pulled Down
TG24 + TG15
CA24
TG24-AM + TG15-AM
C
15%
10%
5%
0%
%TLC1 Pulled Down
EST2
est2Δ
est2-D530A

Figure 3-8

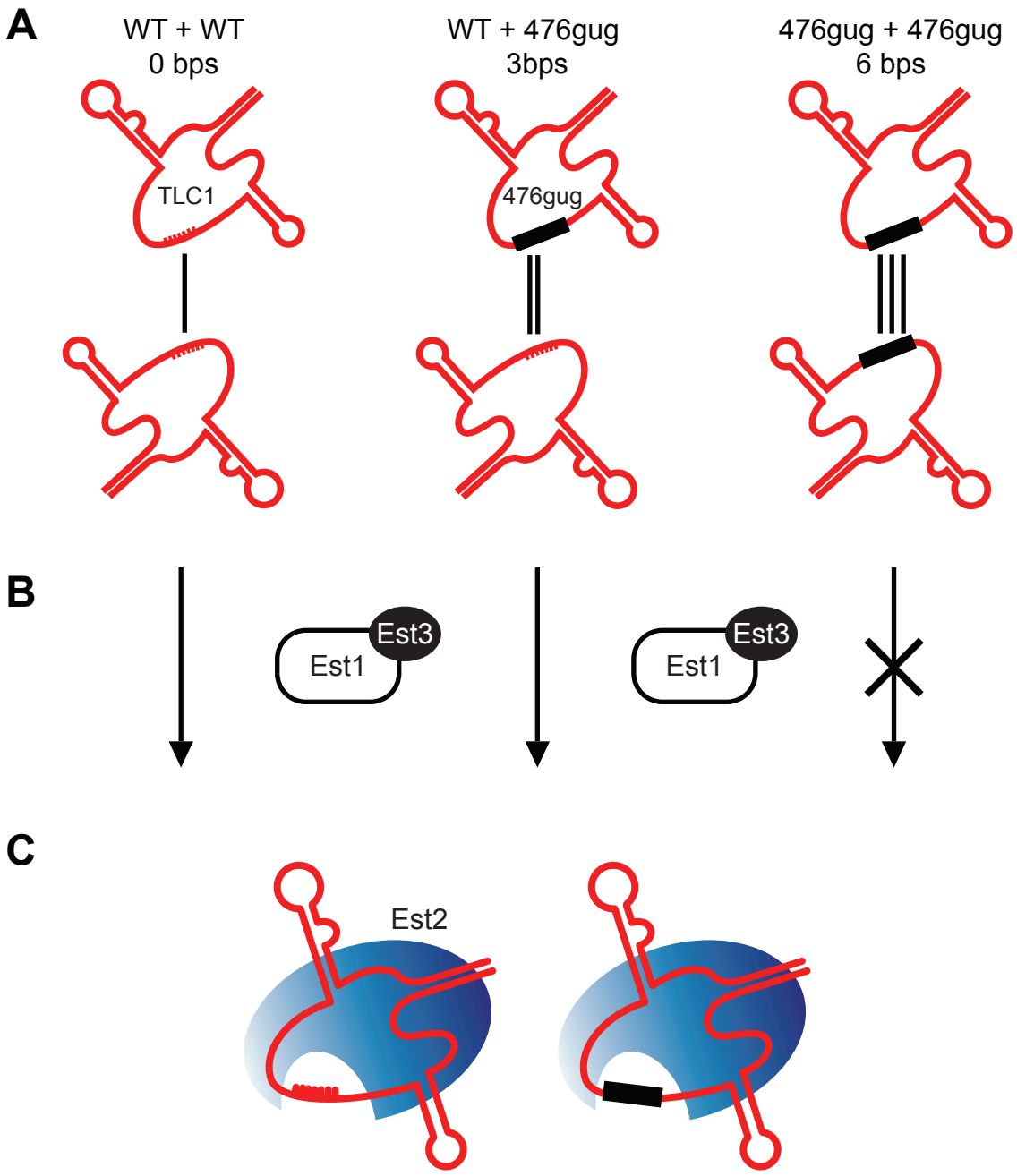
A
WT + WT
0 bps
TLC1
WT + 476gug
3bps
476gug
476gug + 476gug
6 bps
B
Est3
Est1
Est3
Est1
C
Est2

Chapter 4: Conclusions and Future Directions

In this thesis, we explored the nature of telomerase dimerization and its functional significance in *S. cerevisiae*. We showed that yeast telomerase RNA does physically dimerize; however, no evidence for dimerization of yeast telomerase reverse transcriptase protein itself has been found. We also showed that the activation functions of Est1 and Est3 modulate the functional interaction between two templates from two telomerase RNAs. These results are summarized here, and a unified model combining these results is presented.

Physical Dimerization of Telomerase RNA

In Chapter 2, we show evidence for physical dimerization of TLC1. We found two classes of TLC1 dimers and two modes by which TLC1 can dimerize. One class of TLC1 dimer was sensitive to protease treatment, and another (possibly overlapping) class was sensitive to high concentration of anti-sense oligonucleotides. The Ku complex association with TLC1, as well as the silence information regulator protein Sir4, but not silencing, is critical in one of the modes of TLC1 dimerization. The other mode requires the 3' region of TLC1 that is cleaved off in the mature version of TLC1. Abrogating both modes together *in vivo* results in abolition of TLC1-TLC1 interaction to background levels. The relationship between the classes of TLC1 dimers and two modes by which TLC1 dimerize is still under study.

The 3' region that is critical for TLC1 dimerization *in vivo* is also important for TLC1 dimerization *in vitro* (Gipson *et al*. 2007). This region is cleaved off as a part of TLC1 biogenesis pathway, and this process is only active during G1 phase of cell cycle (Chapon *et al*. 1997). This is consistent with the model that dimerization is a step during biogenesis; dimerization of TLC1 increased during G1 phase and decreased when S-phase starts.

The Ku complex and Sir4 are both telomeric-end binding proteins. Unlike Sir2, Sir3, and other subtelomere-associated proteins, Ku and Sir4 bind to more distal regions of telomeres. This suggested that this mode of TLC1 dimerization requires TLC1 recruitment to telomeres. One might expect that dimerization during TLC1 biogenesis would show an epistatic relationship; however, we have found that the cleavage of the 3' region is not a necessary step for telomerase complex formation (data not shown). This is consistent with the lack of interdependence between the two modes of TLC1 dimerization.

Surprisingly, TLC1 dimerization was not substantially affected by the deletion of essential telomerase components. We also show that Est2-Est2 interaction is not stable enough *in vitro* to be observed by the methods similar to the methods used in detecting TLC1-TLC1 interaction. Whether there are two copies of TLC1 in telomerase complex remains to be tested. The human telomerase RNA has been shown to dimerize and that dimerization is important for telomerase activity *in vitro* (Tesmer *et al*. 1999; Ly *et al*. 2003). Electron microscopy of human telomerase complex showed that two telomerase complexes are held together by the RNA and not by the reverse transcriptase (D. Rhodes,

personal communication, 2011). This is consistent with our finding that TLC1 can dimerize but not Est2.

The main unanswered question is the functional significance of the physical dimerization of telomerase RNA. The mutations that cause reduced TLC1 dimerization all result in shorter telomeres, suggesting that dimerization is important for telomerase activity. Our current working model is that TLC1 dimerization during its biogenesis is important for the telomerase assembly. This will be tested by measuring the amount TLC1-associated with Est2 in various mutations that cause TLC1 dimerization defects. Another aspect of the functional significance regarding the template-template interaction is described Chapter 3 and in the next section.

Functional Interaction of Telomerase Templates

In Chapter 3, we explored the functional interaction of TLC1 templates. We focused our studies on a particularly specialized mutation, *tlc1-476gug*, that introduces a palindromic sequence within the template (Prescott and Blackburn 1997a). This mutation was previously thought to be completely inactive, but we have developed a qPCR method that allowed us to measure the very small amount of activity retained in the *tlc1-476gug* telomerase. The qPCR method was used to verify the previous finding that the activity of *tlc1-476gug* telomerase is substantially increased by the presence of wild-type (see Chapter 3; Prescott and Blackburn 1997a). The *tlc1-476gug* mutation results in the ability of two templates to form base-pairing at six consecutive positions. The presence of such base-pairing *in vivo* is partially supported by the correlation with the template-template

intermolecular complementarity and the ability to increase 476gug mutant template usage.

Next we showed that the significant increase of *tlc1-476gug* mutant template usage, or rescue, stimulated by the wild-type TLC1 requires Est1 and Est3. Specifically, conserved residues in Est1 that are shown to be important for the "activation" function of Est1, as well as those conserved residues in the same region, were found to be important for the rescue of 476gug mutant template. Although the ability of Est1 and Est3 to rescue an unusual template mutation that is virtually inactive may be serendipitous, we believe that the mutation allowed us to uncover a function that is normally not manifested by the commonly used assays of telomerase activity.

Finally, our attempts to probe the accessibility of template regions by biotinylated oligonucleotides have shown that a DNA primer substrate of telomerase can remain bound much more stably to the telomerase complex when the substrate is not or cannot be elongated. Biotinylated oligonucleotide-directed purification of telomerase has been carried out in many studies, especially those that probed the oligomeric state of telomerase, and these studies generally do not distinguish between active and inactive telomerase complex purified by this method (Prescott and Blackburn 1997b; Wenz *et al*. 2001; Wang *et al*. 2002). The implications for the interpretation of such experiments are discussed in detail in Chapter 3. Further studies using the biotinylated oligonucleotides designed specifically against 476gug template should allow us to test the model proposed in Chapter 3.

Telomerase Dimerization as a Regulatory Mechanism

The functional interactions between two templates have been described in both human and yeast (Wenz *et al*. 2001; Prescott and Blackburn 1997b). The conservation between human and yeast in this aspect suggests that it might play an important role in telomerase activity. A parsimonious explanation would be that these template regions physically interact or are at least in a close proximity. The crystal structure of the red flour beetle shows that there is clearly not enough space in the catalytic site to accommodate two templates and a single-stranded DNA substrate (Gillis *et al*. 2008; Mitchell *et al*. 2010). If there were any physical interaction of templates at or near the catalytic site of telomerase, it would surely inhibit the activity. This is the basis for our model: that the template-template interaction may act as a self-inhibitory mechanism for telomerase activity. An activation step would involve changing the nature of the template-template interaction (*e.g*. conformational change, removal of secondary template). In this model, *tlc1-476gug* would be an extreme example of increased template-template interaction, with its extended base-pairing potential with itself. We propose that the "activation" function of Est1 and Est3 involves alleviation of a normally much more fluid template-template interaction.

Additionally, we propose that the template-template interaction is facilitated by the dimerization of TLC1. Although telomerase RNA dimerization seems to be important for efficient telomerase activity, it may also be inhibitory before telomerase complex is fully "activated." The increased activity of *tlc1-476gug* telomerase in *ku70Δ* and *ku80Δ*, in which telomerase dimerization is reduced, is consistent with this model. However, the

interpretation has many confounding elements (see Chapter 3). Finally, we suggest a model in which TLC1 dimerization during biogenesis promotes its incorporation into a telomerase complex, but it is formed in such way that it requires an activation step to increase the accessibility to the template region. Therefore, telomerase RNA dimerization can both promote and inhibit telomerase activity, which makes the process of dimerization a potentially important regulatory mechanism for telomerase activity.

Telomerase is a highly thought-after target for pharmaceutical drugs: aging and cancerous cell growth may be modulated by an activator or an inhibitor of telomerase activity. The telomerase RNA dimerization provides a unique avenue by which drugs may be targeted for either activation or inhibition of telomerase activity.

References

Chapon, C., Cech, T.R. and Zaug, A.J., 1997. Polyadenylation of telomerase RNA in budding yeast. *RNA (New York, N.Y.)*, 3(11), pp.1337-1351.

Gillis, A.J., Schuller, A.P. and Skordalakes, E., 2008. Structure of the Tribolium castaneum telomerase catalytic subunit TERT. *Nature*, 455(7213), pp.633-637.

Gipson, C.L., Xin, Z.-T., Danzy, S.C., Parslow, T.G. and Ly, H., 2007. Functional Characterization of Yeast Telomerase RNA Dimerization. *Journal of Biological Chemistry*, 282(26), pp.18857 -18863.

Ly, H., Xu, L., Rivera, M.A., Parslow, T.G. and Blackburn, E.H., 2003. A role for a novel "trans-pseudoknot" RNA–RNA interaction in the functional dimerization of human telomerase. *Genes & Development*, 17(9), pp.1078 -1083.

Mitchell, M., Gillis, A., Futahashi, M., Fujiwara, H. and Skordalakes, E., 2010. Structural basis for telomerase catalytic subunit TERT binding to RNA template and telomeric DNA. *Nat Struct Mol Biol*, 17(4), pp.513-518.

Prescott, J. and Blackburn, E.H., 1997a. Telomerase RNA mutations in Saccharomyces cerevisiae alter telomerase action and reveal nonprocessivity *in vivo* and *in vitro*. *Genes & Development*, 11(4), pp.528 -540.

Prescott, J. and Blackburn, E.H., 1997b. Functionally interacting telomerase RNAs in the yeast telomerase complex. *Genes & Development*, 11(21), pp.2790 -2800.

Tesmer, V.M., Ford, L.P., Holt, S.E., Frank, B.C., Yi, X., Aisner, D.L., Ouellette, M., Shay, J.W. and Wright, W.E., 1999. Two Inactive Fragments of the Integral RNA Cooperate To Assemble Active Telomerase with the Human Protein Catalytic Subunit (hTERT) *In vitro*. *Mol*. *Cell*. *Biol*., 19(9), pp.6207-6216.

Wang, L., Dean, S.R. and Shippen, D.E., 2002. Oligomerization of the telomerase reverse transcriptase from Euplotes crassus. *Nucleic Acids Research*, 30(18), pp.4032 -4039.

Wenz, C., Enenkel, B., Amacker, M., Kelleher, C., Damm, K. and Lingner, J., 2001. Human telomerase contains two cooperating telomerase RNA molecules. *EMBO J*, 20(13), pp.3526-3534.

Appendix 1: An Unbiased Screen to Investigate Any Potential Non-catalytic or Other Functions of Telomerase.

Tetsuya Matsuguchi[1], Eric Jang[1], Sean Collins[2,3], David Breslow[2,3], Nevan Krogan[2], Jonathan Weissman[2,3], and Elizabeth H. Blackburn[1]

[1]Department of Biochemistry and Biophysics

[2]Department of Cellular and Molecular Pharmacology

[3]Howard Hughes Medical Institute

University of California, San Francisco

San Francisco, CA 94158

Introduction

It has been previously reported that lack of telomerase activity on telomeres, caused by either deletion of any of the genes encoding the known core components of telomerase – Est1, Est2, Est3, or TLC1 – or by a mutation causing loss of the ability of telomerase to elongate and maintain telomeres *in vivo* - the *cdc13-2* mutant (formerly called *est4-1*) – were all phenotypically indistinguishable from each other (Lendvay *et al*. 1996). This implied that the only function of telomerase is to elongate telomeres and thereby prevent senescence. To examine this question further, *est1Δ*, *est2Δ*, *est3Δ*, *tlc1Δ*, *est2-D530A*, *est2-ΔN20* mutants were compared. The *est2-ΔN20* mutant was included in this analysis because it had an unusual reported phenotype: it caused not only short telomeres and senescence, but also an immediate slow-growth phenotype (Xia *et al*. 2000). In this

respect, it was unlike the other telomerase mutants, none of which were reported to show growth effects until senescence.

The genetic interaction screen called the Epistatic MiniArray Profile (E-MAP) technique was used (Schuldiner *et al*. 2005). In this approach, each haploid MATα strain carrying a telomerase mutation was crossed to the collection of MATa mutation strains, and the colony growth phenotype was measured in the spores that carried both mutations (Figure A1-1). The collection of mutant strains used contained 754 alleles of 743 genes that are involved in various aspects of chromosome biology (Collins *et al*. 2007). Most of the mutations in this collection were deletions of non-essential genes, and the DAmP allele of 70 essential genes, which had reduced abundance of mRNA (Schuldiner *et al*. 2005).

Results

The colony sizes of single mutants (mutant collection mutation) and double mutants (mutant collection mutation and telomerase mutation) were scored as previously described (Collins *et al*. 2007). The genetic interaction was calculated as the log of the ratio of the actual double mutant growth to the expected double mutant growth based on the growth of each single mutant. The alleviating (yellow), aggravating (blue) or no (black) genetic interactions are represented by the gradient of colors (Figure A2-1A). This new set of data was combined with all of the previous E-MAP data collected in the Weissman Lab. Clustering analysis for the entire set of data was carried out, which

clusters mutant alleles that behave similarly to each other when combined with other mutations. The clustered set of data is shown in Figures A1-2 through A1-5.

Genetic interactions with telomerase complex

All of the telomerase mutants clustered together in this analysis, including the *est1Δ* strain included in previous E-MAPs (Figure A1-5; bottom panel, first seven columns). This clustering concurs with the previous findings that telomerase mutations generally behave similarly. Synthetic lethality between telomerase mutations and deletions of Ku complex (*yku70Δ* and *yku80Δ*) has been reported (Gravel *et al*. 1998; Polotnianka *et al*. 1998; Nugent *et al*. 1998). Indeed, the strongest genetic interactions identified with telomerase mutations were *yku70Δ* and *yku80Δ* (Figure A1-6A). Weaker, alleviating genetic interactions were found with the cochaperon prefoldin complex, *PAC10/GIM2* and *GIM5* (Geissler *et al*. 1998; FigureA1-6B) and the nucleotide excision repair genes, *RAD1* and *RAD14* (Figure A1-6C). The prefoldin complex has been shown to be synthetic lethal to *cdc13-1* mutation (Addinall *et al*. 2008), which is a mutation in the single-stranded telomere binding protein. In addition, the clustering of the all mutations brought together telomerase mutations with cochaperon prefoldin complex (Figure A1-5; bottom panel), indicating that telomerase mutations and the prefoldin complex show similar genetic interactions.

Distinct genetic interactions of the telomerase deletions from the catalytically dead telomerase mutation, *est2-D530A*

To identify genetic interactions that might uncover the non-catalytic functions of telomerase, the growth of double mutants with *est2-D530A* were compared to that of double mutants with telomerase deletions (Figure A1-2B). Genetic interactions with *est2-D530A* that are distinct from deletions indicate functional difference between complete loss of telomerase and telomerase incapable of telomere elongation but may potentially be functional in other processes. The top three such candidates were identified: the Ku complex, the Ino80 complex, and the Bre5/Ubp3 ubiquitin-protease complex (Figure A1-7).

As discussed above, the Ku complex had aggravating interactions with both *est2-D530A* and deletion mutations; however, *est2-D530A* strain had much less synthetically sick phenotype compared to the deletions (Figure A1-7A). The Ku complex plays a role in various aspects of telomere biology, including telomere tethering to nuclear periphery, telomere position effect, telomerase recruitment to telomeres, and replication timing of telomeres. In addition, the Ku complex is essential for non-homologous end-joining (NHEJ), a DNA repair pathway.

The Ino80 complex is an ATP-dependent chromatin-remodeling complex that has been shown to be important in transcriptional regulations as well as at DSBs (Watanabe and Peterson 2010). The Ino80 complex has 10 subunits: Ino80 (the ATPase subunit), Rvb1 and Rvb2 (helicase-like), Arp4, Arp5, and Arp8 (actin-related), Nhp10 (HMG-like), and Ies1-6 (Ino-Eighty Subunit) (Watanabe and Peterson 2010). Of these, Rvb1,

Rvb2, and Arp4 are essential. The screen showed that double deletions of *IES1*, *IES3*, and *IES5* with telomerase deletions had alleviating interactions, while there was no interaction with *est2-D530A*. This relationship was not seen in deletions of *NHP10* and *ARP8* (Figure A1-7B). It has recently been shown that one of the Ino80 complex subunit Ies3 interacts with Est1 in yeast two-hybrid as well as in coIP experiments (Yu *et al*. 2007). Also Ino80 complex is associated with telomeres by ChIP experiments (Yu *et al*. 2007). In addition, *ies3Δ est1Δ* and *ies3Δ est2Δ* double mutants show increased telomere-telomere fusions and extra-chromosomal telomeric circles, while *arp8Δ est2Δ* double mutant did not (Yu *et al*. 2007). This difference between *IES3* and *ARP8* is consistent with the difference we observed in the E-MAP screen, and suggests that increased NHEJ may be the reason for alleviation/buffering of telomerase deletion mutations.

Bre5 and Ubp3 are the subunits of a ubiquitin protease complex (Cohen *et al*. 2003). The double mutants of *BRE5* or *UBP3* with telomerase deletions show synthetic interactions while *est2-D530A* and *est2-ΔN20* did not (Figure A1-7C). Telomere silencing is enhanced in *bre5Δ* and *ubp3Δ* strains (Moazed and Johnson 1996). Bre5 also plays a role in the NHEJ pathway, and down-regulation of NHEJ has been observed in *bre5Δ* strains (Bilsland *et al*. 2007).

Overall, all three complexes identified to have different genetic interactions from *est2-D530A* compared to deletions strains have known telomere-related functions, and most notably, all complexes modulates levels of NHEJ. Intriguingly, *est2-D530A* fared better than deletion mutations when the Ku complex and the Bre5/Ubp3 complex, which promote NHEJ, were mutated, and it fared worse when the Ino80 complex, which

competes with NHEJ, was mutated. If the relationship held true, this would suggest that *est2-D530A* can inhibit the deleterious effects of non-NHEJ processes at telomeres and that NHEJ could increase the survival of telomere shortening, possibly by delaying senescence.

Additionally, *est2-D530A* mutation showed synthetically sick phenotype with DNA replication genes associated with DNA damage: homologous recombination genes (*RAD57*, *RAD54*, *RAD51*), base-excision repair pathway (*POL32* and *RAD27*), and the Sgs1 complex (*TOP3* and *RMI1*) (Figure A1-8). These pathways can affect telomere biology in any number of ways, but when DNA damage is present, these NHEJ and other DNA damage repair pathways compete; therefore, these mutations can be driving the level of NHEJ higher.

Tetrad analysis failed to verify E-MAP results

To verify these findings, the deletions were made in freshly made in diploid yeast cells that are heterozygous at the *EST2* locus, *est2Δ* and *est2-D530A*. Starting with heterozygous strain is ideal, because there will be no confounding effect from slightly different telomere lengths between *est2Δ* and *est2-D530A*. In addition, the diploid strain carried *EST2-CDC13* fusion on a CEN-ARS plasmid. Cells carrying *EST2-CDC13* fusion have longer telomeres, and this will prevent spores from senescing before colony size differences can be determined. This CEN-ARS plasmid was kicked out immediately before the diploids were subjected to sporulation conditions.

One copy of each of the candidate synthetic lethal genes (*e.g. YFG1*) was deleted in this strain. When sporulated, half of the tetrads will be a tetratype containing spores of the genotypes: *est2Δ YFG1*, *est2Δ yfg1Δ*, *est2-D530A YFG1*, and *est2-D530A ygf1Δ*. The spores were dissected and grown on rich medium. The size of the colonies was scored prior to identifying the genotype of each colony in the tetrads. If the synthetic interaction difference between deletion and catalytic mutations were real, the colony size between *est2Δ yfgxΔ* and *est2-D530A yfgxΔ* would be different. However, the visual size scoring of these colonies showed no appreciable difference.

Direct competitive growth assay failed to verify E-MAP results

Visual scoring of colony sizes may not be able to discern small differences in growth rates. Weissman lab has developed a competition assay using cells expressing GFP and cells that don't express GFP (Breslow *et al*. 2008). These strains were combined in equal number in a liquid media and grown several generations. Because both strains are growing under the same condition, if there are no growth rate differences between the strains, the ratio of GFP+ and GFP- strains should remain constant. As cells grow exponentially, the ratio of GFP+ and GFP- strains changes exponentially if one strain has a growth advantage, and this method allows measuring growth rate difference as small as 1%. We carried out these experiments using the strains made above. Again, we observed no discernable differences in the growth rate.

No extra mutations were found in strains used for E-MAP

The strains used to verify the E-MAP findings were derived from the same S288c background, from which deletion collection was created. However, it remained possible that the deletion collection used in the original screen described above contained an extra mutation that does not exist in the strains used in the later experiments. To test this possibility, Eric Jang, a high school volunteer, used the strains from the deletion collection (Walter Lab) to repeat the experiments. He used a random spore selection method that is similar to the one used for the E-MAP analysis. For all the strains he tested, none of them showed different colony sizes between *est2Δ* and *est2-D530A* spores.

Discussion

The E-MAP analysis identified several complexes that genetically interacted with telomerase mutations; many of these have known telomere functions. It seems unlikely that all of these likely candidates were artifacts. The main difference between the E-MAP analysis and other experiments designed to verify the E-MAP data is that verification experiments were carefully designed not to have cells reach senescence, which may confound the analysis. In those verification experiments, a Cdc13-Est2 fusion plasmid had kept the telomeres long prior to sporulation, and even though this plasmid was selected against before scoring for colony growth phenotypes, the telomeres would still have been longer than wild-type for at least some period during the colony size analysis procedures. In contrast, in the E-MAP analysis, there were several selection steps that

require many generations of growth in absence of telomerase; telomeres in these strains could have been critically short or approaching critical shortness by the time cell growth was scored. It is possible, then, that these genetic interactions observed in the E-MAP analysis require short telomeres or senescing cells. Given the recent data on different sensitivity of *est2-D530A* and *est2Δ* cells to G-quartet binding drugs, this seems plausible.

Recently, Eric Jang, a high school volunteer, has looked at the effect of G-quartet binding chemicals on Type I and Type II survivors (cells maintaining telomere via recombination) formed from *est2Δ* and *est2-D530A* mutants. Surprisingly, there were different effects of the chemicals depending on whether the survivors were *est2Δ* or *est2-D530A*. Specifically, in Type I survivors, in which Y' subtelomere region is amplified by homologous recombination, *est2-D530A* strain showed up to 20-fold increase in amplified Y' region while *est2Δ* strain showed up to 60- to 80-fold amplification. This suggests either that survivors formed in *est2Δ* and *est2-D530A* are somehow different, or that non-catalytic *est2-D530A* still goes to telomere in survivors and perhaps "caps" the telomeres, preventing recombination from taking place at the telomeres.

Many of the complexes and pathways identified are involved in DNA damage repair pathways, especially NHEJ. This is consistent with the idea that catalytically-dead telomerase can still act as a protective cap at the telomeres. Although different DNA repair pathways are specialized and preferred for certain types of damage, many of them are versatile and can compete for DNA damage substrates. The reason for why so many

different DNA pathways were identified may be that they all modulate the level of one particular DNA repair pathway (*e.g.* NHEJ).

This model has support from observations in the budding yeast *Candida albicans*. Deletion of the genes encoding Est2 or telomerase RNA components of telomerase in *C. albicans* caused a low fraction of the shortening telomeres to undergo a distinctive, measurable degradation of the 5' end DNA strand, even while the bulk culture cells were still growing, and well before senescence (Hsu *et al*. 2007). In contrast, in the strain corresponding to the *est2-D530A* catalytically-dead point-mutant (*est2-D667A*), even though the culture underwent similar kinetics of bulk telomere shortening and senescence, such telomeric DNA degradation was considerably reduced (Hsu *et al*. 2007). This finding suggested that the Est2, even though catalytically-dead, was protecting the telomeres from these low-frequency but measurable degradation events that occur even while telomeres are long in this species.

Given the strong supporting evidence for complexes identified to have true genetic interactions, senescing and survivor cells that are *est2Δ* and *est2-D530A* should be tested for synthetic interactions. The common theme in NHEJ and other DNA repair pathways suggest that measuring not only the cell growth phenotype but also telomere-telomere fusions or other signs of DNA damage repair would likely be fruitful.

Materials and Methods

Plasmids

Jue Lin provided pEHB4016 (pRS316-EST1) and pEHB4009 (pRS316-EST2). The plasmid pEHB22,298 (pRS316-EST3) was constructed by PCR-amplifying *EST3* ORF and 500 base-pairs of the flanking regions and subcloning the PCR product between NotI and EcoRI sites in pRS316. Shivani Nautiyal provided pRS316-TLC1. Cdc13-Est2 fusion plasmid was provided by Sveta Makovets.

Yeast strains and media

Yeast cultures were grown in standard rich medium or minimal media (YEPD or CSM). Deletion strains were made using a PCR-based transformation method (Longtine *et al*. 1998). The non-deletion mutations, *est2-D530A* and *est2-ΔN20* were introduced by PCR-amplifying the mutation constructs with the natMX6 marker using the fusion PCR method. The standard sporulation conditions were used.

E-MAP

E-MAP experiments were performed using the same collection of mutations as described (Collins *et al*. 2007). Genetic interaction scores were calculated as previously described (Collins *et al*. 2006).

FACS

FACSCalibur was used to measure the GFP fluorescence levels of yeast cells. The GFP-positive and GFP-negative strains were used to define a gate for distinguishing GFP+ and GFP- cells. At least 20,000 cells were used for the measurement.

References

Addinall, S.G., Downey, M., Yu, M., Zubko, M.K., Dewar, J., Leake, A., Hallinan, J., Shaw, O., James, K., Wilkinson, D.J., Wipat, A., Durocher, D. and Lydall, D., 2008. A Genomewide Suppressor and Enhancer Analysis of cdc13-1 Reveals Varied Cellular Processes Influencing Telomere Capping in Saccharomyces cerevisiae. *Genetics*, 180(4), pp.2251 -2266.

Bilsland, E., Hult, M., Bell, S.D., Sunnerhagen, P. and Downs, J.A., 2007. The Bre5/Ubp3 ubiquitin protease complex from budding yeast contributes to the cellular response to DNA damage. *DNA Repair*, 6(10), pp.1471-1484.

Breslow, D.K., Cameron, D.M., Collins, S.R., Schuldiner, M., Stewart-Ornstein, J., Newman, H.W., Braun, S., Madhani, H.D., Krogan, N.J. and Weissman, J.S., 2008. A comprehensive strategy enabling high-resolution functional analysis of the yeast genome. *Nat Meth*, 5(8), pp.711-718.

Cohen, M., Stutz, F., Belgareh, N., Haguenauer-Tsapis, R. and Dargemont, C., 2003. Ubp3 requires a cofactor, Bre5, to specifically de-ubiquitinate the COPII protein, Sec23. *Nat Cell Biol*, 5(7), pp.661-667.

Collins, S.R., Schuldiner, M., Krogan, N.J. and Weissman, J.S., 2006. A strategy for extracting and analyzing large-scale quantitative epistatic interaction data. *Genome Biology*, 7(7), p.R63.

Collins, S.R. *et al*., 2007. Functional dissection of protein complexes involved in yeast chromosome biology using a genetic interaction map. *Nature*, 446(7137), pp.806-810.

Geissler, S., Siegers, K. and Schiebel, E., 1998. A novel protein complex promoting formation of functional [alpha]- and [gamma]-tubulin. *EMBO J*, 17(4), pp.952-966.

Gravel, S., Larrivée, M., Labrecque, P. and Wellinger, R.J., 1998. Yeast Ku as a Regulator of Chromosomal DNA End Structure. *Science*, 280(5364), pp.741 -744.

Hsu, M., McEachern, M.J., Dandjinou, A.T., Tzfati, Y., Orr, E., Blackburn, E.H. and Lue, N.F., 2007. Telomerase core components protect Candida telomeres from aberrant overhang accumulation. *Proceedings of the National Academy of Sciences of the United States of America*, 104(28), pp.11682-11687.

Lendvay, T.S., Morris, D.K., Sah, J., Balasubramanian, B. and Lundblad, V., 1996. Senescence mutants of Saccharomyces cerevisiae with a defect in telomere replication identify three additional EST genes. *Genetics*, 144(4), pp.1399-1412.

Longtine, M.S., Mckenzie III, A., Demarini, D.J., Shah, N.G., Wach, A., Brachat, A., Philippsen, P. and Pringle, J.R., 1998. Additional modules for versatile and economical PCR-based gene deletion and modification in Saccharomyces cerevisiae. *Yeast*, 14(10), pp.953-961.

Moazed, D. and Johnson, A.D., 1996. A Deubiquitinating Enzyme Interacts with SIR4 and Regulates Silencing in S. cerevisiae. *Cell*, 86(4), pp.667-677.

Nugent, C.I., Bosco, G., Ross, L.O., Evans, S.K., Salinger, A.P., Moore, J.K., Haber, J.E. and Lundblad, V., 1998. Telomere maintenance is dependent on activities required for end repair of double-strand breaks. *Current Biology*, 8(11), pp.657-662.

Polotnianka, R.M., Li, J. and Lustig, A.J., 1998. The yeast Ku heterodimer is essential for protection of the telomere against nucleolytic and recombinational activities. *Current Biology*, 8(14), pp.831-835.

Schuldiner, M., Collins, S.R., Thompson, N.J., Denic, V., Bhamidipati, A., Punna, T., Ihmels, J., Andrews, B., Boone, C., Greenblatt, J.F., Weissman, J.S. and Krogan, N.J., 2005. Exploration of the Function and Organization of the Yeast Early Secretory Pathway through an Epistatic Miniarray Profile. *Cell*, 123(3), pp.507-519.

Watanabe, S. and Peterson, C.L., 2010. The INO80 Family of Chromatin-Remodeling Enzymes: Regulators of Histone Variant Dynamics. *Cold Spring Harbor Symposia on Quantitative Biology*, 75, pp.35-42.

Xia, J., Peng, Y., Mian, I.S. and Lue, N.F., 2000. Identification of Functionally Important Domains in the N-Terminal Region of Telomerase Reverse Transcriptase. *Mol. Cell. Biol.*, 20(14), pp.5196-5207.

Yu, E.Y., Steinberg-Neifach, O., Dandjinou, A.T., Kang, F., Morrison, A.J., Shen, X. and Lue, N.F., 2007. Regulation of Telomere Structure and Functions by Subunits of the INO80 Chromatin Remodeling Complex. *Molecular and Cellular Biology*, 27(16), pp.5639-5649.

Figure Legends

Figure A1-1. E-MAP Scheme.

(A) Each of the telomerase mutation (*e.g. est2Δ*) is combined with the mutation collection (*e.g. yfg1Δ*) by mating. (B) The resulting doubly heterozygous diploid is selected and sporulated. (C) *MATa* spores are selected, and the single mutant (*e.g. EST2 yfg1Δ*) and the double mutant (*e.g. est2Δ yfg1Δ*) are scored.

Figure A1-2. E-MAP legends and data.

(A) Rows 7-16 represent the genetic interaction of telomerase mutants with each of the mutation in the collection. All of the strains were newly made for this assay except

*est1Δ**, which was used in the previous E-MAPs. (B) Rows 1-6 represent the fitness difference of each telomerase mutant compared to the geometric mean of all of the telomerase mutants (the mean value of rows 9-16). (C) Each column shows the genetic interactions of the allele indicated at the top with the telomerase mutations. The dendrograms are the result of clustering by the similar phenotypes. Rows 1-16 are described in (A) and (B).

Figure A1-3 through A1-5. Continuation of E-MAP data from A1-2C.

Figure A1-6. Genetic interactions with telomerase components.
Genetic interactions with telomerase components were found with (A) Ku complex, (B) cochaperon prefoldin complex, and (C) the nucleotide excision repair genes. These are zoom-in sections of the figures A1-3 through A1-5.

Figure A1-7. Different genetic interactions between *est2-D530A* and deletion mutations. Row 1 shows the difference between genetic interactions of *est2-D530A* and other telomerase deletion mutations. (A) The Ku complex, (B) the Ino80 complex, and (C) the Bre5/Ubp3 ubiquitin-protease complex are shown. These are zoom-in sections of the figures A1-3 through A1-5.

Figure A1-8. Aggravating interactions between *est2-D530A* and DNA repair pathways. Two of the *est2-D530A* mutations (Row 9 and 11) show fairy strong synthetically sick phenotypes with the base-excision, homologous recombination, and Sgs1 complex genes. This is a zoom-in view of sections from Figures A1-3 and A1-4.

Figure A1-1

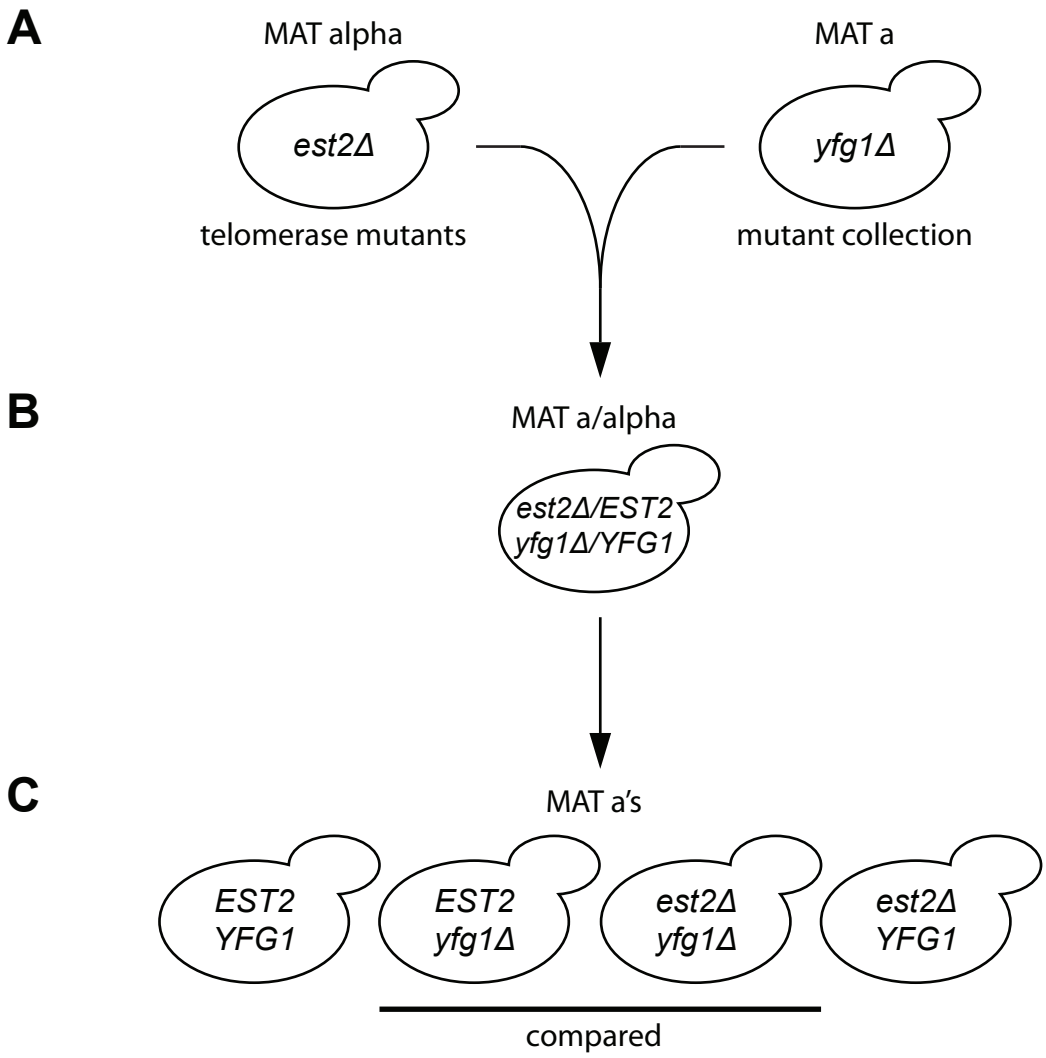
A
MAT alpha
MAT a
est2Δ
yfg1Δ
telomerase mutants
mutant collection
B
MAT a/alpha
est2Δ/EST2
yfg1Δ/YFG1
C
MAT a's
EST2
YFG1
EST2
yfg1Δ
est2Δ
yfg1Δ
est2Δ
YFG1
compared

Figure A1-2

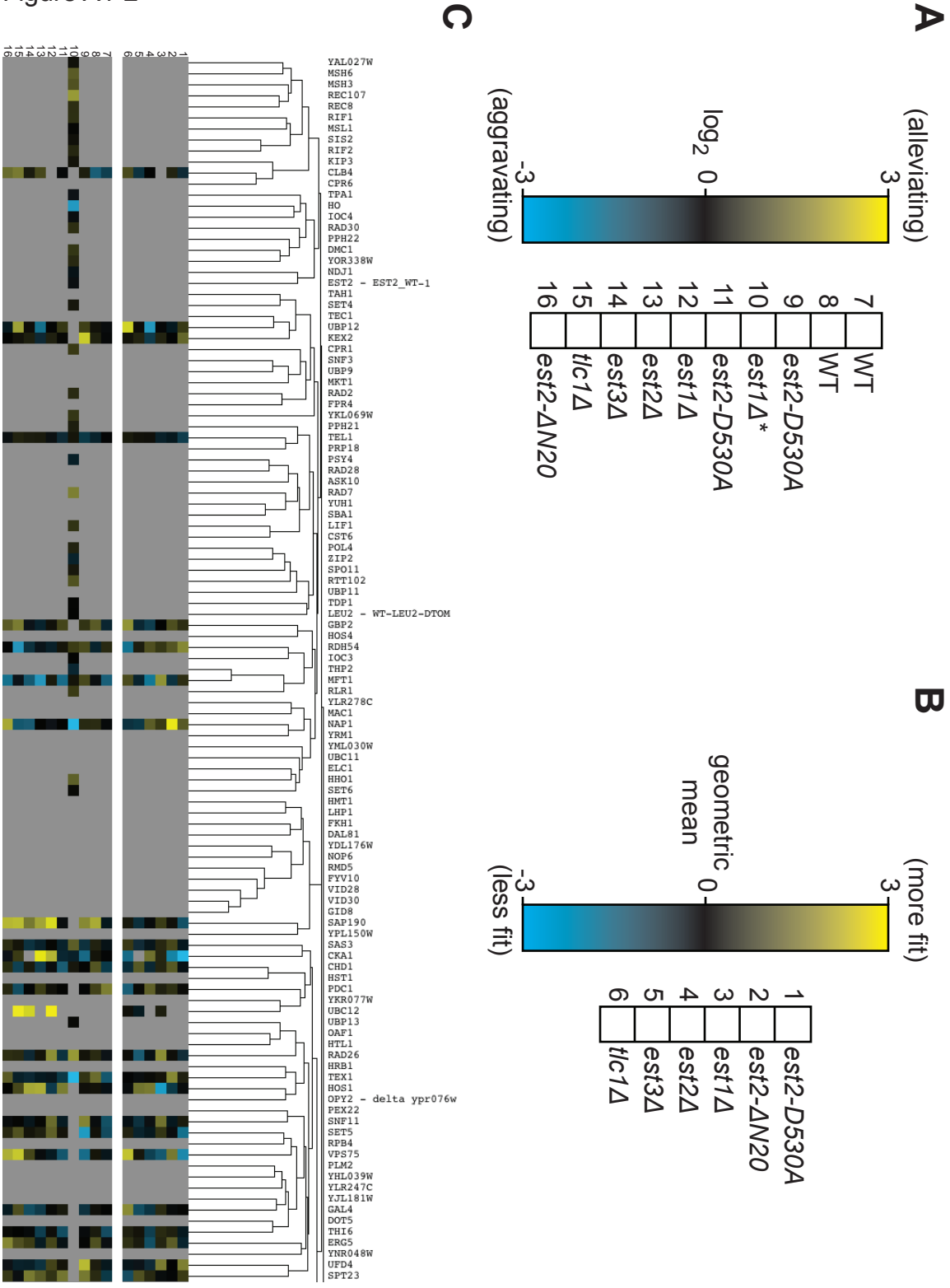
A
(alleviating)
3
0
-3
(aggravating)
log2
7 WT
8 WT
9 est2-D530A
10 est1Δ*
11 est2-D530A
12 est1Δ
13 est2Δ
14 est3Δ
15 tlc1Δ
16 est2-ΔN20
B
(more fit)
3
0
-3
(less fit)
geometric mean
1 est2-D530A
2 est2-ΔN20
3 est1Δ
4 est2Δ
5 est3Δ
6 tlc1Δ
C
YAL027W
MSH6
MSH3
REC107
REC8
RIF1
MSL1
SIS2
RIF2
KIP3
CLB4
CPR6
TPA1
HO
IOC4
RAD30
PPH22
DMC1
YOR338W
NDJ1
EST2 - EST2_WT-1
TAH1
SET4
TEC1
UBP12
KEX2
CPR1
SNF3
UBP9
MKT1
RAD2
FPR4
YKL069W
PPH21
TEL1
PRP18
PSY4
RAD28
ASK10
RAD7
YUH1
SBA1
LIF1
CST6
POL4
ZIP2
SPO11
RTT102
UBP11
TDP1
LEU2 - WT-LEU2-DTOM
GBP2
HOS4
RDH54
IOC3
THP2
MFT1
RLR1
YLR278C
MAC1
NAP1
YRM1
YML030W
UBC11
ELC1
HHO1
SET6
HMT1
LHP1
FKH1
DAL81
YDL176W
NOP6
RMD5
FYV10
VID28
VID30
GID8
SAP190
YPL150W
SAS3
CKA1
CHD1
HST1
PDC1
YKR077W
UBC12
UBP13
OAF1
HTL1
RAD26
HRB1
TEX1
HOS1
OPY2 - delta ypr076w
PEX22
SNF11
SET5
RPB4
VPS75
PLM2
YHL039W
YLR247C
YJL181W
GAL4
DOT5
THI6
ERG5
YNR048W
UFD4
SPT23

Figure A1-3

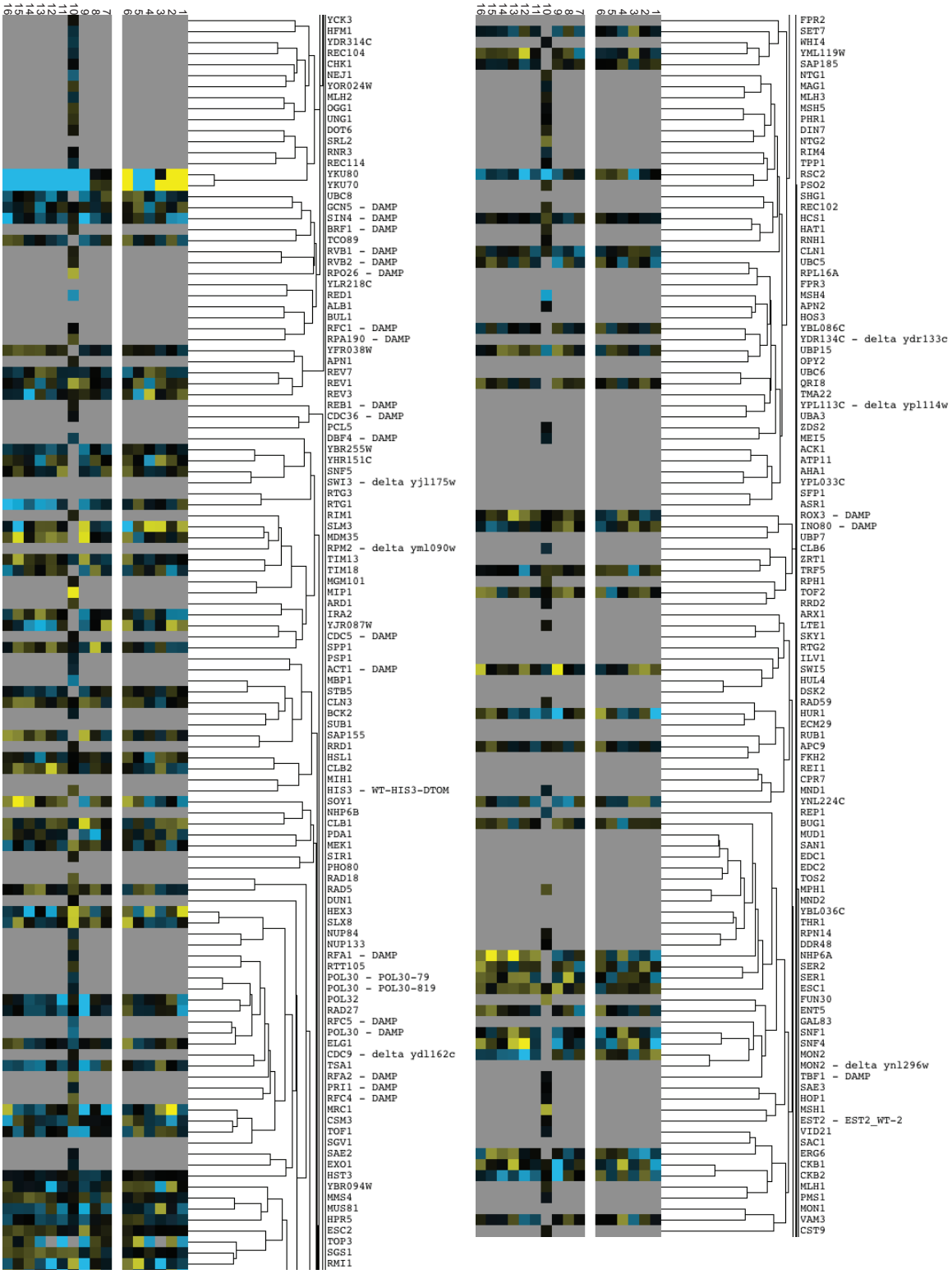
YCK3
HFM1
YDR314C
REC104
CHK1
NEJ1
YOR024W
MLH2
OGG1
UNG1
DOT6
SRL2
RNR3
REC114
YKU80
YKU70
UBC8
GCN5 - DAMP
SIN4 - DAMP
BRF1 - DAMP
TCO89
RVB1 - DAMP
RVB2 - DAMP
RPO26 - DAMP
YLR218C
RED1
ALB1
BUL1
RFC1 - DAMP
RPA190 - DAMP
YFR038W
APN1
REV7
REV1
REV3
REB1 - DAMP
CDC36 - DAMP
PCL5
DBF4 - DAMP
YBR255W
YHR151C
SNF5
SWI3 - delta yjl175w
RTG3
RTG1
RIM1
SLM3
MDM35
RPM2 - delta yml090w
TIM13
TIM18
MGM101
MIP1
ARD1
IRA2
YJR087W
CDC5 - DAMP
SPP1
PSP1
ACT1 - DAMP
MBP1
STB5
CLN3
BCK2
SUB1
SAP155
RRD1
HSL1
CLB2
MIH1
HIS3 - WT-HIS3-DTOM
SOY1
NHP6B
CLB1
PDA1
MEK1
SIR1
PHO80
RAD18
RAD5
DUN1
HEX3
SLX8
NUP84
NUP133
RFA1 - DAMP
RTT105
POL30 - POL30-79
POL30 - POL30-819
POL32
RAD27
RFC5 - DAMP
POL30 - DAMP
ELG1
CDC9 - delta ydl162c
TSA1
RFA2 - DAMP
PRI1 - DAMP
RFC4 - DAMP
MRC1
CSM3
TOF1
SGV1
SAE2
EXO1
HST3
YBR094W
MMS4
MUS81
HPR5
ESC2
TOP3
SGS1
RMI1
FPR2
SET7
WHI4
YML119W
SAP185
NTG1
MAG1
MLH3
MSH5
PHR1
DIN7
NTG2
RIM4
TPP1
RSC2
PSO2
SHG1
REC102
HCS1
HAT1
RNH1
CLN1
UBC5
RPL16A
FPR3
MSH4
APN2
HOS3
YBL086C
YDR134C - delta ydr133c
UBP15
OPY2
UBC6
QRI8
TMA22
YPL113C - delta ypl114w
UBA3
ZDS2
MEI5
ACK1
ATP11
AHA1
YPL033C
SFP1
ASR1
ROX3 - DAMP
INO80 - DAMP
UBP7
CLB6
ZRT1
TRF5
RPH1
TOF2
RRD2
ARX1
LTE1
SKY1
RTG2
ILV1
SWI5
HUL4
DSK2
RAD59
HUR1
ECM29
RUB1
APC9
FKH2
REI1
CPR7
MND1
YNL224C
REP1
BUG1
MUD1
SAN1
EDC1
EDC2
TOS2
MPH1
MND2
YBL036C
THR1
RPN14
DDR48
NHP6A
SER2
SER1
ESC1
FUN30
ENT5
GAL83
SNF1
SNF4
MON2
MON2 - delta ynl296w
TBF1 - DAMP
SAE3
HOP1
MSH1
EST2 - EST2_WT-2
VID21
SAC1
ERG6
CKB1
CKB2
MLH1
PMS1
MON1
VAM3
CST9

Figure A1-4

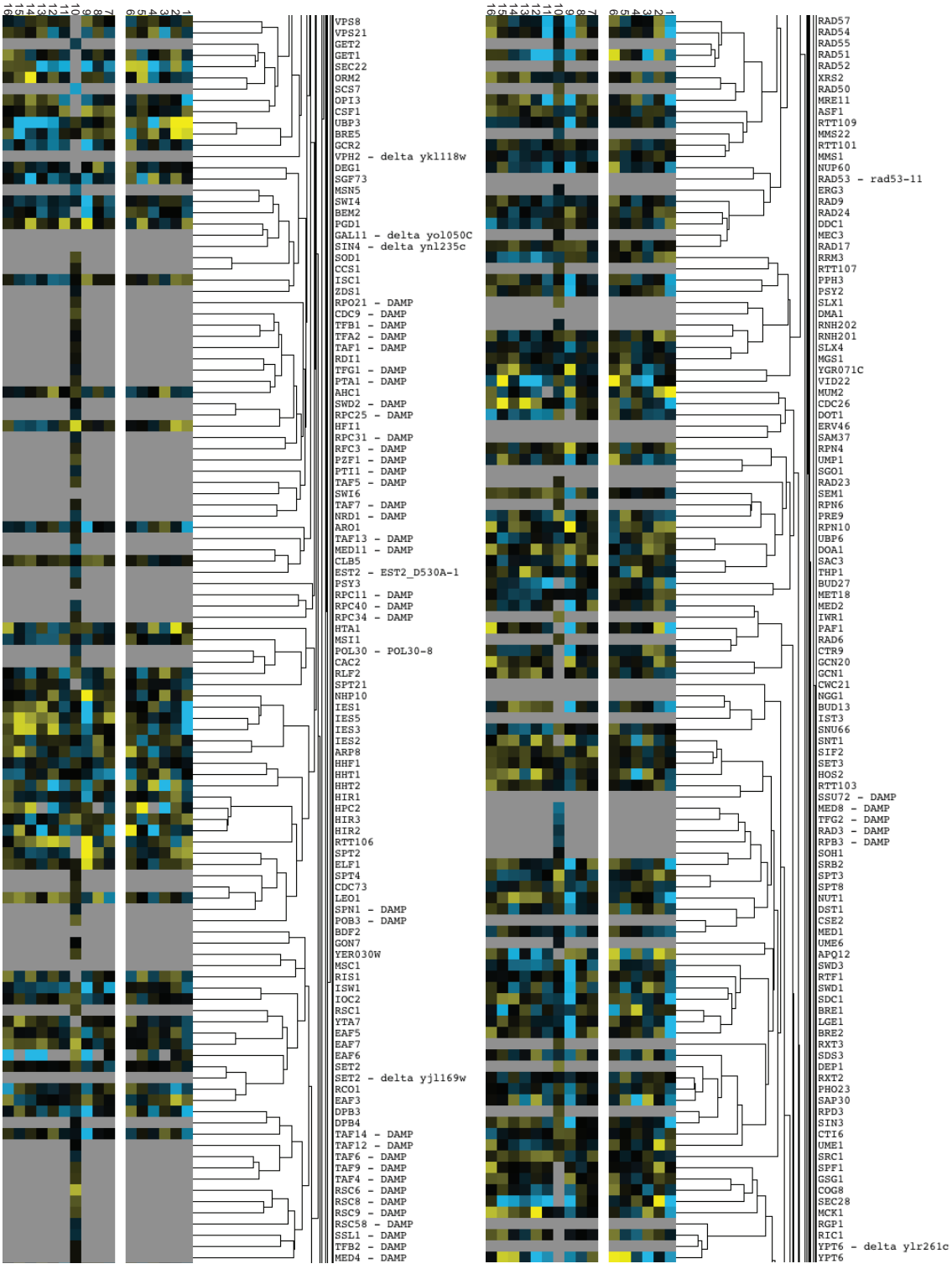
VPS8
VPS21
GET2
GET1
SEC22
ORM2
SCS7
OPI3
CSF1
UBP3
BRE5
GCR2
VPH2 - delta ykl118w
DEG1
SGF73
MSN5
SWI4
BEM2
PGD1
GAL11 - delta yol050C
SIN4 - delta ynl235c
SOD1
CCS1
ISC1
ZDS1
RPO21 - DAMP
CDC9 - DAMP
TFB1 - DAMP
TFA2 - DAMP
TAF1 - DAMP
RDI1
TFG1 - DAMP
PTA1 - DAMP
AHC1
SWD2 - DAMP
RPC25 - DAMP
HFI1
RPC31 - DAMP
RFC3 - DAMP
PZF1 - DAMP
PTI1 - DAMP
TAF5 - DAMP
SWI6
TAF7 - DAMP
NRD1 - DAMP
ARO1
TAF13 - DAMP
MED11 - DAMP
CLB5
EST2 - EST2_D530A-1
PSY3
RPC11 - DAMP
RPC40 - DAMP
RPC34 - DAMP
HTA1
MSI1
POL30 - POL30-8
CAC2
RLF2
SPT21
NHP10
IES1
IES5
IES3
IES2
ARP8
HHF1
HHT1
HHT2
HIR1
HPC2
HIR3
HIR2
RTT106
SPT2
ELF1
SPT4
CDC73
LEO1
SPN1 - DAMP
POB3 - DAMP
BDF2
GON7
YER030W
MSC1
RIS1
ISW1
IOC2
RSC1
YTA7
EAF5
EAF7
EAF6
SET2
SET2 - delta yjl169w
RCO1
EAF3
DPB3
DPB4
TAF14 - DAMP
TAF12 - DAMP
TAF6 - DAMP
TAF9 - DAMP
TAF4 - DAMP
RSC6 - DAMP
RSC8 - DAMP
RSC9 - DAMP
RSC58 - DAMP
SSL1 - DAMP
TFB2 - DAMP
MED4 - DAMP
RAD57
RAD54
RAD55
RAD51
RAD52
XRS2
RAD50
MRE11
ASF1
RTT109
MMS22
RTT101
MMS1
NUP60
RAD53 - rad53-11
ERG3
RAD9
RAD24
DDC1
MEC3
RAD17
RRM3
RTT107
PPH3
PSY2
SLX1
DMA1
RNH202
RNH201
SLX4
MGS1
YGR071C
VID22
MUM2
CDC26
DOT1
ERV46
SAM37
RPN4
UMP1
SGO1
RAD23
SEM1
RPN6
PRE9
RPN10
UBP6
DOA1
SAC3
THP1
BUD27
MET18
MED2
IWR1
PAF1
RAD6
CTR9
GCN20
GCN1
CWC21
NGG1
BUD13
IST3
SNU66
SNT1
SIF2
SET3
HOS2
RTT103
SSU72 - DAMP
MED8 - DAMP
TFG2 - DAMP
RAD3 - DAMP
RPB3 - DAMP
SOH1
SRB2
SPT3
SPT8
NUT1
DST1
CSE2
MED1
UME6
APQ12
SWD3
RTF1
SWD1
SDC1
BRE1
LGE1
BRE2
RXT3
SDS3
DEP1
RXT2
PHO23
SAP30
RPD3
SIN3
CTI6
UME1
SRC1
SPF1
GSG1
COG8
SEC28
MCK1
RGP1
RIC1
YPT6 - delta ylr261c
YPT6

Figure A1-5

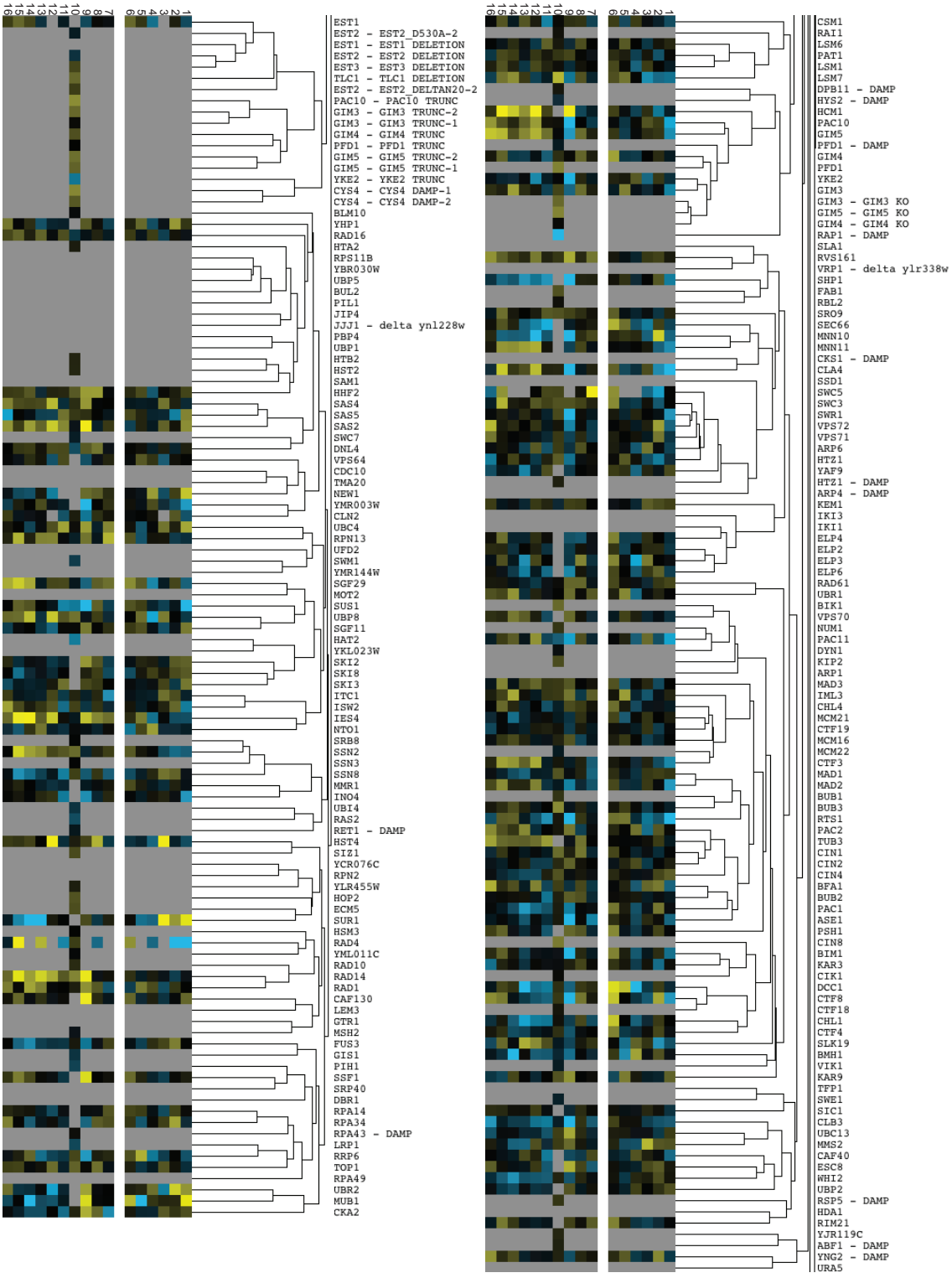
EST1
EST2 - EST2_D530A-2
EST1 - EST1 DELETION
EST2 - EST2 DELETION
EST3 - EST3 DELETION
TLC1 - TLC1 DELETION
EST2 - EST2_DELTAN20-2
PAC10 - PAC10 TRUNC
GIM3 - GIM3 TRUNC-2
GIM3 - GIM3 TRUNC-1
GIM4 - GIM4 TRUNC
PFD1 - PFD1 TRUNC
GIM5 - GIM5 TRUNC-2
GIM5 - GIM5 TRUNC-1
YKE2 - YKE2 TRUNC
CYS4 - CYS4 DAMP-1
CYS4 - CYS4 DAMP-2
BLM10
YHP1
RAD16
HTA2
RPS11B
YBR030W
UBP5
BUL2
PIL1
JIP4
JJJ1 - delta ynl228w
PBP4
UBP1
HTB2
HST2
SAM1
HHF2
SAS4
SAS5
SAS2
SWC7
DNL4
VPS64
CDC10
TMA20
NEW1
YMR003W
CLN2
UBC4
RPN13
UFD2
SWM1
YMR144W
SGF29
MOT2
SUS1
UBP8
SGF11
HAT2
YKL023W
SKI2
SKI8
SKI3
ITC1
ISW2
IES4
NTO1
SRB8
SSN2
SSN3
SSN8
MMR1
INO4
UBI4
RAS2
RET1 - DAMP
HST4
SIZ1
YCR076C
RPN2
YLR455W
HOP2
ECM5
SUR1
HSM3
RAD4
YML011C
RAD10
RAD14
RAD1
CAF130
LEM3
GTR1
MSH2
FUS3
GIS1
PIH1
SSF1
SRP40
DBR1
RPA14
RPA34
RPA43 - DAMP
LRP1
RRP6
TOP1
RPA49
UBR2
MUB1
CKA2
CSM1
RAI1
LSM6
PAT1
LSM1
LSM7
DPB11 - DAMP
HYS2 - DAMP
HCM1
PAC10
GIM5
PFD1 - DAMP
GIM4
PFD1
YKE2
GIM3
GIM3 - GIM3 KO
GIM5 - GIM5 KO
GIM4 - GIM4 KO
RAP1 - DAMP
SLA1
RVS161
VRP1 - delta ylr338w
SHP1
FAB1
RBL2
SRO9
SEC66
MNN10
MNN11
CKS1 - DAMP
CLA4
SSD1
SWC5
SWC3
SWR1
VPS72
VPS71
ARP6
HTZ1
YAF9
HTZ1 - DAMP
ARP4 - DAMP
KEM1
IKI3
IKI1
ELP4
ELP2
ELP3
ELP6
RAD61
UBR1
BIK1
VPS70
NUM1
PAC11
DYN1
KIP2
ARP1
MAD3
IML3
CHL4
MCM21
CTF19
MCM16
MCM22
CTF3
MAD1
MAD2
BUB1
BUB3
RTS1
PAC2
TUB3
CIN1
CIN2
CIN4
BFA1
BUB2
PAC1
ASE1
PSH1
CIN8
BIM1
KAR3
CIK1
DCC1
CTF8
CTF18
CHL1
CTF4
SLK19
BMH1
VIK1
KAR9
TFP1
SWE1
SIC1
CLB3
UBC13
MMS2
CAF40
ESC8
WHI2
UBP2
RSP5 - DAMP
HDA1
RIM21
YJR119C
ABF1 - DAMP
YNG2 - DAMP
URA5

Figure A1-6

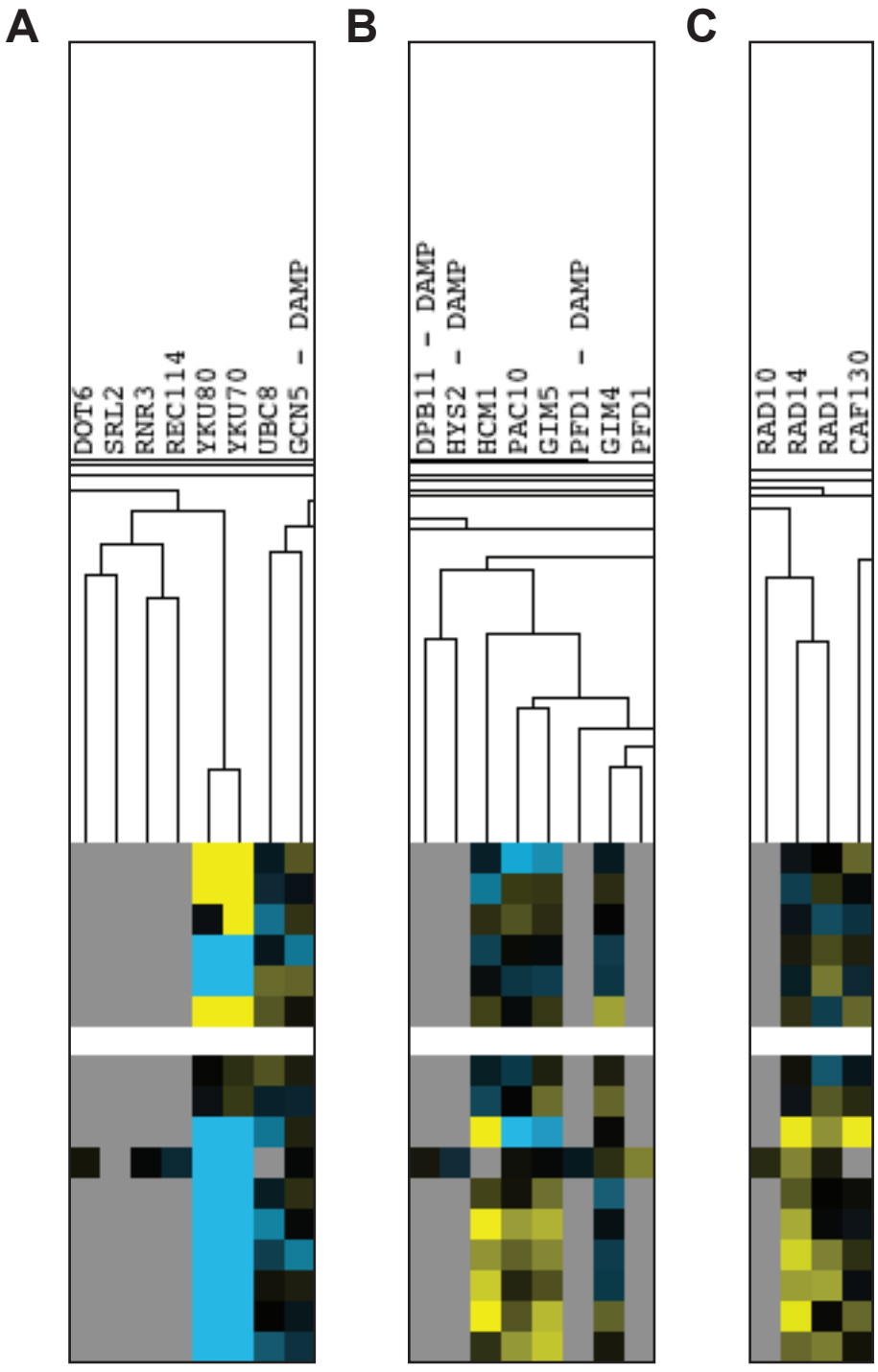
A
DOT6
SRL2
RNR3
REC114
YKU80
YKU70
UBC8
GCN5 - DAMP
B
DPB11 - DAMP
HYS2 - DAMP
HCM1
PAC10
GIM5
PFD1 - DAMP
GIM4
PFD1
C
RAD10
RAD14
RAD1
CAF130

Figure A1-7

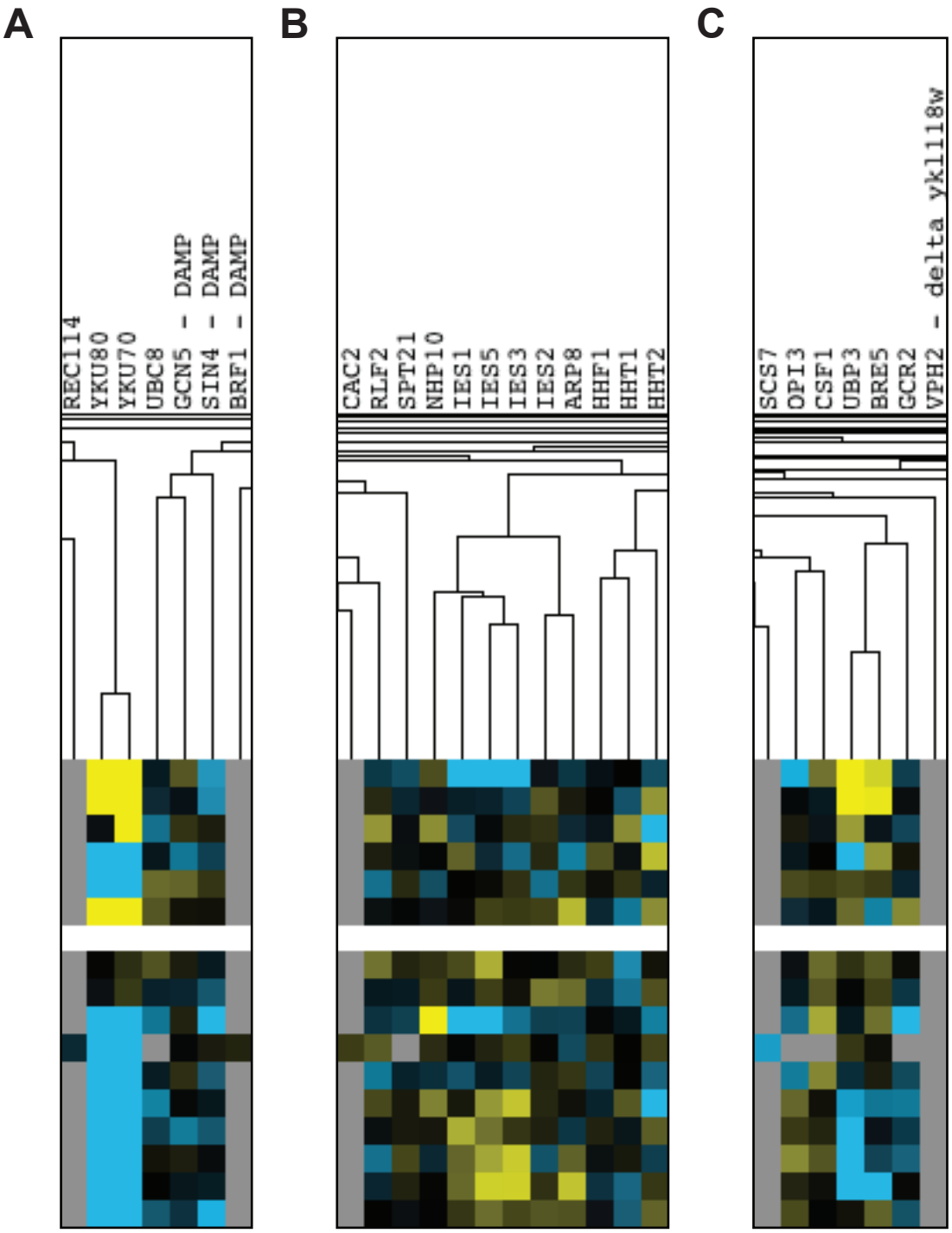
A
REC114
YKU80
YKU70
UBC8
GCN5 - DAMP
SIN4 - DAMP
BRF1 - DAMP
B
CAC2
RLF2
SPT21
NHP10
IES1
IES5
IES3
IES2
ARP8
HHF1
HHT1
HHT2
C
SCS7
OPI3
CSF1
UBP3
BRE5
GCR2
VPH2 - delta yk1118w

Figure A1-8

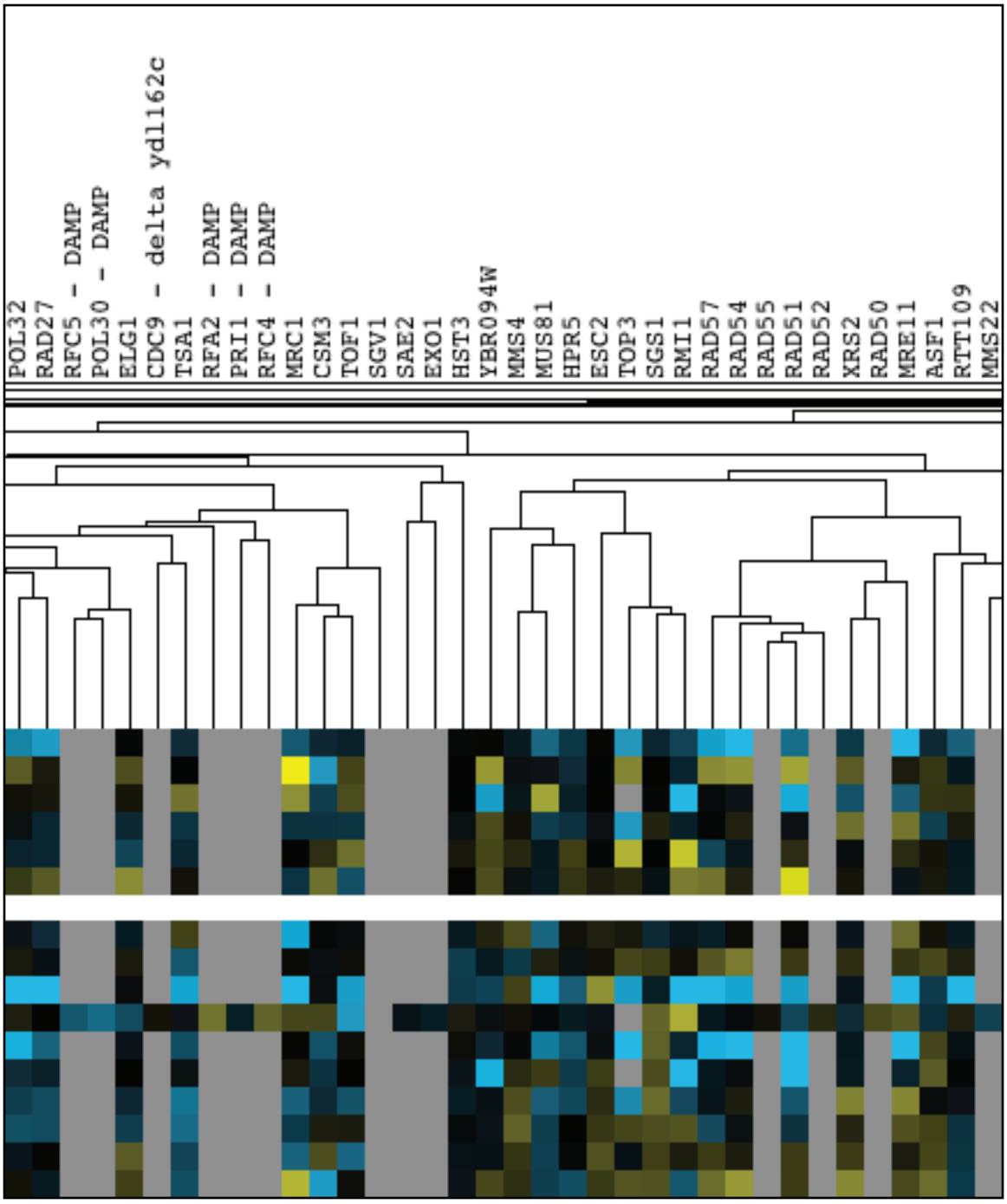
POL32
RAD27
RFC5 - DAMP
POL30 - DAMP
ELG1
CDC9 - delta yd1162c
TSA1
RFA2 - DAMP
PRI1 - DAMP
RFC4 - DAMP
MRC1
CSM3
TOF1
SGV1
SAE2
EXO1
HST3
YBR094W
MMS4
MUS81
HPR5
ESC2
TOP3
SGS1
RMI1
RAD57
RAD54
RAD55
RAD51
RAD52
XRS2
RAD50
MRE11
ASF1
RTT109
MMS22

Appendix 2: Transcriptional Regulation of *TLC1* in Senescent Cells

Tetsuya Matsuguchi and Elizabeth H. Blackburn

Department of Biochemistry and Biophysics

University of California, San Francisco

San Francisco, CA 94158

Results and Discussion

Mozdy and Cech showed that the TLC1 levels do not change throughout the cell cycle, and that there is a slight increase in TLC1 levels in the whole cell population when the yeast culture is saturated versus logarithmically-growing. It has been reported that telomeres are slightly longer in saturated cultures. This prompted us to check the level of TLC1 as cells undergo senescence. Senescent yeast cultures undergo a DNA damage response, and transcriptional profile changes (Nautiyal *et al*. 2002). However, in such analyses the TLC1 levels had not been measured.

To test whether senescence evoked a response in the form of resulting in altered TLC1 levels, wild-type, *est1Δ*, *est2Δ*, *est2-D530A*, *est2-ΔN20*, *est3Δ*, and *tlc1Δ* cells were successively streaked on plates four times. Total RNA was directly purified from these cells scraped from the plates. The amounts of TLC1 and U2 snRNA were quantified using qRT-PCR. As expected, TLC1 levels in wild-type cells did not change substantially from streak to streak (Figure A2-1). Interestingly, in *est1Δ*, *est3Δ*, and *est2-D530A* strains, the level of TLC1 was higher when the colony shape and number showed

senescence phenotype (striped bars marked "heterogeneous" in Figure A2-1), but not before senescence (when telomeres are shortening but the cells are still growing relatively robustly) or after senescence (in survivors that also grow quite well). One possible exception was in the *est2-D530A* cells, in which the first streak showed a colony phenotype. Notably, in *est2Δ* cells, there was no increase in TLC1 levels even during senescence.

It is also interesting to note that in both *est2Δ* and *est2-ΔN20* cells, the TLC1 levels were less than that of wild-type cells (Figure A2-1). Though *est2-ΔN20* cells have shorter telomeres, they do not senesce. This suggests that N-terminal region encompassed by the first 20 amino acids of Est2 is important for stabilizing TLC1. This result identifies an additional region of Est2 important for *TLC1* function or stability; the previous identification of domains and amino acids of TERT (Est2 in *S. cerevisiae*) important for telomerase RNA interaction had not identified this region.

The increase in TLC1 levels during senescence raised two intriguing, non-mutually exclusive possibilities: a) that transcriptional regulation occurs at the *TLC1* promoter during senescence; b) that the stability of TLC1 is increased during senescence. Evidence for the latter possibility came from the observation that, specifically in *est2Δ* cells, the TLC1 level did not change in cells during senescence. In contrast, it increased as *est1Δ*, *est3Δ*, and *est2-D530A* strains underwent senescence. Therefore, Est2 may be playing a role in keeping TLC1 stable.

Most CEN-ARS plasmids used in the lab contain ~500 base pairs of the promoter region and express similar levels of TLC1, as does the endogenous *TLC1*. However,

effects of promoter deletions had not been previously examined. To test how different regions of the *TLC1* promoter influence *TLC1* expression, different lengths of the 5' region of endogenous *TLC1* were cloned in front of a *TLC1* gene that was marked within the transcribed mature RNA region such a way as to allow distinction from the endogenous TLC1 by qRT-PCR. These constructs were introduced on CEN-ARS plasmids into otherwise wild-type yeast strains, and the total RNA was extracted. The amount of marked TLC1 was quantified and normalized to the amount of U2 snRNA. Most of the constructs containing segments of the endogenous promoter upstream regions of sizes raging from 50 to 950 base-pairs showed similar levels of TLC1, except the TLC1 expressed with 150 base-pairs of the upstream region, which showed almost 3-fold more TLC1 than the others. These data suggested that a repression factor (or more than one) may bind in the region 150 bp or more upstream of *TLC1*.

The potential presence of an inhibitory signal for the transcription of *TLC1* fits with the regulatory mode of other telomerase components (Est1, Est2, and Est3), which show very limited expression levels. Est1 expression is tightly regulated by the cell-cycle phase and proteolysis, and Est3 level is kept at a minimum through its in-frame stop codon (Larose *et al*. 2007; Osterhage *et al*. 2006; see Appendix 3). It is possible that tight regulation of telomerase is required to minimize telomerase incorrectly adding telomeric DNA to chromosomal breaks instead of the breaks being repaired by other processes such as NHEJ or recombination. Such control of telomerase at DNA breaks has been shown to involve tight control via phosphorylation of Pif1 helicase, for example (Schulz and Zakian 1994; Makovets and Blackburn 2009)

It would be interesting in future work to see whether the region farther upstream of 150 bp is required for the higher levels of TLC1 in senescent cells. Further promoter mutations can also probe the region in question in more detail. Identifying the repressor that responds to senescence would be interesting, especially if it responds specifically to senescence and not to general stress conditions.

Materials and Methods

Plasmids

The different sizes of *TLC1* promoters (50, 150, 250, …, 950 bp) were PCR amplified with a common reverse primer that introduced GCAG sequence immediately before the NcoI site at +450 position of *TLC1*. The PCR products were subcloned into pEHB22,254 (pRS415-TLC1) between the XbaI site in the multiple cloning site and the NcoI site in the *TLC1* sequence.

Yeast strains and growth media

Yeast strains used were of S288c background. Yeast cultures were grown in standard rich medium or minimal media (YEPD or CSM). Deletion strains were made using a PCR-based transformation method (Longtine *et al*. 1998).

Quantitative reverse transcription and PCR

Total RNA was extracted from yeast cells scraped from plates or from liquid cultures in log phase of growth using the RNeasy Mini Kit (Qiagen), including the DNase step as

described by the manufacturer. The primer set for U2 snRNA was designed based on the previously published sequences (Mozdy and Cech 2006). The primer set for wild-type TLC1 was designed using IDT's PrimerQeust. The GCAG-tagged TLC1 expressed from plasmids was quantified using the primer ending in the sequence complementary to the GCAG tag. One-step reverse transcription and PCR kits were used for all RNA quantifications (Stratagene). All quantitative PCR runs included serially diluted RNA samples to make a standard curve, from which relative quantitative values were derived using the Stratagene software. Primers used for the qRT-PCR are listed in Table A2-1.

References

Larose, S., Laterreur, N., Ghazal, G., Gagnon, J., Wellinger, R.J. and Elela, S.A., 2007. RNase III-dependent Regulation of Yeast Telomerase. *Journal of Biological Chemistry*, 282(7), pp.4373 -4381.

Longtine, M.S., Mckenzie III, A., Demarini, D.J., Shah, N.G., Wach, A., Brachat, A., Philippsen, P. and Pringle, J.R., 1998. Additional modules for versatile and economical PCR-based gene deletion and modification in Saccharomyces cerevisiae. *Yeast*, 14(10), pp.953-961.

Makovets, S. and Blackburn, E.H., 2009. DNA damage signalling prevents deleterious telomere addition at DNA breaks. *Nat Cell Biol*, 11(11), pp.1383-1386.

Mozdy, A.D. and Cech, T.R., 2006. Low abundance of telomerase in yeast: Implications for telomerase haploinsufficiency. *RNA*, 12(9), pp.1721 -1737.

Nautiyal, S., DeRisi, J.L. and Blackburn, E.H., 2002. The genome-wide expression response to telomerase deletion in Saccharomyces cerevisiae. *Proceedings of the National Academy of Sciences*, 99(14), pp.9316 -9321.

Osterhage, J.L., Talley, J.M. and Friedman, K.L., 2006. Proteasome-dependent degradation of Est1p regulates the cell cycle-restricted assembly of telomerase in Saccharomyces cerevisiae. *Nat Struct Mol Biol*, 13(8), pp.720-728.

Schulz, V.P. and Zakian, V.A., 1994. The saccharomyces PIF1 DNA helicase inhibits telomere elongation and de novo telomere formation. *Cell*, 76(1), pp.145-155.

Figure Legends

Figure A2-1. TLC1 levels are higher in senescing cells.

TLC1 levels from strains shown are quantified. The wedge above each strain represents increasing number of streaks (Streak 1-4). Solid bars represent RNA collected from colonies that were uniform and circular, and dotted bars represent samples collected from colonies with heterogeneous size and shape, indicative of cells undergoing senescence or crisis due to short telomeres. The ratio of TLC1 level to U2 RNA were normalized to the wild-type levels and plotted here. The error bars indicate standard deviation from triplicate measurements of qRT-PCR.

Figure A2-2. TLC1 expressed with different lengths of the upstream sequence. TLC1-GCAG expressed from plasmids with indicated length of upstream sequence was quantified. The level of TLC1 was normalized to U2 RNA level. The error bars indicate standard deviation of measurements from three independent clones collected at different times. Within each experiment, the values were normalized to the average of all values from that particular experiment. The vector control was run only twice.

Table A2-1. Primer sequences for qRT-PCR

Amplicon	Primer number	Sequence (5' to 3')
U2 snRNA	oEHB22,0422	TCGATGGGAAGAAATGGTGCTATAG
	oEHB22,0423*	GTCGAAAAACTTCCTCTTGCAGCG
TLC1	oEHB22,0555	GGCCTCAGAAATTTGGTAGGCACT
	oEHB22,0556*	TTGCGCACACACAAGCATCTACAC
GCAG-tagged *TLC1*	oEHB22,0559	TGCTTGTGTGTGCGCAATTTGTGG
	oEHB22,0595*	GATGGTAGGCTTCCCATGGctgc

*Primer used in the reverse transcription step

Figure A2-1

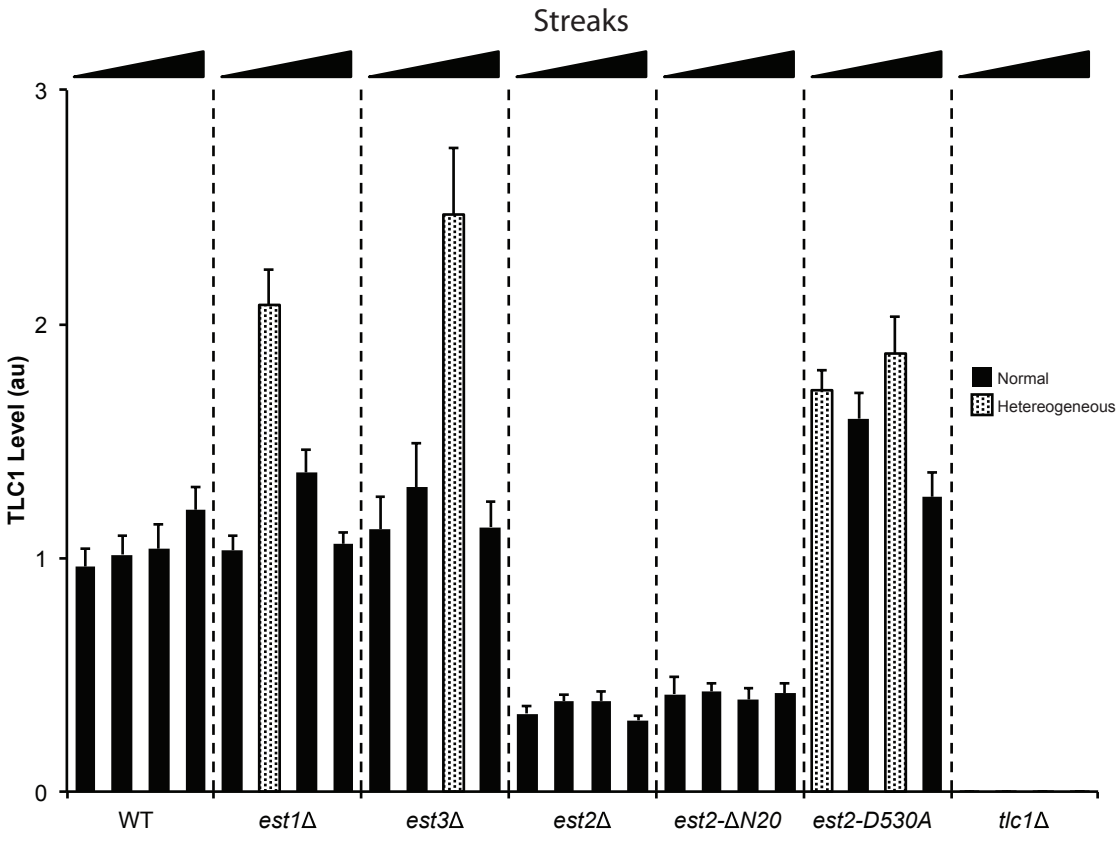
Streaks
TLC1 Level (au)
3
2
1
0
Normal
Hetereogeneous
WT
est1Δ
est3Δ
est2Δ
est2-ΔN20
est2-D530A
tlc1Δ

Figure A2-2

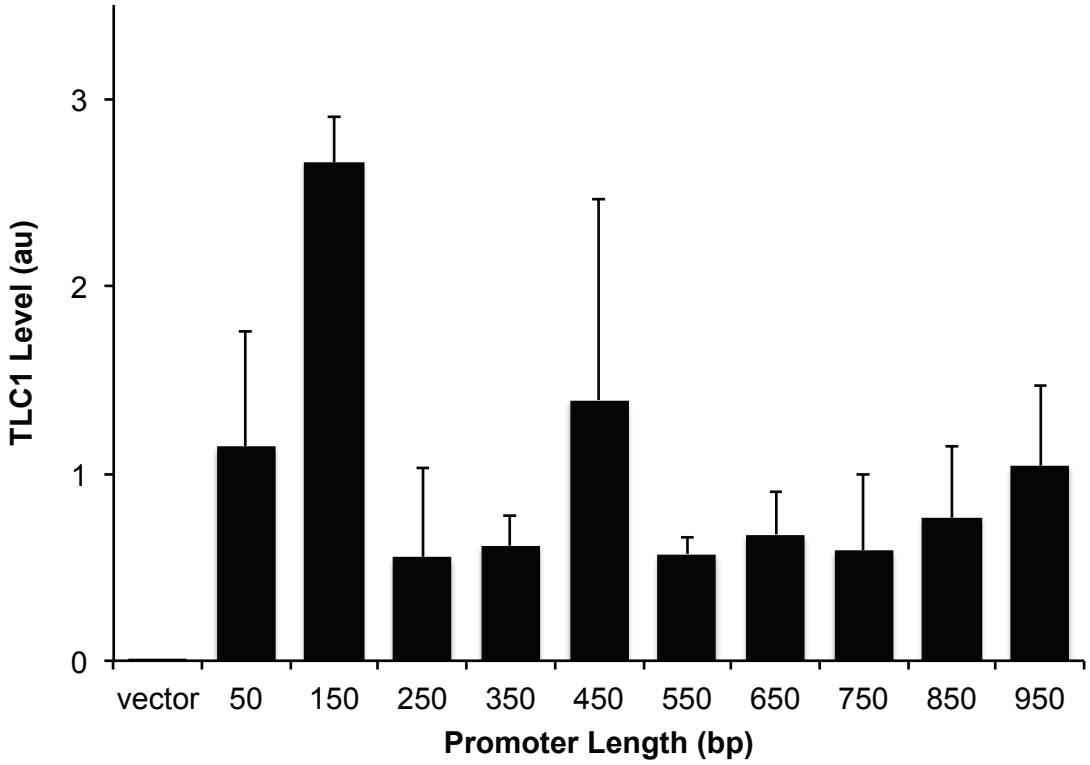
TLC1 Level (au)
0
1
2
3
vector
50
150
250
350
450
550
650
750
850
950
Promoter Length (bp)

Appendix 3: Post-transcriptional Regulation of Est3

Tetsuya Matsuguchi and Elizabeth H. Blackburn

Department of Biochemistry and Biophysics

University of California, San Francisco

San Francisco, CA 94158

Results and Discussion

Est3 is one of the most enigmatic of the telomerase complex components. Est3 is a small protein that co-immunoprecipitates with the telomerase RNA-and Est2-containing telomerase complex of *S. cerevisiae* (Hughes *et al*. 2000). Est3 is required for telomerase to maintain telomere length and prevent senescence *in vivo*, but Est3 is not absolutely required for telomerase activity assayed *in vitro*, as shown by using cell extracts from *est3* deletion strain cells, under enzyme activity assay conditions with saturating amounts of DNA oligonucleotide primer and moderate to high concentrations of dNTP substrates (Lendvay *et al*. 1996; Lingner *et al*. 1997). Hence Est3 is required for *in vivo* telomerase activity but not *in vitro*. Est3 physically interacts with the telomerase complex and requires Est1 for this interaction, and the N-terminal region of Est2 is also critical for Est3 association with telomerase (Tuzon *et al*. 2011). The function of Est3 has remained largely unknown, although there is some evidence for its role in the processivity of telomerase activity.

Interestingly, in *S. cerevisiae* there is a stop codon within *EST3*'s coding region, and a frameshift during translation is required for the production of full-length Est3 protein (Figure A3-1; Morris and Lundblad 1997). In *E. coli*, two of the processivity factors for DNA replication, gamma and tau, are encoded by a single gene, dnaX (Kodaira *et al*. 1983). The tau subunit is a product of the 5' half of the gene encoded by dnaX. A larger Gamma subunit is produced when a frameshift occurs during the reading of the dnaX gene (Flower and McHenry 1990; Blinkowa and Walker 1990). Similarly, *EST3* mRNA also has a potential to code for two proteins, a smaller N-terminal half (Est3N) and the full-length Est3. It has previously been shown that production of the Est3N protein fragment is dispensable for telomerase activity; however, full-length still contains Est3N, and therefore the previous findings did not rule out the possibility that production of just the Est3 full-length protein (which encompasses all the amino acids in Est3N as well as the C-terminal portion of full length Est3) potentially may be sufficient to compensate for the loss of Est3N (Morris and Lundblad 1997).

To test the possibility that there is a function for the Est3N, the Est3 N-terminal region was overexpressed to produce Est3N itself, in a cell that also expressed the wild type *EST3* locus, and telomere lengths were measured. No significant differences in telomere lengths were observed, indicating no dominant negative property of the overexpressed Est3N, which is a truncated version of full-length Est3 protein. It is also possible that other telomerase factors are limiting and that overexpression of Est3N is not sufficient to change the telomere length. In fact, overexpression of wild-type Est3 (which produces a mixture of overexpressed Est3N and overexpressed full-length Est3) is not

sufficient to change telomere length (Zhang *et al*. 2010). It is also possible that Est3N has a function outside the realm of telomere biology.

To test whether Est3N plays any role in DNA damage response pathways, *EST3-fsc* mutation was used to test the sensitivity to MMS, UV, and phleomycin (Figure A3-1 and data not shown). This mutation leads to loss of Est3N expression (and, as shown below, causes an increased level of Est3 full-length protein to be expressed) but did not change the sensitivity to these DNA damaging agents.

Generally, a stop codon in the middle of a transcript signifies an error during the transcription and triggers a nonsense mediated decay (NMD) pathway that degrades the mRNA. A very small number of *EST3* transcripts per cell are required to maintain wild-type telomere length; therefore, we tested whether *EST3* mRNA levels are kept low by the NMD pathway. When NMD was mutated (*upf1Δ, upf2Δ, upf3Δ*), the *EST3* mRNA transcript level was two-fold higher than the wild-type (Figure A3-2; blue bars). To verify that the effect of NMD on *EST3* mRNA level is due to the in-frame stop codon, the frameshift-corrected allele of *EST3* (*EST3-fsc*), in which the stop codon in the middle is removed, was also measured. Indeed, the *EST3-fsc* mRNA level was also two-fold higher than that of the wild-type *EST3* mRNA level (Figure A3-2; red bars). The *EST3-fsc* mRNA level was not further increased by inactivating the NMD pathway (Figure A3-2; green and yellow bars). These results suggested that the in-frame stop codon in the *EST3* mRNA reduces the steady-state transcript level from the wild-type *EST3* gene via NMD.

To test whether Est3 protein level is similarly controlled by the NMD pathway, Est3 was tagged at its N-terminus with a 3xMyc or 3xFLAG epitope. Est3 protein was

difficult to detect in wild-type cells, but when *EST3-fsc* mutation was introduced, a robust signal was observed (Figure A3-3), indicating that the removal of in-frame stop codon results in the expected more efficient translation and hence overproduction of full-length Est3 protein. Next, the NMD pathway was inactivated in wild-type *EST3* and *EST3-fsc* cells by deleting *UPF1*, *UPF2*, or *UPF3*. Though *EST3* mRNA levels are two-fold higher in NMD-defective cells, the lack of NMD produced no significant increase in Est3 protein level (Figure A3-3; compare Lane 1 and 3). The overproduction effect of *EST3-fsc* was not affected by the NMD status (Figure A3-3; compare Lane 2 and 4). Therefore, the Est3 protein level is normally kept very low largely by requiring frameshift to occur during translation, with little if any contribution from the NMD pathway, despite there being an NMD-canonical substrate (an in-frame stop codon) in the *EST3* mRNA protein coding region.

The in-frame stop codon is conserved among *Saccharomyces* species, but it is not conserved in other species of budding yeast. There seems to be no deleterious effect of over-expressing Est3; the only function of the in-frame stop codon seems to be conservation of resources by not producing any more Est3 than necessary. As discussed in Appendix 2, it may be important to keep telomerase levels under strict negative regulation, and the frame-shift mechanism of controlling Est3 protein levels would provide an independent way of limiting telomerase action *in vivo* that may reinforce or otherwise complement negative regulation of the action of telomerase through other mechanisms acting on other components of telomerase. For example, it has been noted that the *EST1* mRNA sequence upstream to the canonical AUG protein coding start site

has a series of predicted short open reading frames, an arrangement that has been shown to result in down-regulation and responsiveness to cell growth conditions for other genes such as *GCN5* in *S. cerevisiae*. It would be interesting to test whether the effect of maintaining such a reduced level of Est3 at minimal levels, as occurs in wild type cell, is substantial enough confer a selective advantage over otherwise isogenic cells engineered to be missing the frame-shift.

Materials and Methods

Plasmids

pEHB22,107 (pRS406-EST3-fsc) was cloned by separately PCR-amplifying 5' and 3' halves of *EST3-fsc* and then performing a fusion PCR using these halves. pEHB12,009 (pMPY-3xFLAG) was made by Jeffrey Seidel.

Yeast strains and growth media

Strains used were derived from S288c background (Baker Brachmann *et al*. 1998). Gene deletions were made using a standard PCR-based protocol (Longtine *et al*. 1998). Loop-in/loop out method was used to introduce *EST3-fsc* using pEHB22,107. EST3 was N-terminally tagged using loop-in/loop-out method using URA3 marker flanked by the tag amplified from pMPY-3xMyc (Schneider *et al*. 1995) and pEHB12,009.

Quantitative RT-PCR of RNA

Total RNA was prepared per manufacture's instructions using RNeasy Mini Kit including the optional DNase step (Qiagen). One-step qRT-PCR kit (Brilliant II SYBR® Green QRT-PCR Master Mix Kit, 1-Step; Stratagene) was used to carry out all RNA quantification in 20 uL reactions with the Stratagene Mx3000P qPCR machine. Primers used for the qRT-PCR are listed in Table A3-1.

Immunoblotting

Standard protocols for SDS-PAGE, protein transfer to membrane, and immunoblotting were used. Briefly, whole lysates were prepared by vortexing and boiling the yeast cells in Loading Buffer (40 mM Tris-HCl pH6.8, 2% SDS, 2 mM DTT, 4% glycerol, 0.01% bromophenol blue) with glass beads. The samples were run on a 15% polyacrylamide gel and transferred to Hybond-P membrane (GE Healthcare). Anti-Myc 9E10 (Clontech) or anti-FLAG M2 (Sigma-Aldrich) antibody was used as the primary antibody, and the sheep anti-mouse antibody conjugated to HRP was used as the secondary antibody (Abcam). ECL Plus (Amersham) kit was used to detect HRP activity on Kodak BioMax Film.

Acknowledgement

We thank Jeffrey Seidel for plasmids for N-terminal tagging, and the members of Blackburn lab for helpful discussions.

References

Baker Brachmann, C., Davies, A., Cost, G.J., Caputo, E., Li, J., Hieter, P. and Boeke, J.D., 1998. Designer deletion strains derived from Saccharomyces cerevisiae S288C: A useful set of strains and plasmids for PCR-mediated gene disruption and other applications. *Yeast*, 14(2), pp.115-132.

Blinkowa, A.L. and Walker, J.R., 1990. Programmed ribosomal frameshifting generates the Escherichia coli DNA polymerase III gamma subunit from within the tau subunit reading frame. *Nucleic Acids Research*, 18(7), pp.1725-1729.

Flower, A.M. and McHenry, C.S., 1990. The gamma subunit of DNA polymerase III holoenzyme of Escherichia coli is produced by ribosomal frameshifting. *Proceedings of the National Academy of Sciences of the United States of America*, 87(10), pp.3713-3717.

Hughes, T.R., Evans, S.K., Weilbaecher, R.G. and Lundblad, V., 2000. The Est3 protein is a subunit of yeast telomerase. *Current Biology*, 10(13), pp.809-812.

Kodaira, M., Biswas, S.B. and Kornberg, A., 1983. The dnaX gene encodes the DNA polymerase III holoenzyme tau subunit, precursor of the gamma subunit, the dnaZ gene product. *Molecular & General Genetics: MGG*, 192(1-2), pp.80-86.

Lendvay, T.S., Morris, D.K., Sah, J., Balasubramanian, B. and Lundblad, V., 1996. Senescence mutants of Saccharomyces cerevisiae with a defect in telomere replication identify three additional EST genes. *Genetics*, 144(4), pp.1399-1412.

Lingner, J., Cech, T.R., Hughes, T.R. and Lundblad, V., 1997. Three Ever Shorter Telomere (EST) genes are dispensable for *in vitro* yeast telomerase activity. *Proceedings of the National Academy of Sciences*, 94(21), pp.11190 -11195.

Longtine, M.S., Mckenzie III, A., Demarini, D.J., Shah, N.G., Wach, A., Brachat, A., Philippsen, P. and Pringle, J.R., 1998. Additional modules for versatile and economical PCR-based gene deletion and modification in Saccharomyces cerevisiae. *Yeast*, 14(10), pp.953-961.

Morris, D.K. and Lundblad, V., 1997. Programmed translational frameshifting in a gene required for yeast telomere replication. *Current Biology*, 7(12), pp.969-976.

Schneider, B.L., Seufert, W., Steiner, B., Yang, Q.H. and Futcher, A.B., 1995. Use of polymerase chain reaction epitope tagging for protein tagging in Saccharomyces cerevisiae. *Yeast (Chichester, England)*, 11(13), pp.1265-1274.

Tuzon, C.T., Wu, Y., Chan, A. and Zakian, V.A., 2011. The Saccharomyces cerevisiae Telomerase Subunit Est3 Binds Telomeres in a Cell Cycle– and Est1–Dependent Manner and Interacts Directly with Est1 *In vitro*. *PLoS Genet*, 7(5), p.e1002060.

Zhang, M.-L., Tong, X.-J., Fu, X.-H., Zhou, B.O., Wang, J., Liao, X.-H., Li, Q.-J., Shen, N., Ding, J. and Zhou, J.-Q., 2010. Yeast telomerase subunit Est1p has guanine quadruplex-promoting activity that is required for telomere elongation. *Nat Struct Mol Biol*, 17(2), pp.202-209.

Figure Legends

Figure 3A-1. *EST3* locus.

The wild-type EST3 open reading-frame has a stop codon (top), which can be removed by a single nucleotide deletion (ΔT, bottom). The squiggly lines represent protein products made by *EST3* and *EST3-fsc*, Est3N and Est3.

Figure 3A-2. Nonsense-Mediated Decay (NMD) pathway and in-frame stop codon limit EST3 mRNA level.

Total RNA was prepared from *EST3 UPF*, *EST3 upfΔ*, *EST3-fsc UPF*, and *EST3-fsc upfΔ* strains. The results from *upf1Δ*, *upf2Δ*, and *upf3Δ* were aggregated, as they had nearly identical levels of respective RNAs. EST3, CPA1 (known NMD target), and U2 (not an NMD target) RNA levels were measured. The ratios of RNA levels from *EST3 upfΔ* and *EST3 UPF*; *EST3-fsc UPF* and *EST3-fsc upfΔ*; *EST3-fsc UPF* and *EST3 UPF*; and *EST3-fsc upfΔ* and *EST3 upfΔ* are shown in blue, green, red and yellow bars, respectively. The error bars represent the standard deviations of six data points (two strains each of *upf1Δ*, *upf2Δ*, and *upf3Δ* samples). The fold-difference is shown on log scale axis.

Figure 3A-3. Overproduction of full-length Est3 protein in *EST3-fsc* strains.

Western blots of N-terminally tagged Est3 from (A) wild-type EST3 and *EST3-fsc* strains, tagged with either 3xMyc or 3xFLAG and (B) wild-type *EST3* and *EST3-fsc*

strains that are *UPF1* or *upf1Δ*. Myc-tagged Est3 was probed with 9E10 (anti-Myc) antibody, and FLAG-tagged Est3 was probed with M2 (anti-FLAG) antibody.

Table A3-1. Primer sequences for qRT-PCR

Amplicon	Primer number	Sequence (5' to 3')
U2 snRNA	oEHB22,0422	TCGATGGGAAGAAATGGTGCTATAG
	oEHB22,0423*	GTCGAAAAACTTCCTCTTGCAGCG
EST3	oEHB22,0406	CCGAAAGTAATTCTGGAGTCTCATTCA
	oEHB22,0407*	TTTGGTGTGAGGAATCTCTTATCGATG
CPA1	oEHB22,0553	AATGGACCAGGCAACCCAGAACTA
	oEHB22,0554*	AGCCAAGAGTTGATGGCCTAGACA

*Primer used in the reverse transcription step

Figure A3-1

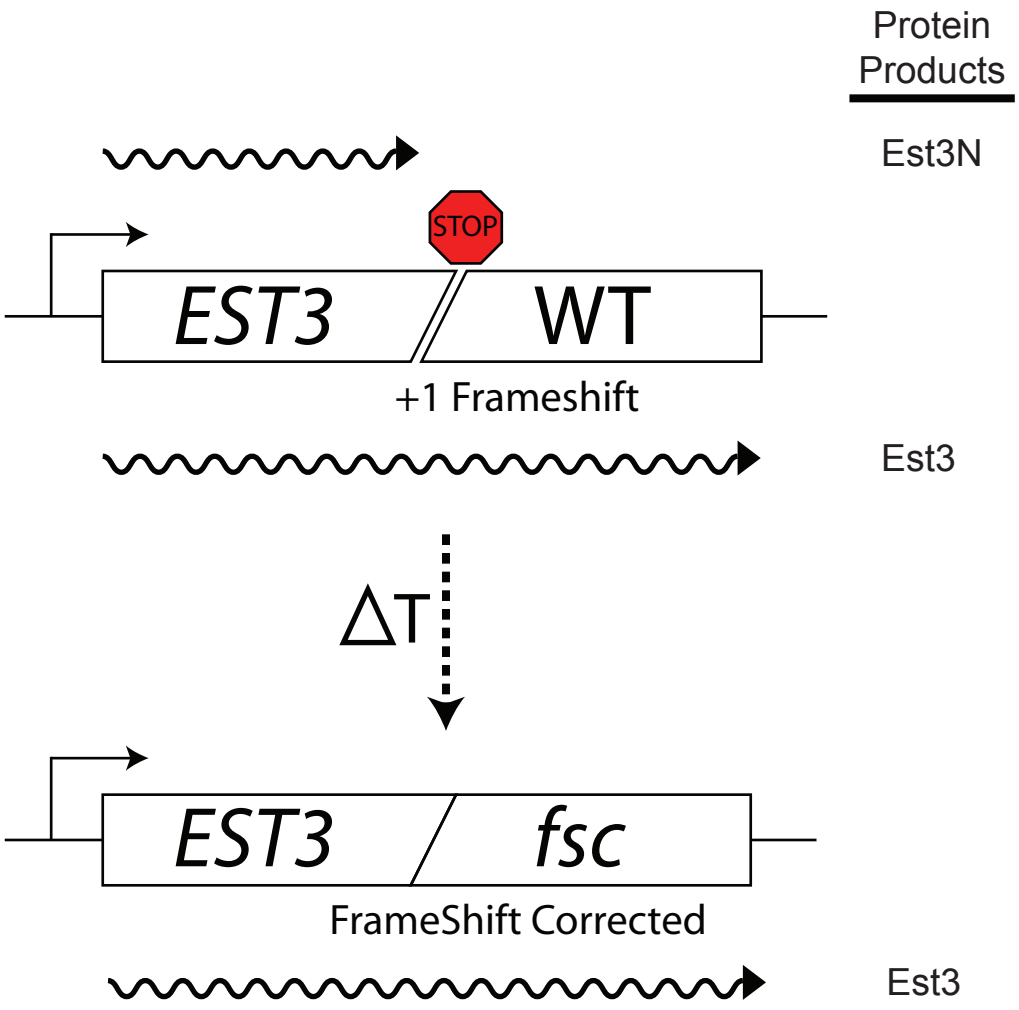
Protein Products
Est3N
STOP
EST3
WT
+1 Frameshift
Est3
ΔT
EST3
fsc
FrameShift Corrected
Est3

Figure A3-2

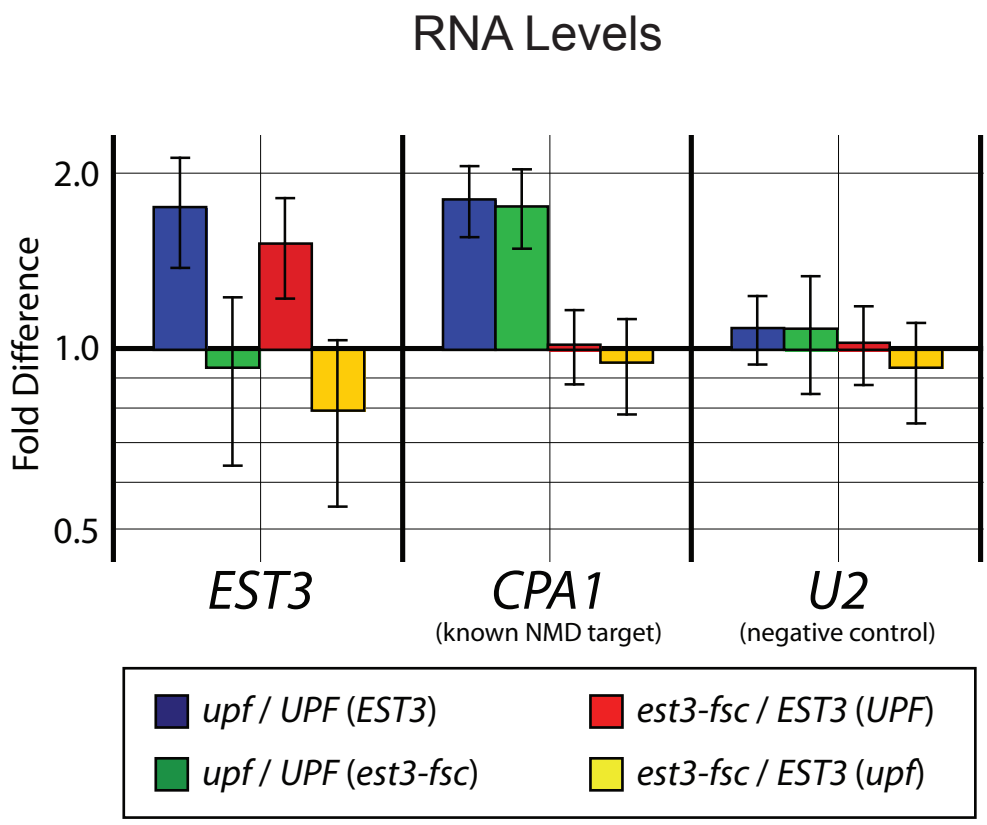
RNA Levels
Fold Difference
2.0
1.0
0.5
EST3
CPA1
(known NMD target)
U2
(negative control)
upf / UPF (EST3)
upf / UPF (est3-fsc)
est3-fsc / EST3 (UPF)
est3-fsc / EST3 (upf)

Figure A3-3

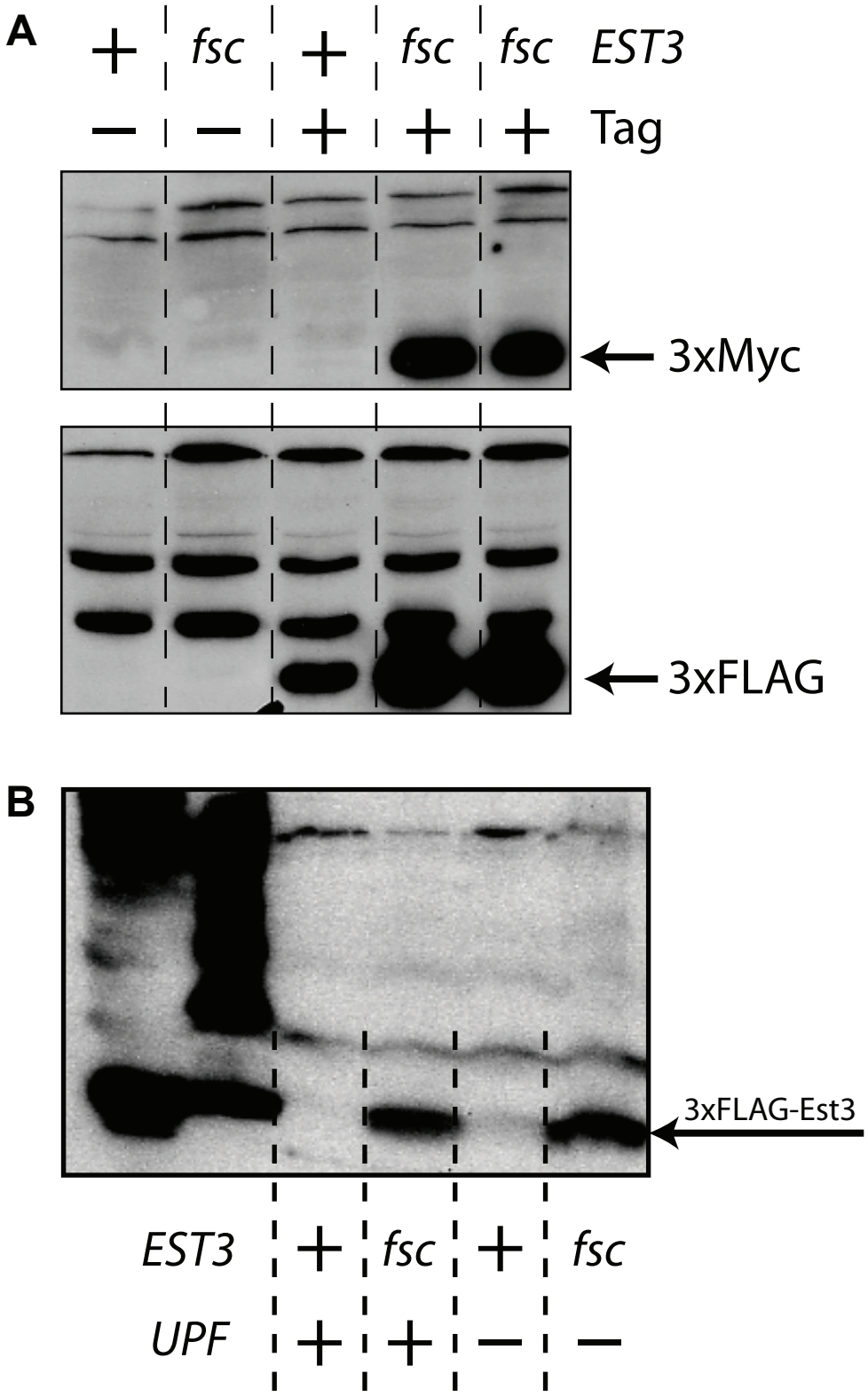
A
+ fsc + fsc fsc EST3
− − + + + Tag
3xMyc
3xFLAG
B
3xFLAG-Est3
EST3 + fsc + fsc
UPF + + − −

Appendix 4: Yeast Two-Hybrid Systems for Analysis of Interactions Between the Telomerase Core Subunits

Tetsuya Matsuguchi and Elizabeth H. Blackburn

Department of Biochemistry and Biophysics

University of California, San Francisco

San Francisco, CA 94158

Results and Discussion

In attempts to study the potential dimerization of telomerase RT subunit Est2, the yeast two-hybrid system was used. It was previously reported that there is no interaction between Est2's, using the classic yeast two-hybrid system in which Gal4 DNA binding domain (Gal4DB) and a Gal4 activation domain (Gal4AD) are fused separately to copies of Est2 (personal communication, EHB). Negative results in assessing interactions can result for various reasons when the yeast two-hybrid system is employed, but one of the main concerns in detecting Est2 dimerization was the dimerization of the Gal4DB itself. Like most DNA binding proteins, Gal4 dimerizes (Carey *et al*. 1989), and each of the two DNA binding domains binds to a half-site of the DNA binding sequence. While some dimerization interaction has been seen in some cases using this system, it was possible that Gal4DB-Est2 dimerization may have been preventing Gal4DB-Est2 interactions with Gal4AD-Est2.

To circumvent this problem, the SKN-1 DNA binding protein from *C. elegans* was cloned and used as a DNA binding domain. Skn-1 is known to bind to DNA as a monomer (Weintraub *et al*., with Blackwell, Bowerman, *et al*., Priess 1994). Unfortunately, the DNA binding sequence is also half the size of most DNA binding sequences. This meant that there are several DNA binding sequence elsewhere in the yeast genome, and in fact, Skn-1-Gal4AD was not able to induce the expression of a reporter gene.

There are also other two-hybrid systems, such as the split-GFP system, in which the N-terminal and C-terminal halves of the GFP are fused to a bait protein and a prey protein, and only when the two proteins interact does a full GFP fluorophore form that can fluoresce (Cabantous *et al*. 2005). In addition, this interaction can occur anywhere in the cell and is not restricted to the nucleus. While screening by fluorescence using FACS machine is useful, this system cannot be used to select for particular mutations.

Given the above shortcomings and problems, to make a selectable, monomeric, and cytoplasmic yeast two-hybrid system, a split-Ade2 system was developed that may be useful for assessing Est2-Est2 and other interactions *in vivo*. The yeast *ADE2* gene is an evolutionary fusion of two bacterial genes (Figure A4-1A): Phosphoribosylaminoimidazole-succinocarboxamide synthase (purK; N-terminal half) and phosphoribosylaminoimidazole carboxylase (purE; C-terminal half) (Watanabe *et al*. 1989; Tiedeman *et al*. 1989). When these two domains were separately expressed, the yeast colony showed red colored ade2$^-$ phenotype, which is caused by an accumulation of a red pigment intermediate. When these two domains were fused to GST, which

homodimerizes, the color phenotype was restored to wild-type (Figure A4-1B), showing that when the two domains are brought together by the fused subunit, the Ade2 enzymes work more efficiently.

In addition to being able to screen interactions by color phenotype, the selectivity can be modulated by changing the amount of adenine in the media, thereby changing the stringency of the interaction required to allow cells to form colonies.

Materials and Methods

Plasmids

Skn-1 gene was PCR-amplified from *C. elegans* genomic DNA prepared with a standard protocol and cloned into pRS415 vector. The 5' and 3' regions were separately PCR-amplified and subcloned into PacI and AscI sites of pFA6a-3HA-KanMX6 and pFA6a-GFP(S65T)-TRP1 (Longtine *et al*. 1998).

Yeast strains and growth media

Yeast cultures were grown in standard rich medium or minimal media (YEPD or CSM), except "low Ade" plates were made using half the amount of adenine normally used. The PCR-based transformation method was used to introduce N-terminal and C-terminal Ade2's (Longtine *et al*. 1998).

References

Cabantous, S., Terwilliger, T.C. and Waldo, G.S., 2005. Protein tagging and detection with engineered self-assembling fragments of green fluorescent protein. *Nature Biotechnology*, 23(1), pp.102-107.

Carey, M., Kakidani, H., Leatherwood, J., Mostashari, F. and Ptashne, M., 1989. An amino-terminal fragment of GAL4 binds DNA as a dimer. *Journal of Molecular Biology*, 209(3), pp.423-432.

Longtine, M.S., Mckenzie III, A., Demarini, D.J., Shah, N.G., Wach, A., Brachat, A., Philippsen, P. and Pringle, J.R., 1998. Additional modules for versatile and economical PCR-based gene deletion and modification in Saccharomyces cerevisiae. *Yeast*, 14(10), pp.953-961.

Tiedeman, A.A., Keyhani, J., Kamholz, J., Daum, H.A., 3rd, Gots, J.S. and Smith, J.M., 1989. Nucleotide sequence analysis of the purEK operon encoding 5'-phosphoribosyl-5-aminoimidazole carboxylase of Escherichia coli K-12. *Journal of Bacteriology*, 171(1), pp.205-212.

Watanabe, W., Sampei, G., Aiba, A. and Mizobuchi, K., 1989. Identification and sequence analysis of Escherichia coli purE and purK genes encoding 5'-phosphoribosyl-5-amino-4-imidazole carboxylase for de novo purine biosynthesis. *Journal of Bacteriology*, 171(1), pp.198-204.

Weintraub, H., with Blackwell, T. and Bowerman, B., Priess, 1994. Formation of a monomeric DNA binding domain by Skn-1 bZIP and homeodomain elements. *Science*, 266(5185), pp.621 -628.

Figure Legend

Figure A4-1. Split-Ade2.

(A) Yeast *ADE2* gene is a fusion of two bacterial proteins purK and purE. N-terminal (straight lines) and C-terminal (squiggly lines) constructs were made by fusing either HA or GST epitope to each region. (B) N-terminal and C-terminal halves with HA and GST epitopes were co-expressed. The GST epitope is known to dimerize, but the HA epitope does not dimerize. Active Ade2 enzyme results in white colonies, while inactive or weaker Ade2 enzyme results in an accumulation of red pigment.

Figure A4-1

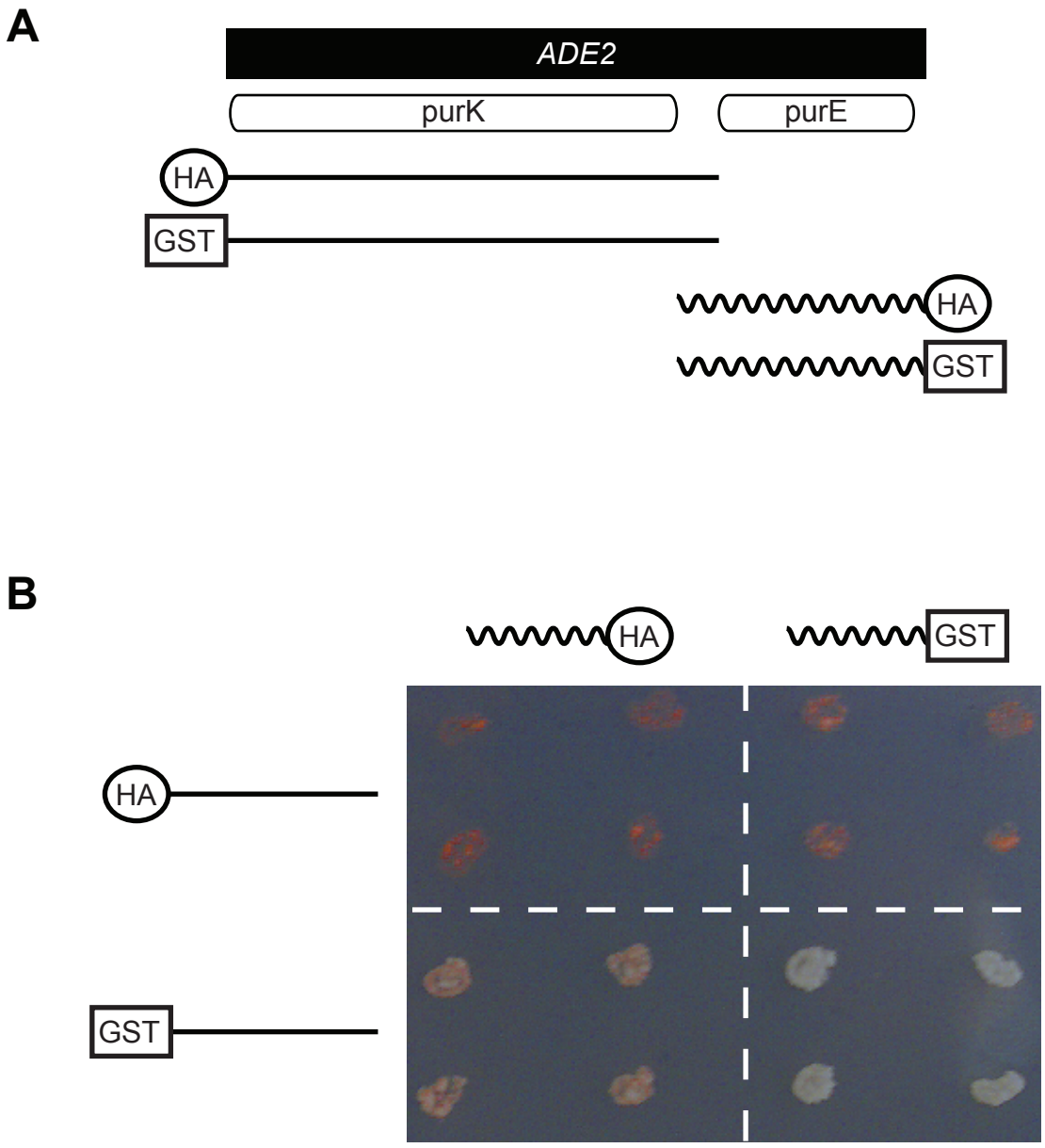

Publishing Agreement

It is the policy of the University to encourage the distribution of all theses, dissertations, and manuscripts. Copies of all UCSF theses, dissertations, and manuscripts will be routed to the library via the Graduate Division. The library will make all theses, dissertations, and manuscripts accessible to the public and will preserve these to the best of their abilities, in perpetuity.

Please sign the following statement:

I hereby grant permission to the Graduate Division of the University of California, San Francisco to release copies of my thesis, dissertation, or manuscript to the Campus Library to provide access and preservation, in whole or in part, in perpetuity.

Author Signature

June 8, 2011

Date